Title
Acoustic Methods of Pulmonary Disease Diagnosis

Author
Rao, Adam

Publication Date
2019

Peer reviewed|Thesis/dissertation

Acoustic Methods of Pulmonary Disease Diagnosis

by

Adam Rao

DISSERTATION

Submitted in partial satisfaction of the requirements for degree of

DOCTOR OF PHILOSOPHY

in

Bioengineering

in the

GRADUATE DIVISION

of the

UNIVERSITY OF CALIFORNIA, SAN FRANCISCO
AND
UNIVERSITY OF CALIFORNIA, BERKELEY

Approved:

DocuSigned by:
Shuvo Roy
C1B7512AE288433...

Shuvo Roy

Chair

DocuSigned by:
Daniel Fletcher

Daniel Fletcher

DocuSigned by:
5E4BA1E695CB406...

Adithya Cattamanchi

Committee Members

Ideas may come to us out of order in point of time. We may discover a detail of the facade before we know too much about the foundation.

Simon Flexner

Acknowledgments

I cannot express the depth of gratitude I have for my parents. It is thanks to their support and their unique strengths that I have the patience and dogged persistence necessary to pursue this work. Thank you, Mom and Dad.

I also want to thank two of my closest friends whose academic diligence has always kept me hungry to learn more. Jeff and Emily, without your help and positive influence I never would have been able to pursue a PhD.

My friends made during my time at UCSF continued to push me to be the best scientist that I can be and many collaborated on projects contributing to this thesis in many different ways. Including my entire MSTP class, especially Jonathan Schor for listening to my crazy ideas and contributing crazy ideas of your own and David Wu for convincing me to buy a 3D printer and then helping to print enclosures for devices. All of my fellow medical school classmates, for showing me what it means to strive to be the best doctors we can be and motivating me to make devices to supplement our practice. Especially thanks to Sam Zetumer for your contributions in both clinical knowledge and data science, Simon Chu for your clinical expertise and help critically designing and running clinical studies. Tina Otero and Tiffany Chong for your help collecting data for the studies, without which there would be nothing to analyze.

I also would like to thank my friends outside of medical school for keeping me sane and contributing your unique skills to helping move the project forward. To Brian Jacobe: two decades down many more to come. Thanks for being such a great friend and helping advise us on database design. To Neil Batlivala: thank you for charging headfirst into the project when our data was in shambles and lending your computer science expertise to

get us a solid codebase. To Kendall Rogers: thank you for proofreading sections of this thesis on short notice, and for reminding me of my appreciation for the written word.

I want to thank the MTM team for working hard to take the Tabla project further. Liya Abraha for lending your unique experience practicing medicine in Eritrea. Audrey Denman for lending your consulting and business skills to the project. Grant Pemberton for lending your excitement and drive in improving the codebase for the project. Justin Olshavsky for helping to lead patent investigation together with the UC Hastings team. Thank you all.

I also want to thank three excellent engineers for their work on the project. Yasha Saxena your work was inimitable thanks to your work developing analysis methods, hardware and for helping to manage the MTM team. Ryan Williams, you helped both me and the project by challenging me to be a better manager and helping refine the codebase. Emily Huynh your work was invaluable and persistence laudable for trudging through a great many academic papers to construct a review of this field with me and for being a fantastically driven mentee.

To the host of advisors and collaborators across academia and industry, your advice and mentorship was indispensable. Thank you to Tejal Desai for being my MSTP advisor and helping encourage me along the way; Aaron Korblith, for not only your clinical expertise and guidance but also the excitement you brought to the project and your encouragement, which helped me realize I was learning and moving things forward even when things seemed bleak. To Dan Fletcher, thank you for serving on my committee and for your insightful guidance and for pushing me to think about the engineering problems and research in different ways. Likewise, thank you to Adithya Cattamanchi for your clinical guidance and for reminding me of important clinical considerations during the

development of the device.

A deep and resounding thank you is owed to my dissertation advisor and mentor Shuvo Roy. When I first met you, I was an engineer with some consulting experience. I distinctly remember being extremely impressed that your slide deck was better than many consulting decks. I was shocked at how your research was managing to bridge the gap between engineering and medicine. I had always seen engineering and medical research as two separate and distinct entities, you showed me that truly translational research was not only possible but critical to design of medical devices. You also taught me that academia and industry do not need to stay in their own lanes. You pushed me to be independent while providing me with every possible resource to succeed. I feel truly honored to have been your student.

Finally, I want to again extend a special thank you to the members of my dissertation committee and quals committee. Tejal Desai, Adithya Cattamanchi, Dan Fletcher and Shuvo Roy. Thank you all for spending hours discussing my research, asking pointed questions during quals, and for helping make this device a reality. Your guidance has significantly impacted my practice as an engineer and your words of advice will stay with me in years to come.

Contributions

I would like to acknowledge all of the co-authors on manuscripts that in part are contained in this dissertation. This includes Jorge Ruiz, Chen Bao, and Shuvo Roy for a manuscript entitled "Tabla: A Proof-of-Concept Auscultatory Percussion Device for Low-Cost Pneumonia Detection," which appeared in MDPI Sensors. As well as Simon Chu, Neil Batlivala, Sam Zetumer, and Shuvo Roy for a manuscript entitled "Improved Detection of Lung Fluid with Standardized Acoustic Stimulation of the Chest," which appeared in the IEEE Journal of Translational Engineering in Health and Medicine. And Emily Huynh, Thomas J. Royston, Aaron Kornblith, Shuvo Roy for a manuscript entitled "Acoustic Methods for Pulmonary Diagnosis," which appeared in IEEE Reviews of Biomedical Engineering.

Abstract

Acoustic Methods of Pulmonary Disease Diagnosis

by

Adam Rao

Respiratory diseases are a leading cause of death worldwide. Despite modern antibiotics, treatment of pneumonia and other lung diseases is often limited by the tools available to diagnose these disorders in low resource settings. While tools such as chest x-ray and CT scans are highly accurate, their high cost provides a prohibitive barrier for many patient populations. On the other hand, the physical exam provides a time-honed method for diagnosis of many common lung diseases. Unfortunately, due to limited sensitivity, the pulmonary physical exam is often insufficient for diagnosis. The goal of the research presented in this dissertation is to take advantage of the simplicity of the clinical physical exam, but to quantify its findings using modern sensors. We present a standardized approach to analysis which differentiates a healthy lung from a diseased lung with 91.7% accuracy. For pneumonia specifically, we demonstrated 92.3% accuracy when distinguishing healthy subjects from pneumonia subjects in a pilot study. In addition to these findings, we also review this work in the context of the current work in the field and provide suggestions for next steps to continue quantified acoustic analysis of the lungs.

Contents

1 Clinical Motivation **1**

1.1 Imaging of fluid in the lungs 1

1.2 Pathophysiology of Common Lung Diseases 5

1.3 Automating the Pulmonary Physical Exam 6

1.4 Objectives 7

2 Acoustic Signals and Lung Disease **9**

2.1 Introduction 10

2.2 Types of Acoustic Signals 12

2.3 Physics of the human thorax 20

3 Methods of Measurement and Device Design **23**

3.1 Methods of Measurement 23

3.2 Methods of actuation for external sources 29

3.3 Materials and Methods 41

3.4 Tabla System Load Testing 52

3.5 Results and Discussion 53

3.6 Conclusions 57

4 Signal Processing and Analysis **60**

4.1 Frequency range for analysis 60
4.2 Analysis methods 62
4.3 Classification algorithms 66
4.4 Methods 70
4.5 Results & Discussion 80
4.6 Conclusion 83

5 Designing Human Subject Studies **85**
5.1 Designing a Clinical Protocol for Medical Device Studies 86
5.2 From Bench to Bedside 91
5.3 Human Subjects Studies 92

6 Conclusions **103**
6.1 Automating the pulmonary physical exam 104
6.2 Challenges and prospects: The path to standardization 106
6.3 Looking ahead: Telemedicine and mobile health 108
6.4 Recommendations 109

A Device Storyboard **111**

Bibliography **118**

List of Figures

1.1 Common Lung Pathologies 4

2.1 Internal and External Acoustic Signals used in Pulmonary Diagnosis 10

3.1 Actuators used in Pulmonary Diagnosis 32
3.2 Ultrasound Artifacts used in Pulmonary Diagnosis 37
3.3 Tabla System Components 42
3.4 Tabla Auscultatory Percussion Device Usage 44
3.5 Early Tabla Device Prototypes 45
3.6 Tabla Device Block Diagram 46
3.7 MP3 Decoder Circuit Diagram 49
3.8 Audio Amplifier Circuit Diagram 50
3.9 Spectrogram of Chirp Signal 51
3.10 Tabla and Eko Device Load Testing 53
3.11 Benchtop Phantom Acoustic Response 56
3.12 Frequency Spectrum of Healthy Subjects Compared with Pneumonia Patients . 58

4.1 Onset Detection Function for Chirp Signal 74
4.2 Sinusoidal Modeling for Chirp Signal 76
4.3 Data Analysis Block Diagram 78

List of Tables

2.1 Sound Stimuli 13

3.1 CORSA Specification Recommendations for Sensors 26
3.2 Methods of Measurement: Microphones 30
3.3 Methods of Measurement: Accelerometers 31
3.4 UNICEF design requirements. 42
3.5 Actuator Pugh chart: Scored from 1 (low) to 5 (high). 47

4.1 Clinical features of healthy subjects and patients 72
4.2 KNN with and without Clinical Features 81
4.3 KNN between percussion sounds and breath sounds feature set with Clinical Features 82

5.1 Comparison of acoustic methods for lung disorder diagnosis 97

Chapter 1

Clinical Motivation

Respiratory diseases are a leading cause of death worldwide. Despite modern antibiotics, treatment of pneumonia and other lung diseases is often limited by the tools available to diagnose these disorders in low resource settings. While tools such as chest x-ray and CT scans are highly accurate, their high cost provides a high barrier for many patient populations. On the other hand, the physical exam provides a time-honed method for diagnosis of many common lung diseases. Unfortunately, due to limited sensitivity, the pulmonary physical exam is often insufficient for diagnosis. The goal of the research presented in this dissertation is to take advantage of the simplicity of the clinical physical exam, and to quantify its findings using modern sensors.

1.1 Imaging of fluid in the lungs

Accumulation of excess air and water in the lungs leads to breakdown of respiratory function and is a common cause of patient hospitalization. Shortness of breath, or dyspnea, is a common chief complaint among patients admitted to the hospital, accounting

for 3.7 million visits to emergency departments in the US in 2011 [1]. Rapid and reliable diagnosis of the undifferentiated adult patient presenting with acute dyspnea is critical for appropriate triage, medical management, and identification and/or prevention of imminent respiratory collapse. Physical examination is the standard procedure for initial evaluation of patients who present with respiratory symptoms. A respiratory physical exam consists of several procedures, including listening to the patient's thorax with a stethoscope (auscultation) and tapping on the chest or back to check for areas of dullness corresponding to pathology (percussion) [2].

Percussion is a technique in which one introduces a sound stimulus through the chest wall in order to detect change of respiratory functions, as can be an indicator of lung pathology. By tapping on the patient's back and listening for certain sounds, a clinician can determine if a lung field is abnormally occupied by air, fluid, or solid mass. Structural changes induced by disease cause alterations in acoustic transmission of frequencies through the thoracic cavity [3]. While valuable, appropriate execution of this technique and interpretation of the findings are both subjective and highly skill dependent [4]. Exam results often suffer from a high degree of variability and a low interobserver agreement [5]. This qualitative physical exam has led to the introduction of adjunctive imaging modalities to assist in the diagnosis of respiratory disease.

Radiographic imaging is one of the most common diagnostic methods used to evaluate the presence of lung disease that might not be detected by the physical exam. While a key supplement in the diagnosis and management of respiratory patients, the chest radiograph has its drawbacks. The use of high-energy ionizing radiation to penetrate tissue for imaging can lead to mutations that increase the risk of cancer. In addition, certain obstructive airway diseases such as chronic obstructive pulmonary disease (COPD) and asthma

may also be missed in an x-ray analysis [6]. Furthermore, the equipment may be cost-prohibitive in resource-poor settings, where the burden of respiratory disease is greatest. For example, the cost of deploying an x-ray machine in Northern India is estimated at $51,500, plus an additional $5,900 per year for operational costs [7]. Consequently, adjunctive pulmonary monitoring methods that are low-risk, inexpensive, and accurate are the subject of active research.

Ultrasound does not carry radiation risks and has established diagnostic utility for the heart, kidneys, and other major organs. Unfortunately, its utility for directly imaging lung tissue is still being researched [8]. This is largely due to acoustic impedance mismatch at high frequencies (on the order of MHz) between the chest wall and air inside the lungs, resulting in the reflection of ultrasound waves at the surface of the lungs [4]. Lung ultrasound, like the physical exam, also has limitations that are both operator- and patient-dependent. Utilizing ultrasound and correctly interpreting its findings requires extensive formal training.

Audible sound shares the advantages of ultrasound while providing a more quantitative method of analysis compared with physical exam techniques. The past few decades has seen a surge in research into quantifying audible sound to provide metrics for pulmonary disease diagnosis. Audible sound techniques generally fall into two main categories: internal sound analysis and external sound analysis [9]. Internal sound analysis uses signals generated by the human body to provide diagnostic information. External sound analysis, which is the subject of this study, uses low frequency sound transmitted into the respiratory system by an acoustic actuator for detection on the chest surface. In this technique, the frequency and time information of the signal are used to provide diagnostic information about the patient.

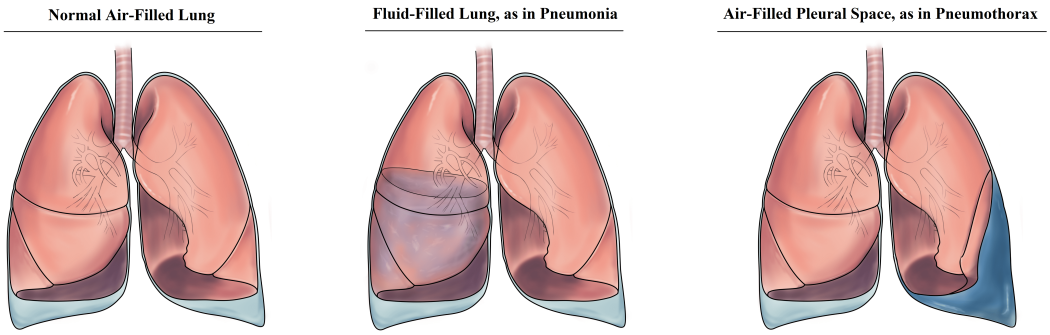

Figure 1.1: A healthy lung, a lung with consolidation characteristic of pneumonia and a lung with air in the pleural space characteristic of pneumothorax. Pneumonia leads to the accumulation of protein-rich fluid (exudate) in the lungs. The presence of exudate and air accumulation can be detected using different techniques, e.g., chest X-rays and acoustic analysis

Here, we present a proof of concept for the acoustic detection of structural lung pathologies. We will utilize a low-cost acoustic actuator to provide a fixed signal input and a digital stethoscope system paired with an innovative audio processing algorithm for automated classification. The system, named Tabla after the percussive instrument of the same name, utilizes the technique of auscultatory percussion, wherein a percussive input sound is sent through the chest and recorded with a digital stethoscope for analysis. Standardizing the acoustic stimulation is designed to reduce patient and operator variability. The cost for an acoustic based system is hundreds (rather than thousands) of dollars, providing a feasible and scalable diagnostic solution for the developing world. Our investigation into distinguishing features characteristic of normal and abnormal lung function provides a foundation upon which future studies that examine disease-specific lung changes can be based. This system aims to provide rapid and accurate diagnosis in the emergent patient who presents in respiratory distress.

1.2 Pathophysiology of Common Lung Diseases

Due to both infectious and non-infectious diseases, the lung can become abnormally occupied by air and fluid. Structural changes induced by disease cause alterations in acoustic transmission of frequencies through the thoracic cavity [3]. For the purposes of this review, we focus on pneumonia, pleural effusion, pneumothorax, chronic obstructive pulmonary disease (COPD), and asthma. These diseases in particular have pronounced acoustic findings, and the majority of the research in the field has focused on these disorders. The diseases can be grouped into two broad categories based on their pathophysiology: fluid accumulation and air accumulation. Pneumonia is the result of a lung infection which leads to inflammation and the accumulation of exudate (a protein-rich fluid) in the lungs [10]. The accumulation of this fluid provides the physiological basis for the acoustic physical exam findings of abnormal breath sounds and dullness to percussion [11]. The term "consolidation" refers to the area of the lungs suffering from fluid accumulation. Pleural effusion is similar to pneumonia in that it also results in the accumulation of fluid; however, the location of the fluid accumulation is in the cavity surrounding the lungs, called the pleura [10]. In addition to fluid, air can also abnormally occupy the chest cavity and lead to the collapse of the lungs in an acute disease called pneumothorax [12]. The presence of this air measurably changes the acoustic properties of the lungs [13]. Asthma and COPD are inflammatory disorders which affect the larger airways; this inflammation leads to the characteristic wheezes and other pathological breath sounds associated with these diseases [14, 15]. This inflammation also primarily inhibits exhalation, leading to a trapping of air in the chest cavity, which may affect the resonance of the chest [16]. Unlike pneumothorax, asthma and COPD are chronic in nature.

1.3 Automating the Pulmonary Physical Exam

The accumulation of fluid at the site of infection provides the physiological basis for physical exam findings of pneumonia: egophony, dullness to percussion, increased tactile fremitus, changes in breath sounds and crackles, among others [11]. A brief explanation of these common pulmonary physical exam maneuvers and other acoustic signals is covered in Chapter 2, but a detailed summary can be found in [17]. Our device relies specifically on automation of the physical exam procedure of auscultatory percussion.

Percussion involves the physician tapping on the sternum and specific areas of the back while listening to the resulting sounds. Experience allows the physician to determine if these sounds correspond to the presence of healthy or abnormal tissue. In a normal lung, much of the sound is reflected at the interface between the soft lung tissue and the semi-rigid chest wall, due to the large impedance mismatch. This leads to a "clear long lasting sound described as resonant" [3]. In the case of pneumonia, exudate surrounds the soft lung tissue and the acoustic impedance mismatch between the chest wall and the consolidation is minimal. Vibrations on the surface rapidly propagate to the exudate, leading to a "sound of low amplitude and short duration described as dull" [3]. The principle of operation for our device is the same as for auscultatory percussion, in which a physician applies a sound input by tapping the sternum with one hand while listening via a stethoscope held against the back with the other hand [10]. The physician assesses the acoustic properties of the sound that travels through the chest.

Controlled studies have shown that auscultatory percussion (the physical examination technique in which the physician taps on the patient's chest and listens to the patient's back via a stethoscope), is a method capable of detecting various presentations

of pneumonia [10]. Unfortunately, compared to a chest X-ray, the sensitivity (58%) and specificity (67%) of physical examination for detection of pneumonia are fairly low [5]. This is due in part to differences in the interpretation of the findings; rates of interobserver agreement between two internists and a pulmonologist for diagnosing pneumonia via physical exam ranged from 60–72% in one study [5]. The undesirably high interobserver error of physical exams for diagnosing pneumonia has inspired researchers to seek new, low-cost methods that offer improved sensitivity and specificity by quantifying physical findings.

1.4 Objectives

The objective of this thesis is to investigate the diagnosis of pulmonary diseases by using sound transmission into the lungs and to evaluate the performance of the Tabla system in the detection of fluid accumulation in the chest during various pulmonary diseases. To achieve these aims the following sub-aims are investigated:

- Review existing acoustic methods of pulmonary diagnosis, including both internal and external sound sources.
- Explore and analyze measurement systems, including both sensors and actuators, for acoustic assessment of the lungs.
- Build and perform bench-top and clinical testing with a device utilizing the custom Tabla measurement system that meets diagnostic and usability requirements set forth by UNICEF.

- Devise a signal processing pipeline for data acquisition and exploring classification accuracy of the Tabla system.
- Explore and reflect upon the best practices for future development of acoustic diagnostics.

Chapter 2

Acoustic Signals and Lung Disease

Recent developments in sensor technology and computational analysis methods enable new strategies to measure and interpret lung acoustic signals that originate internally, such as breathing or vocal sounds, or are externally introduced, such as in chest percussion or airway insonification. A better understanding of these sounds has resulted in new instrumentation that allows for highly accurate as well as portable options for measurement in the hospital, in the clinic, and even at home. This review outlines instrumentation for acoustic stimulation and measurement of the lungs. We first review the fundamentals of acoustic lung signals and the pathophysiology of the diseases that these signals are used to detect. Then, we focus on different methods of measuring and creating signals that have been used in recent research for pulmonary disease diagnosis. These new methods, combined with signal processing and modeling techniques, lead to a reduction in noise, and allow improved feature extraction and signal classification. We conclude by presenting the results of human subject studies taking advantage of both the instrumentation and signal processing tools to accurately diagnose common lung dis-

eases. This paper emphasizes the active areas of research within modern lung acoustics, and encourages the standardization of future work in this field.

2.1 Introduction

The stethoscope has been developed and used for almost two centuries to allow physicians to evaluate the health of the lungs by listening to breath sounds using a technique called auscultation [18]. Other physical exam procedures, such as percussion, which involves tapping on the patient's chest, and tactile fremitus, which involves assessing the way that vocal vibrations travel through the chest, have also remained core components of the respiratory physical exam [19, 20]. These methods are commonly employed in the preliminary diagnosis of lung pathologies due to their quick and inexpensive utility. Utilizing acoustic findings, trained physicians are able to differentiate between normal and pathological lungs in patients suffering from diseases such as pneumonia, pleural effusion, pneumothorax, chronic obstructive pulmonary disease (COPD), and asthma [19, 21–24].

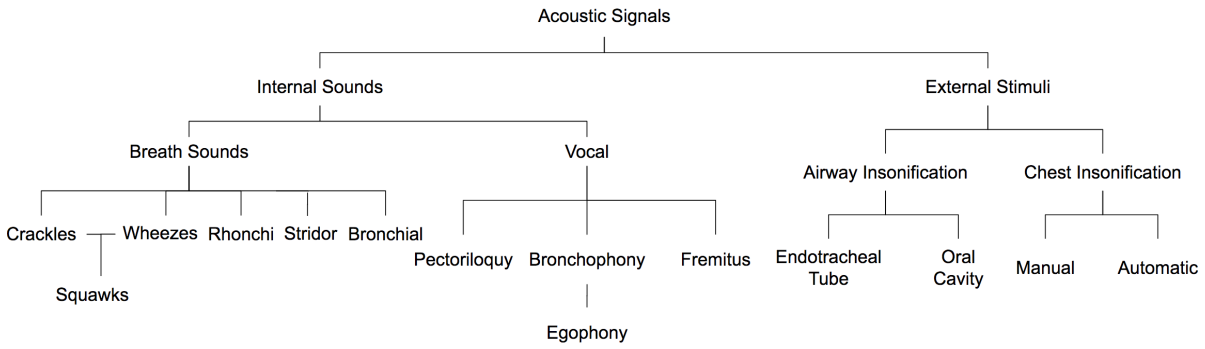

Figure 2.1: Summary of the different types of acoustic signals for pulmonary disease diagnosis. This includes both internal sounds, such as breath sounds, and external stimuli, such as percussion.

In spite of the clinical utility of the respiratory physical exam, these techniques suffer from subjectivity leading to interobserver variability in patient diagnoses [25, 26]. Further challenges include the training required to recognize the specific signals necessary to make a diagnosis. However, over the years, studies into the physics of the lungs have given us a holistic understanding of their response to acoustic stimuli, including factors such as how sound travels through the lung tissue (parenchyma) and the specific characteristics of the lung sound signals under healthy and pathologic conditions [27–30].

This understanding has enabled acoustic methods to advance beyond the stethoscope to employ different hardware and software tools. This paper has been organized to quickly review basic sound types associated with the lung and provide an overview of the physics that govern sound transmission in the respiratory system (Sections II-IV). This is followed by presenting the diverse methods and procedures required for proper measurement of pulmonary acoustics for disease diagnosis, while focusing on presenting recent work in the field (Sections V-X). Recent advances include the use of microphone arrays [31, 32] and ultrasound [33, 34], as well as more sophisticated signal processing methods for processing and classification [35] such as wavelet analysis and support vector machines (SVM) [23].

Approaches rooted in these recent advances have been used for analysis of breath sounds, as well as other internal signals, such as vocal vibrations, together with the introduction of external stimuli into the lungs via the throat or chest. While thorough reviews of breath sound analysis have been conducted [36–38], to our knowledge a broader review of different acoustic analysis techniques for lung disease has not been performed. For this purpose, we review automatic classification methods that have been developed and tested in tandem with various acoustic signals both internal and external. This paper

surveys current acoustic methods, including both measurement and actuation hardware; evaluates signal processing methods used to process and analyze measured sound; reviews selected human subject studies for validation of various methods; and outlines future challenges in the field.

2.2 Types of Acoustic Signals

In this review, we break down the analysis of lung acoustics into two categories: analysis of "internal" signals, in particular, analysis of the sounds produced during breathing and from the vocal chords; and "external" signals, like those that result from chest percussion and airway insonification [19]. The types of acoustic signals are summarized in Fig. 2.1. A summary of the frequency ranges, signal types and analysis techniques for both internal and external signals is provided in Table 2.1.

Internal: Breath sounds

Respiratory sounds occur as the result of air flowing through the lungs and are categorized as normal or abnormal (adventitious). Normal respiratory sounds are defined here as those that are in healthy airways by physiological unforced breathing. These sounds are generally subdivided into tracheobronchial and vesicular; the former originate in the trachea and larger bronchial airways, and the latter may originate in small branches of the airway tree further from the trachea or from other mechanisms at distal regions of the lung parenchyma [62]. Absence or deficiency of normal breath sounds or manifestation of adventitious sounds may be an indicator of pulmonary disease.

Table 2.1: Sound Stimuli

Sound	**Frequency Ranges (Hz)**	**Signal Type**	**Analysis Methods**
Breath sounds	10–1200 Hz [20, 39, 40], 60–2000 Hz [41], 100–600 Hz [42], 37.5–1000 Hz [23, 36], 75–2000 Hz [43], 80–2000 Hz [44, 45], 75–1000 Hz [46], 0–800 Hz [47]	Non-stationary	Meyer wavelet [22, 23], Autoregressive [44], Hilbert transform (envelopes) [22, 46], Fourier transform [40, 47–49]
Vocal fremitus	0–1000 Hz [50]	Non-stationary	Autoregressive [50]
Chest insonification	80–1000 Hz [4, 51], 2–10 MHz [33, 34, 52, 53]	Stationary	Cross-correlation [51], Frequency response function [4, 54]
Airway insonification via mouth	80–1000 Hz [32], 50–1600 Hz [55, 56], 75–2000 Hz [57], 200–2000 Hz [58], 50–2000 Hz [12], 0–20000 Hz [59], 3–35 Hz [60]	Stationary	FFT [32, 58, 60], FRF [55, 57], Convolution [58], Transit time analysis [57], Power analysis [57], Spectrogram [59]
Airway insonification via endotracheal tube	20–1600 Hz [13, 61], 50–1600 Hz [12]	Stationary	PSD [12], FFT [13, 61]

This table provides typical ranges for internal and external sounds useful for analyzing lung structure and/or function. *FFT = Fast Fourier Transform, PSD = Power spectral density, FRF = Frequency response function*

Adventitious respiratory sounds have been classified into several different types, depending on their spectral-temporal characteristics and their location [19, 20]. A variety of lung pathologies and injuries result in adventitious respiratory sounds and/or alter sound transmission pathways, with both spectrally and regionally differing effects that, if properly quantified, may provide additional information about the severity and location of the trauma or disease. We briefly review the different types of breath sounds and their spectral characteristics in this section, and refer the reader seeking more detailed explanations to the definitions and spectral characteristics set forward by the European Respiratory Society (ERS) [63].

Crackles

Crackles, also termed “crepitations" or “rales," are short, discontinuous, and non-stationary sounds that can be detected during inspiration [14]. Key features often extracted from crackles include their duration, waveform, and timing, which can be correlated to several pathologies, such as pneumonia, fibrosis, and other parencymal diseases [14, 62, 64, 65].

Wheezes

Wheezes are adventitious *continuous* sounds that are typically heard at end expiration with mild obstruction of small airways. They are often detected in subjects affected by obstructive diseases, in particular asthma and COPD [14, 65–67], as well as in sickle cell patients experiencing an acute pain crisis [64]. Their dominant spectral content is usually between 100 to 1000 Hz, with higher harmonics above 1 kHz.

Rhonchi

Rhonchi are musical low-pitched sounds characterized by a sinusoidal waveform [14]. The duration is generally higher than 100 ms and frequency content lower than 300 Hz. They are associated with abnormal airway collapsibility and the creation of breaches in fluid films [14]. Rhonchi can be considered indicators of obstruction of large airways with mucus or other pathologies [14].

Stridor

Stridor, often mistakenly considered a type of wheezing, refers to intense continuous monophonic sounds best heard over extra-thoracic airways during inspiration. Stridor is usually considered an indicator of upper airway obstruction. Signal analysis reveals

that stridor tends to have a sinusoidal waveform, with a fundamental frequency generally above 500 Hz [14, 68].

Squawks

Squawks are defined as a mixed sound since they are characterized by a crackle followed by a short musical component resembling a wheeze [14]. They are likely to occur in fibrotic pulmonary disorders. Acoustically, their waveform is similar to that of short wheezes, but they are often preceded by a crackle. Mean squawk duration is approximately 90–320 ms.

Bronchial

Bronchial breath sounds are blasting sounds, audible throughout inspiration and expiration, with a frequency range of 600–1000 Hz [38]. Although normal when heard over the neck, close to the bronchus, when bronchial sounds are heard over the lung fields it is usually due to a reduction in the amount of parenchyma through which the sounds pass resulting from disease [28]. Generally, they have a higher frequency content with respect to normal sounds; this is because consolidation causes a reduction of the low-pass filtering role of the alveolar region.

Internal: Vocal sounds

Vocal sounds can be viewed as internal to the body but are also an external stimulus to the airways and lungs. Vocal sounds consist of a fundamental frequency and several overtones that make up higher frequencies. In healthy patients, auscultation of vocal sounds often appear muffled due to poor transmission of sound in air-filled lungs, which

filters out higher frequencies often with a peak at 130–250 Hz [17, 50]. Consolidation has been found to increase this transmission to 400 Hz [69]. Auscultation of vocal sounds has been used to exploit its frequency content and response, and is a valuable tool as certain vocal findings have been found to precede abnormal breath sounds [69]. Different methods of initiating vocal sounds have been explored by researchers, pairing different methods of actuation such as ultrasound or sound delivered via speakers with different types of sensors; however, as they are based on the same principles, it is often up to the physician to decide which method to use [28].

Pectoriloquy

Pectoriloquy refers to an abnormal increase in the clarity of whispered vocal sounds during auscultation due to the presence of lung consolidation, which increases the sound speed and thus lowers the damping of the vocal signal due to the efficiency of sound transmission through fluid. A study comparing different methods of diagnosing pneumonia, including auscultation of percussion, breath sounds, pectoriloquy, and bronchophony, showed that pectoriloquy had the lowest inter-rater agreement and was rarely detected by physicians [5, 70].

Bronchophony

Bronchophony applies the same principles of pectoriloquy, but is spoken instead of whispered. Egophony is a specific type of bronchophony. When a patient speaks the letter “E" it is normally heard on the chest wall as a muffled “E" in healthy patients, but in the presence of consolidation, it sounds like a spoken “A" [69]. “E” consists of a fundamental frequency between 100–400 Hz and overtones ranging from 2000–3500 Hz, while

“A" consists of a higher fundamental frequency of up to 600 Hz [17]. Increased density in the parenchyma from pleural effusion or lung consolidation transmits the higher frequencies of “A" better than the lower frequencies of “E" with no significant transmission above 1000 Hz, and may stifle transmission from 100–300 Hz, causing the apparent “A" sound [17]. In several studies, egophony was found to have increased the likelihood of diagnosing pneumonia but had highly variable positive predictive values, from 20–56% [71].

Fremitus

For vocal fremitus, the input to the chest is the speech signal at the vocal chords and the output is the sound heard at the chest wall. To generate the speech in a standard way, the patient is asked to vocalize a constant sound, such as *EEE* [19]. The vibrations initiated by fremitus are decreased in the presence of conditions such as bronchial asthma, emphysema, obstruction, pleural effusion, and pneumothorax. Air trapping or accumulation decreases the transmission of lower frequency vibrations, while consolidation and inflammation increases transmission [72].For these reasons, fremitus is often more useful in male patients, and has been observed to be ineffective in obese patients [69, 72]. Wipf et al. found that, along with pectoriloquy, vocal fremitus was rarely detected in patients with pneumonia [5]. Another study corroborates these findings, but suggests that it is difficult to calculate the reliability of fremitus because it occurs infrequently [70]. For pleural effusion, fremitus has been shown to have a high sensitivity (82%), specificity (86%), and negative predictive value (95%) for diagnosis, though the positive predictive value was low (56%) [73].

External: Airway insonification

The process of analyzing abnormalities in lung structure can also be done electronically, by introducing external sound through the oral cavity or the endotracheal tube [12, 13, 51, 55, 57, 61, 74]. Sounds introduced to the oral cavity have ranged from 50–2000 Hz [55, 57, 74], while sounds introduced through the endotracheal tube have ranged from 20–1600 Hz [13, 61]. A transfer function with the chest as the output has been used to characterize the structure and/or content of the parenchyma. By utilizing a fixed input signal, the specific frequencies of interest can be isolated and the differences between patients' vocalization discussed above can be avoided [69, 72].

External: Chest insonification

In addition to the vocal tract, sound can also be introduced directly to the chest, which can be done via percussion, electronic actuators, and ultrasound. Percussion is a term that refers to exciting a tissue with an impulsive force [3]. The input is a percussive stroke generated manually by a finger or automatically by an external tool; the output is the sound heard at the chest wall [3]. If the vibrations from the percussive stroke are less damped, they persist, known as a resonant or tympanic note. This occurs due to a significant acoustic mismatch between the gas-filled lungs and chest wall, causing reflections at the lung–chest wall interface, and thus longer vibrations. In contrast, flat percussive notes, which die out quickly, are caused by similar tissue beneath the chest wall, such as over the heart or due to the presence of fluid, which decreases the amount of acoustic mismatch [28].

In previous studies, dullness from percussion has been shown to be associated with in-

creased likelihood of pneumonia, though its measurement is hindered by low inter-rater agreement [5, 70]. Auscultatory percussion, first described by Guarino, is a variation of direct percussion in which one side of the body is percussed and the sound assessed with a stethoscope at a distance or on the other side of the body [10]. Bohadana et al. expanded Guarino's findings in a study of 98 patients with abnormal chest films; in the blinded study, direct percussion and auscultatory percussion were compared, demonstrating that both were about equally effective at detecting pleural effusions, but that neither technique could detect intrapulmonary masses less than 6 cm in diameter [75]. In a follow-up study, the same researchers recorded data from several sensors to create a sound map of the backs of three healthy subjects and four patients with large intrapulmonary lesions (from 6–10 cm), finding that scapulae play a large role in sound transmission for percussion of the sternum and that intrapulmonary lesions were not detectable [76]. This limitation in part arises from the low bandwidth of manual percussion sounds (less that 100 Hz), and in part due to the characteristic transmission of sound through bony structures as well as through the lung parenchyma.

Automated methods have attempted to address these limitations by expanding the bandwidth of the input signal to 1000 Hz and recording from areas that exclude the scapulae. Recent studies have introduced a frequency range of 50–1000 Hz at the chest to measure changes in velocity and arrival time, the transfer function, or reflections of sound waves [4, 28, 51, 54]. Apart from an impulsive signal, a controlled input signal such as a chirp can be input at the chest wall to analyze any abnormalities in its transmission through the chest structure [4, 54, 77].

In addition to audible range stimulation, ultrasound provides input into the chest of frequencies above 20 kHz, with most clinical ultrasound systems in the range of 2 to 10

MHz [33]. As the sound travels into the tissue, a reflection beam called an echo is formed; production and detection of echos is the basis for all diagnostic ultrasound systems [33]. If two adjacent tissues have different acoustic impedances, they will produce an echo. If the difference between the two tissues is very large, as is the case in the chest–lung interface, not enough ultrasound signal will remain to image beyond this interface, creating challenges for thoracic imaging [33]. Despite these challenges, several methods utilizing the artifacts of the ultrasound image can be used to great effect for pulmonary diagnosis, these methods are explored in Section V.E.

2.3 Physics of the human thorax

The human thorax is comprised of four different types of materials with significantly different acoustic properties: hard tissue (bone), soft tissue (muscle, fat, etc.), air in the major conducting airways of the bronchial tree, and parenchymal tissue that is a heterogeneous mixture of soft tissue and air found in the alveolar sacs and smaller bronchioles. The characteristics of these different components affect how sound is transmitted through the thorax.

Absorption

Sound in the lumen of the lung airways experiences a frequency-dependent absorption into the airway walls and surrounding parenchymal tissue, in which high-frequency sounds propagate further within the airway branching structure, while low-frequency sounds tend to couple into the airway walls sooner [20, 28, 78]. However, due to the attenuation of higher frequency sounds in the surrounding parenchymal tissue, most of

the signal energy of breath sounds recorded on the torso surface is concentrated at lower frequencies [20, 56].

Analysis of sound transmission in the chest cavity suggests that the chest, overall, acts as a low-pass filter, absorbing higher frequencies as sound travels through it [28, 43, 50, 55, 57]. This filtering effect is altered with the presence of different lung conditions, such as consolidation or fluid build-up, which on the one hand can create large acoustic impedance mismatches with healthy parenchymal tissue and air, but on the other hand acoustically couples better to surrounding soft tissue of the chest wall and inherently allows sound to propagate with less attenuation, as compared to healthy parenchymal tissue [4].

Transmission and reflection

Transmission and reflection of sound waves is caused by interfaces between the semi-rigid chest wall, pleural spaces which normally contain air but can fill with fluid in disease, and the lung tissue, which is typically approximated as a homogeneous mixture of gas and tissue [79].

Sound intensity is a quantitative measure of transmission. At a given interface, assuming normal incidence, the fraction of sound intensity transferred, T_I, is a function of the relative acoustic impedances of the two media, Z_1, Z_2 [80]:

$$T_I = \frac{4Z_1Z_2}{(Z_2 + Z_1)^2}.$$

If $Z_1 \approx Z_2$, the two media are very similar, so $T_I \approx 1$, meaning that almost all of the sound intensity is transferred to the next medium. At the other extreme, $T_I \approx 0$ and

most of the sound intensity is reflected back at the interface. Thus, imaging the lungs via ultrasound was initially thought to be impossible due to the high acoustic impedance mismatch between the soft tissue and parenchyma [33].

Resonance

Resonant frequencies are those frequencies at which acoustic waves are reflected back and forth due to interaction with boundaries or interfaces, leading to constructive interference and an amplified response. When a short (percussive) impulse, with broad frequency content, is applied to a system, the response at its resonant frequencies will persist longer than at other frequencies, particularly as damping (viscosity) in the system is reduced [81]. For the chest overall, this characteristic depends on several factors, including the size of the thorax. The first, or lowest, resonant frequency of the chest for men is around 125 Hz; for women it is slightly higher, at 150–175 Hz; for children it is 300–400 Hz [28]. For sound traveling in the lumen of the airways, the resonant frequencies are a strong function of the geometry and wall properties of the airways whereas direct chest stimulation will generally bypass these differences [82]. Resonances may also occur when pathologies create trapped air cavities below the torso surface, such as in the case of pneumoperitoneum [83, 84].

Chapter 3

Methods of Measurement and Device Design

3.1 Methods of Measurement

The classic method of measuring lung sounds is with the stethoscope, which works by isolating the sounds from the vibrating chest wall and filtering out certain frequencies of interest mechanically. These sounds can be recorded for analysis by converting the acoustic pressure or vibrations of the chest–wall interface into electrical signals. In this section, we review the filtering characteristics of the stethoscope, discuss common types of sensors used to digitize this signal and their methods of transduction and end with a discussion of multi-point measurement systems. These sensors are discussed in the context of Computerized Respiratory Sound Analysis (CORSA) specification recommendations, which are based on a project of the European Respiratory Society [63].

The Stethoscope

Conventional stethoscopes rely on analog filtering and amplification of sound for interpretation by a trained professional [46]. Stethoscopes have two sides, a bell and a diaphragm, with different frequency characteristics. Bell chestpieces amplify sound below 112 Hz [85], demonstrating superior sound transmission at these frequencies compared to the diaphragm, which attenuates low frequencies [86]. Both bells and diaphragms have an important attenuation above 200 Hz, which limits the ability to discern sounds in this frequency range [85]. The sensitivity of the human ear ranges from 20–20,000 Hz [42, 86]. Despite the range of human hearing, because the ear follows a logarithmic sensitivity to frequency, greater changes are required at higher frequencies to discern them as different [46]. Electronic stethoscopes utilize a variety of sensors including condenser microphones and piezoelectric sensors in order to convert acoustic waves into electrical signals for filtering and processing [13, 22, 61]. Compared to the conventional version, electronic stethoscopes allow amplification of the acoustic signals, electronic removal of noise artifacts, and recording for playback and post-processing [86]. In spite of these advantages, electronic stethoscopes also suffer from excessive ambient noise, which is exacerbated by amplification; however, this is reduced with the implementation of low-pass filters from the bell and diaphragm [86]. Depending on the type of sensor utilized, and the analog and digital filters that are applied, the frequency range varies for these methods of measurement. The main strength in the electronic stethoscope is the integration of a familiar technology with advancements in electronics and signal processing (see Section VII). Low barriers of adoption for medical professionals can facilitate quicker clinical usage of lung acoustic diagnostics; however, its main weakness is site-specific dependencies

with a single point of measurement.

Sensors

The vibrations of the chest–wall can be recorded using several different methods of transduction, such as condenser and piezoelectric transduction [63]. An ideal sensor should be small and lightweight, cost-efficient, produce reliable and sensitive measurements with little noise, and have reproducible frequency response [38]. Due to its flat frequency response, high SNR, and advancements in MEMS technology, we recommend condenser microphones for such an ideal sensor. CORSA provides standard considerations for picking a condenser microphone for respiratory recordings [87] A majority of recent studies reviewed in this article (see Table 5.1) have also utilized condenser microphones.

The two main types of microphones used for lung sound analysis are air-coupled and contact microphones. An air-coupled microphone converts changes in dynamic air pressure within the drum of a stethoscope created by the oscillatory movement of the diaphragm or bell pressed against the torso surface into electrical signals, while contact microphones convert mechanical stress caused by chest movements using piezoelectric transduction principles [35].

Condenser microphones

Condenser microphones are a type of air-coupled microphone. Condenser microphones such as electret microphones utilize condenser transduction to detect changes in acoustic pressure that change the nominal capacitance values [35, 38, 88]. These microphones have a nearly flat frequency response over the audio range, leading to minimal distortion

Table 3.1: CORSA Specification Recommendations for Sensors

Parameter	**Specification**
Frequency response	50–5000 Hz
Dynamic range	60 dB
Sensitivity	Defined as the voltage generated when the input sound pressure is 0.1 Pa; must be stable across all frequencies, sound directions, and varying noise. Typical value is 1 mV/Pa.
Signal-to-noise ratio (SNR)	Defined as the ratio of the output voltage to the noise when no input signal is applied. Recommended to be $>$60 dB.
Coupling	*Piezoelectric*: contact *Condenser microphones*: Conical, diameter 10-25 mm
Fixing	*Piezoelectric*: adhesive ring *Condenser microphones*: Adhesive ring or elastic belt
Noise and interference	*Acoustic*: shielded microphone, protection from mechanical vibrations *EM*: Shielded twisted pair or coaxial cable

This table describes the recommended specifications from CORSA (Computerized Respiratory Sound Analysis) for sensors that detect human pulmonary sounds. *EM* = *Electromagnetic* [63]

[38, 88]. However, they require acoustic coupling to the chest wall with an air cavity [66, 87]. Microelectromechanical systems (MEMS) microphones utilize condenser principles and provide a similar frequency range and SNR as compared to conventional condenser microphones while providing a smaller form factor [35, 89]. Due to their wide bandwidth, high sensitivity, established coupling methods, high SNR (according to CORSA recommendations), and low costs, condenser microphones are widely used [38, 66, 88].

Contact microphones

Contact microphones typically utilize piezoelectric transduction principles to create an output voltage proportional to the displacement of the sensor placed directly onto the skin without the use of an air chamber [87]. These sensors can be characterized by extremely high sensitivity (50 mV/Pa) and have the advantage of not picking up as much ambient noise as condenser microphones, but are conversely very sensitive to motion artifacts [87, 88]. A study found that loading effects due to the method of coupling from the transducer to the hand piece of the stethoscope is a significant noise source [90]. One design solution to this noise source is utilizing foam between the transducer and hand piece of the stethoscope; progressively softer foam results in reduction of physician hand noise but also lowers the sensitivity of the piezo sensor [90].

Contact accelerometers

Similar to the contact microphone, contact accelerometers make use of the piezoelectric effect, but the output voltage is instead proportional to the acceleration of the sensor. The accelerations involved in lung acoustics are on the order of 0.1 milligravity, thus requiring high sensitivity to detect [41]. Low-mass piezoelectric accelerometers are feasible, but suffer from similar shortcomings as contact microphones [32, 66, 87]. Because of their miniature size, MEMS accelerometers are useful for continuous respiratory monitoring and have been used to detect wheezing in asthma and COPD patients [41].

Multi-point measurements: Sensor array

Lung pathologies alter sound transmission pathways and have both spectral and regional effects that can benefit from simultaneous measurements at multiple points across the chest surface. Understanding the location of abnormal lung sounds can help identify areas of pathology as well as assessing the severity of the pathology based on its spatial distribution. To better assess location, simultaneous multi-sensor auscultation methods have been advanced to “map" sounds on the thoracic surface by several groups [42, 66, 91–93].

One multi-sensor system that has undergone considerable study into its efficacy has been branded as “vibration response imaging" (VRI). VRI involves creating a 2D representation of breath sounds using an array of electronic stethoscopes that pick up sounds from the chest using 18–40 piezo-acoustic sensors to create a gray scale image in real time that can dynamically track acoustic variation throughout the respiratory cycle [42]. The sensors in the array have a flat frequency response from 50–400 Hz [42]. This sensor array has been investigated for distinguishing between healthy subjects versus subjects with pleural effusion or pneumonia [21, 94, 95], differences in lung sounds between asthmatic and healthy subjects [96], and differences between subjects with obstructive airway disease (OAD) and non-OAD subjects [65]. While this system has been applied to a variety of disorders, it remains bulky compared to systems with fewer sensors, as it relies on 40 different sensors coupled to the patient’s back via a low-suction vacuum. Another limitation is the fact that the signal is filtered from 150–250 Hz, which may reduce lung sound characteristics contained in frequency bands above 250 Hz [97].

While 2D visualization of breath sounds is an improvement over individual sensor

recordings, 3D mapping of sound sources may provide further localization for diagnosis. Kompis et al. [20] attempted to form a three-dimensional (3D) acoustic image of the likely sound source location(s) by using multiple sensors and assuming “ray acoustic," i.e., “incident field," models for how sound propagated away from these sources. For future work, Kompis et al. noted that a useful imaging system for the human lung should: (a) be robust with respect to acoustic properties, especially speed of sound, which varies and is not precisely known; (b) provide 3D data sets and resulting images that are intuitively interpretable; and (c) be robust with respect to missing sensors or noisy data in individual sensors [20]. While sensor arrays are ideal for providing a 2D or 3D visualization of the lungs, as opposed to the stethoscope which can only provide one location at a time, current solutions remain bulky, and adoption in the clinic will be more difficult due to increased costs compared to point based measurements.

3.2 Methods of actuation for external sources

Unlike internal sounds, which are non-stationary and not precisely repeatable signals [22], externally introduced sounds have the advantage of providing a fixed input signal generated using a variety of methods.

Actuators

Relatively few studies have investigated the use of fixed input signals for pulmonary diagnosis, leading to a lack of standardization for the transducers used to provide the input signal. Actuators rely on the same principles of transduction as sensors, such as electromotive and piezoelectric transduction but provide inverse functionality by converting an

Table 3.2: Methods of Measurement: Microphones

	(Ref)	Sampling Rate (Hz)	Frequencies (Hz)	Method
Microphone				
	[20]	10240	100–1000	Subjects breathed through a pneumotachograph in a soundproof room for at least six complete breath cycles. Heart sounds and background noise were recorded separately with the patient's breath held.
	[55]	–	20–500	A sinusoidal signal source driven by a loudspeaker was inserted into patients' mouths.
	[12]	8192	50–1600	A sound source was connected to the patient's mouth to be inserted into the endotracheal tube when PTX was induced during thoracic surgery. Sounds recorded for 20 s
	[44]	5000	80–2000	Piezoelectric contact microphone was attached to the trachea using an elastic band. Patients also breathed into a pneumotachograph. Data were measured for 3 forced expirations.
	[58]	8000	80–2500	An acoustic detector was placed on a region of interest and subjects either spoke a phrase ("three-three") or breathed normally.
	[57]	4000	75–2000	Sound generated was delivered through a loudspeaker to the patient's mouth via a cardboard mouthpiece. Measurements were taken 15 times.
	[32]	10000	100–700	A probing frequency from 80–1000 Hz retuned within 20 s was injected into the mouth
	[98]	10000	100–2000	A sensor was placed in a stethoscope for testing; lung sounds were measured in commonly used positions in the abdominal region.
	[59]	115000	0–20000	A sound source from a noise generator was transmitted to the patient's mouth via loudspeaker, with measurements taken for 15 s at 1024 samples per impulse response (8.85 ms).
	[45]	4800	80–2000	Four electret microphones attached to patient via an elastic belt, with a measurement taken for 13.6 s.
	[99]	4000	20–2000	An array of five microphones was used for measuring lung sounds when the volunteer coughed twice.

This table provides a comparison of microphone measurements for acoustic detection for lung disorders. The sampling rate and frequencies used for analysis is included where possible.

Table 3.3: Methods of Measurement: Accelerometers

	(Ref)	Sampling Rate (Hz)	Frequencies (Hz)	Method
Accelerometer				
	[51]	–	80–1000	Sound to the mouth was fed from a PC card. Sound to the chest was provided by a compact shaker that was attached to the reference accelerometer.
	[56]	4096	75-1400	Sound to the mouth was fed through an acoustic driver and tube, and spectral characteristics of acceleration were measured by an accelerometer at three locations attached using double-sided tape.
	[100]	10000	100-2000	Subjects were seated in a soundproof chamber and breathed through a calibrated pneumotachograph. Contact sensors were affixed with double sided tape.
	[29]	4096	0–600	Sound inserted at mouth and measurements taken 8 times for 250 ms at the T_6 chest wall site and extrathoracic trachea.
	[55]	–	20–500	A sinusoidal signal driven by a loudspeaker was inserted into patients' mouths.

This table provides a comparison of accelerometer measurements for acoustic detection for lung disorders. The sampling rate and frequencies used for analysis is included where possible.

electrical signal into a mechanical signal. Several parameters are considered in choosing an actuator, such as bandwidth, displacement, force, power, size, and weight. The ideal actuator is a transducer that can generate a strong signal via displacement or force for a wide range of frequencies, without excessive power consumption [77].

Dynamic loudspeakers

Dynamic loudspeakers utilize electromagnetic induction to transduce an electrical signal into sound waves [101]. Surface exciters are a specific type of loudspeaker that do not have the cone or frame, so their vibrations are coupled to a surface instead of to the air. They are capable of producing a strong signal at low frequencies as low as 50 Hz, and can

Figure 3.1: The frequency of different actuators determines the ranges that can be probed. Solenoids have the lowest range of frequencies while piezoelectric material has the highest range. Numbers provided here are estimates based on experiments with a variety of actuators in each category.

be made relatively small [77].

Electromechanical solenoids

Electromechanical solenoids consist of an electromagnet with a plunger, the plunger will move in or out depending on the direction of the current [102]. They are also capable of actuating strong low frequency signals but are bulky and require large amounts of current for operation, which reduces battery life [77].

Piezoelectric

Piezoelectric transducers have found use in generating and detecting ultrasound waves [103]; therefore, they are notable for their ability to generate large forces at high frequencies with a small size.

Audible sound: Chest input

Use of a fixed audible input signal into the chest is still an area of active research with fewer studies compared to breath sound analysis. Several recent studies have introduced sound through the chest to investigate how sound travels through the chest structure [4, 51, 77]. These studies utilized low frequency audio range transducers which produced signals generated within the range of 50–1000 Hz [4, 51, 77].

The first of these studies used an electromagnetic shaker (ET-132, Lab-works Inc., Costa Mesa, CA) to drive a periodic chirp signal with spectral content from 50–400 Hz into the sternum [4]. The upper limit of frequency was set by the signal-to-noise ratio (SNR) for the system, which was limited by the sensitivity of sensors available at the time of the study. Its goal was to investigate changes in acoustic signals during pneumothorax, which leads to air accumulation in the lungs and collapse of lung tissue. Simulations using finite element analysis (COMSOL) predicted changes in pneumothorax in the range of 100–200 Hz; initial human subject data comparing healthy recordings to two pneumothoracies of different severity demonstrated reduction in signal transmission at 120 Hz which tracked with severity. A later study utilized a compact shaker (Model 4810, Bruel & Kjaer) placed on the clavicle with a reference accelerometer attached to the shaker, and expanded the range to 80–1000 Hz, a range determined by the accelerometer's sensitivity [51].

The most recent of these studies utilized a surface exciter to send a linear chirp from 50–1000 Hz into the chest at the sternum [77]. This study investigated changes in acoustic transmission during pneumonia, which leads to fluid accumulation in the chest. The study demonstrated reduction in signal transmission in the 200–400 Hz range when com-

paring healthy subjects to patients with lobar pneumonia. Another study using the same equipment expanded the frequency range to 50–1000 Hz and utilized a classification algorithm to classify subjects lungs as healthy or pathological with an accuracy of 92% [54].

These studies indicate potential for a fixed input signal in the range of 50–1000 Hz for pulmonary disease diagnosis; however, more studies with larger numbers of patients are needed to confirm these findings and establish a baseline for disease specific changes.

Audible sound: Oral cavity input

Several studies have investigated the introduction of sound through the mouth with external recording from the subject's chest [51, 55, 57, 60, 74]. For mouth-to-chest wall transmission, sound propagation is primarily through the parenchyma, as determined by the consistency of sound transmission across different gases [57]. Studies have focused on both frequency based analysis of transmission, transit time analysis as well as a respiratory acoustic impedance approach to identify changes in lung pathology.

These studies produce an external sound using a signal generator which is sent directly into the patient's mouth and may be broken up into high frequency analysis (50–2000 Hz) and low frequency analysis [55, 57, 74]. The frequency range of 5–20 kHz has also been investigated, and found to result in data variability between healthy subjects, motivating the use of data below 5 kHz for analysis [59]. Controlled inputs via the oral cavity control for the intersubject variability of breath sounds.

Low frequency analysis can be used to obtain the respiratory impedance by utilizing a pneumotachograph to measure flow combined with a loudspeaker, which generates low frequencies. Two approaches exist, each sending a different signal into the oral cavity: the

forced oscillation technique (FOT) and impulse oscillometry system (IOS) [60, 104].These techniques assess lung function by measuring acoustic impedance using sound waves inserted into the patients' mouth. The FOT works by sending a sinusoidal signal of single frequencies into the mouth over a range of 3–35 Hz [104, 105], providing good time resolution with measures of respiratory impedance but taking longer because it only sends one frequency at a time [104]. In contrast, the IOS sends a square wave impulse containing frequencies ranging from 4–32 Hz. Though this results in inferior temporal resolution and can cause discomfort for patients at higher frequencies, it offers improved SNR and can show pressure-flow relationships using frequency analysis [104, 106].

Advantages of FOT/IOS include higher sensitivity in detecting peripheral airway obstruction, short duration, and a requirement for little patient cooperation compared to spirometry, which is difficult for children, the elderly, and physically or cognitively impaired patients [104, 105]. For these reasons, FOT/IOS have proven useful in human studies for diagnosing asthma and COPD [60, 107, 108]. Current challenges to FOT/IOS come from its relatively recent introduction to the clinical setting, making it difficult to compare results due to the lack of standardized, healthy values. There have also been mixed reports regarding the effect of demographics such as age and race on IOS measurements [105], though a study using artificial neural networks (ANNs) to classify asthma in IOS patterns achieved an accuracy of 94% without including race as a parameter [105, 109].

Audible sound: Endotracheal input

Studies have also investigated introduction of sound directly into the lungs through an endotrachial tube [12, 13, 61]. Initial studies in a canine model suggested that a frequency range of 20–1600 Hz with uniform amplitude could be used distinguish between differences in lung structure due to pneumothorax [13, 61]. At frequencies below 100 Hz, the disease and control states were comparable; however, for higher frequencies from 300–1600 Hz clear attenuation occurred due to disease in all subjects. Specifically, for structural changes due to air accumulation in the lungs, the canine model demonstrated an important metric for measuring the impact on the frequency response. Since the spectrum contained a large number of values not well suited for diagnostic analysis, a ratio between the low ($<$220 Hz) and high (550–770 Hz) spectral energies was used to detect accumulation of air [13]

Ultrasound: Chest input

The transmission characteristics for ultrasound are similar to audible sound. Longitudinal waves are used in ultrasound, and the speed of ultrasound in soft tissue is about 1540 m/sec [28]. In ultrasound, the frequencies generated are high (1–15 MHz), which allow a short wavelength (1 to 0.1 mm) [33]. Therefore, it is suitable for detecting small differences in tissue boundaries which may not be picked up by an audible sound. Like audible sound, when the ultrasound wave encounters a boundary between two different media, some of the wave energy bounces back toward the source as an "echo" or reflection. The higher the difference in acoustic impedance between two objects, the higher the amount of reflection [28]. For example, at a soft tissue–bone boundary the ultrasound wave is

highly reflected, and thus appears as a white (hyperechoic) line followed by a posterior acoustic shadow beyond the boundary (Fig 2a).

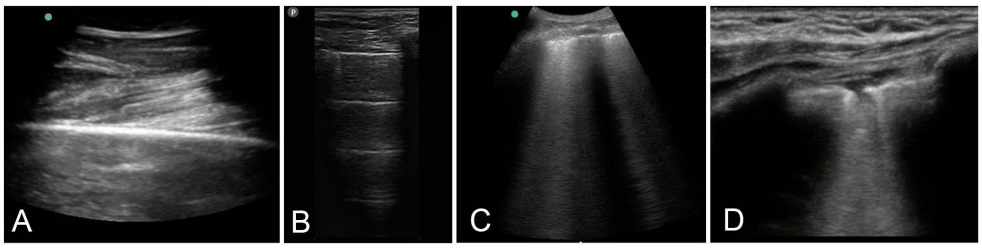

Figure 3.2: (a) This soft tissue–bone boundary in which the ultrasound wave is highly reflected, and thus appears as a white (hyperechoic) line of the femur. (b) A-lines are static horizontal regularly-spaced hyperechoic lines that represent an aerated lung created by reverberation artifact. (c) B-lines are discrete, laser-like vertical projections arising from the pleural line and extending to the bottom of the screen without fading. (d) Shred (fractal) sign shows echo-poor areas of the pleura, represented as a non-smooth pleural line.

Lung ultrasound involves the interpretation of ultrasound artifacts instead of evaluation of the actual lung parenchyma. The soft tissue and pleural boundary has a high acoustic impedance mismatch, such that there is typically a reflection of 99.9% of ultrasound waves, rendering this interface virtually impenetrable to ultrasound [28, 33]. Since there is no ultrasound wave left to image beyond this boundary, performing an ultrasound of the lungs was initially thought to be impractical [28]; however, several studies have shown the usefulness of ultrasound in diagnosing several lung diseases through the identification of artifacts in the ultrasound signal [52]. There are a variety of static and dynamic artifacts that represent normal lung parenchyma.

As for electrocardiograms, a nomenclature has been created to describe and characterize these artifacts for communication. A-lines are static horizontal regularly-spaced hyperechoic lines that represent an aerated lung created by reverberation artifact (Fig 2b). A reverberation artifact is the bouncing of echo between pleural line and the ultrasound

transducer. Likewise, lung sliding is a typical dynamic finding and represents the regular movement of the parietal pleura sliding along the visceral pleura. Lastly, Z-lines appear as bright beads with hyperechoic tails and are a common finding thought to be from microbubbles existing between the pleural layers [110].

There are also many ultrasound artifacts that represent pulmonary disease processes. In particular, comets, echo-graphic signs formed due to water thickened septa, as well as other static image irregularities combined with dynamic signs formed due to the gravity dependence of fluid in the lungs have proven to have diagnostic value [34, 53]. These signs hold particular weight when the alveolar air adjacent to the chest wall is replaced with fluid, allowing ultrasonic detection [111]. Various artifacts and syndromes associated with diseases are explored below.

Interstitial syndrome is a diffuse pulmonary process in which an ultrasound reverberation artifact, B-lines, represent fluid accumulation within pulmonary septa. B-lines are discrete, laser-like vertical projections arising from the pleural line and extending to the bottom of the screen without fading (Fig. 2c). Interstitial syndrome represents a variety of diseases such as pulmonary edema, interstitial pneumonia, acute respiratory distress syndrome, and pneumonitis. The specific distribution of B-lines and the patient's clinical presentation can help elucidate the cause of interstitial fluid [112]. For example, in patients with a moderate to high pretest probability for acute cardiogenic pulmonary edema, an ultrasound study showing B-lines can be used to strengthen a physician's suspicion for pulmonary edema, while in patients with a low pretest probability of pulmonary edema, a negative ultrasound study can almost exclude the possibility of pulmonary edema [113].

Alveolar syndrome represents the loss of air within alveoli secondary to collapse or fluid accumulation (lung consolidation). Alveolar syndrome can be characterized by sev-

eral ultrasonographic findings, including shred sign and tissue-like sign. Shred (fractal) sign shows echo-poor areas of the pleural, represented as a non-smooth pleural line (Fig 2d). Likewise, tissue-like sign, in which extensive consolidation will allow visualization of the underlying pulmonary tissue, is represented as a structure that appears like tissue. For these two findings, pulmonary ultrasound relies on the fact that 98% of consolidations reach the pleural surface and are thus viewable [114].

Recent reports show that ultrasound for pneumonia detection may be superior to chest radiograph; sensitivity and specificity for the diagnosis of pneumonia using ultrasound were 94% and 96% [115]. Lichtenstein et al. used a combination of static signs (irregular boundaries) and dynamic signs (absence of a sinusoidal irregularity) to diagnose alveolar consolidation, as in pneumonia, with a sensitivity of 90% and specificity of 98% when compared to CT [34]. Using visible air bronchograms on mechanically ventilated patients, Lichtenstein et al. also showed 94% specificity in distinguishing between pneumonia from atelectasis for mechanically ventilated patients who would have appeared the same by chest radiography [116].

Ultrasound evaluation of pleural effusion is an established technique with excellent test characteristics [117]. Fluid is an efficient conductor of ultrasound waves and can be visualized on evaluation [118]. Ultrasound is also helpful before thoracentesis, since it can reveal septations, estimate the size of effusion, and localize optimal needle placement. Similarly to alveolar consolidation, pleural effusion has also been diagnosed on ultrasound by using a combination of a static sign (sharp borders) and a dynamic sign (sinusoidal irregularity) which provided a sensitivity and specificity of 93% [34].

For pneumothorax, Lichtenstein et al. published an approach to evaluating pneumothorax with ultrasound by evaluating the artifact created as the visceral pleura slide

against the parietal pleura [52]. A pneumothorax is represented as a loss of standard lung sliding seen in the healthy lung. A recently published review of eight high-quality studies found that overall, ultrasound had a sensitivity of 90.0% and a specificity of 98.2% for detecting pneumothorax [119].

Point-of-care ultrasound has been gaining traction within the medical community, and portable ultrasound that is relatively inexpensive has facilitated this increased usage. While extensive studies have been done on pulmonary diagnosis using ultrasound, its use requires years of training to detect the artifacts associated with lung diseases. Furthermore, the presence of dynamic images in addition to static signs for disease detection make development of machine classifiers for disease more complex.

Audible Shear Waves: Chest input

While compression waves are useful in determining the effects of short range inter-molecular interactions and essential to high-resolution ultrasound imaging, acoustic shear waves can provide information about the shear elasticity and viscosity of a tissue [120–122]. Large changes in shear wave speed caused by diseases affecting the stiffness of the lungs and other tissues can provide diagnostic information [122]. Previous studies have used the modulated radiation force of ultrasound or a mechanical shaker to create a harmonic force in frequencies ranging from 100 to 500 Hz to detect viscoeleastic properties in a phantom and a pig lung using a laser doppler vibrometer or ultrasound for detection [123–125]. Future studies investigating the generation of surface waves on the lung through the intercostal spaces would be particularly interesting.

Acoustic shear wave motion throughout the lung parenchyma can be imaged using

magnetic resonance (MR) elastography, a phase contrast MR imaging method [126]. Typically, an external vibration source applied to the chest is driven at frequencies on the order of 50 Hz. The shear wavelength and attenuation will be altered by changes in the lung mechanical properties. While MR imaging in general is particularly challenging in the lungs due to its heterogeneity and air content leading to lack of hydrogen (^{1}H) atoms (abundant in soft tissue due to its water content), a few groups have had some success in applying MR elastography to the lung using both ^{1}H [126, 127] and polarized rare gas isotope (^{3}He) MR imaging [128]. Measurable increases in lung stiffness have been observed in patients suffering from pulmonary fibrosis [129].

Shear wave motion can also be imaged via ultrasound. In this method, surface wave propagation is induced by an electromagnetic shaker and detected by an ultrasound probe. Zhang et al. were able to show the feasibility of this method in differentiating between interstitial lung disease (ILD) and healthy patients, observing higher wave speed in ILD patients [130].

3.3 Materials and Methods

In this section, we describe the design of the Tabla device from basic principles. Our design choices are intended to comply with the guidelines for a practical diagnostic tool for pneumonia set forth by United Nations Children's Fund (UNICEF) [131], summarized in Table 3.4.

Table 3.4: UNICEF design requirements.

Priority	Design Parameters
5 (high)	Ease of use, high accuracy
4	Long operational lifespan ($>$ 2 years)
3	Highly portable, low cost, reliable, safe, automated diagnosis, robust
2	Low training requirements, long battery life, low maintenance
1 (low)	Little to no familiarity with technology required

Different design requirements were assigned a numerical weight by UNICEF to communicate the importance of each parameter as judged by literature review, research, surveys and interviews. Adapted from [131].

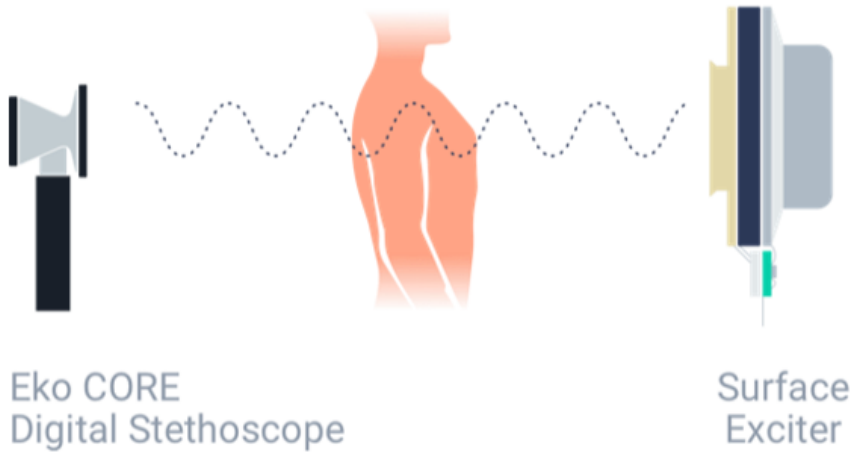

Figure 3.3: the Tabla system consists of a surface exciter which sends sound into the chest, and the Eko CORE digital stethoscope which records sound from the back

Approach and Statement of Contributions

The objective of this paper is to propose a quantitative alternative to the pulmonary physical exam that provides improved sensitivity and specificity, in addition to reducing interobserver error. The contributions of this paper are threefold. First, we propose diagnosing pneumonia by measuring the acoustics of the lungs with automated input and output devices. This has the dual advantages of improving the quality of the test (sen-

sitivity and specificity) and clarity of the results (reducing interobserver error). While previous work has focused on fully automated tests for pneumothorax [4, 12] or partially automated tests for pneumonia [21, 50], this approach is novel because it automates both input and output for detecting pneumonia and provides quantitative results. Second, we provide a small, easy-to-use prototype which follows design criteria set forth by UNICEF [131]. The device consists of an automated input unit which we constructed together with a commercial, off-the-shelf electronic stethoscope (see Figure 3.4). When a button is pressed, the input unit generates a 'chirp' signal and the vibrations on the back are recorded. A spectrogram of the recording is used to estimate the acoustic frequency response of the chest, which gives quantitative information useful for diagnosing pneumonia. Finally, we present initial clinical data with five patients collected under Institutional Review Board (IRB) study number 15-16814 at University of California, San Francisco Medical Center, and a proposed quantitative method of discrimination between healthy and consolidated lung tissue based on Mel-Frequency Cepstral Coefficients (MFCC) and spectral centroid features of the frequency response of the chest.

Principle of Operation

We chose to focus on an acoustic approach because the sensitivity and specificity of such systems in diagnosing pneumonia has been demonstrated (as mentioned in Chapter 1). This choice addresses the two primary design criteria of accuracy and reliability, and has the additional benefit of removing the radiation exposure inherent in methods such as the chest X-ray.

Much like the physician's hand and stethoscope in auscultatory percussion, our device

Figure 3.4: The Tabla device is placed on the sternum and the stethoscope is moved to different quadrants of the lungs to record audio data, which is transmitted via Bluetooth to a smartphone (not shown).

consists of two components: a sound source (actuator) and a sensor (stethoscope) (Figure 3.4). The actuator uses a surface exciter to send a sound wave with a frequency sweep from 50 to 1000 Hz into the chest. The stethoscope is placed on the back and records the sound waves transmitted through the chest. All patient data is collected and stored on a Health Insurance Portability and Accountability Act (HIPAA)-compliant server for later analysis with Matlab (R2017b, MathWorks, Natick, Massachusetts).

We initially experimented with a method analogous to regular percussion, sending the signal in on the same side as the sensor. Early prototypes are shown in Figure 3.5. Unfortunately, although this allowed for a compact design that could snap onto the stethoscope, the cross talk between the tabla device and stethoscope limited the extent to which the sound waves interacted with the lungs. We therefore decided to switch to a design mimicing auscultory percussion and sending sound through the chest.

Figure 3.5: Early prototypes of the Tabla device.

Previous work suggests that breath sounds in the frequency range 150–250 Hz provide vital information for pneumonia diagnosis (as discussed in Section **??**). Characterization of the cutoff frequency of normal lungs suggests that frequencies above 1000 Hz do not contain useful data [43, 50, 132]. Furthermore, fixed-input studies of pneumothorax suggest that an upper limit of 400 Hz is necessary to keep the signal-to-noise ratio (SNR) in an appropriate range [12]. We expanded this range to 1000 Hz for our human subject recordings without undesirable effects on SNR.

Actuator

The choice of actuator was based on several considerations: its size, which affects the portability, cost and comfort of the device; and its intensity at low frequencies as well as its frequency range, both of which affect the ease of use and reliability of the device.

We considered several types of actuator diagrammed in Figure 3.1, including piezoelectric transducers, push/pull solenoids, speakers, and surface exciters. The frequency range and power of each of the potential inputs was measured by its application to two different body parts: the knee, which is solid and provides a dull response; and the stomach, which is hollow and provides a resonant response. A comparison of each actuator type's performance on each of the UNICEF criteria summarized in Table 3.4 is provided

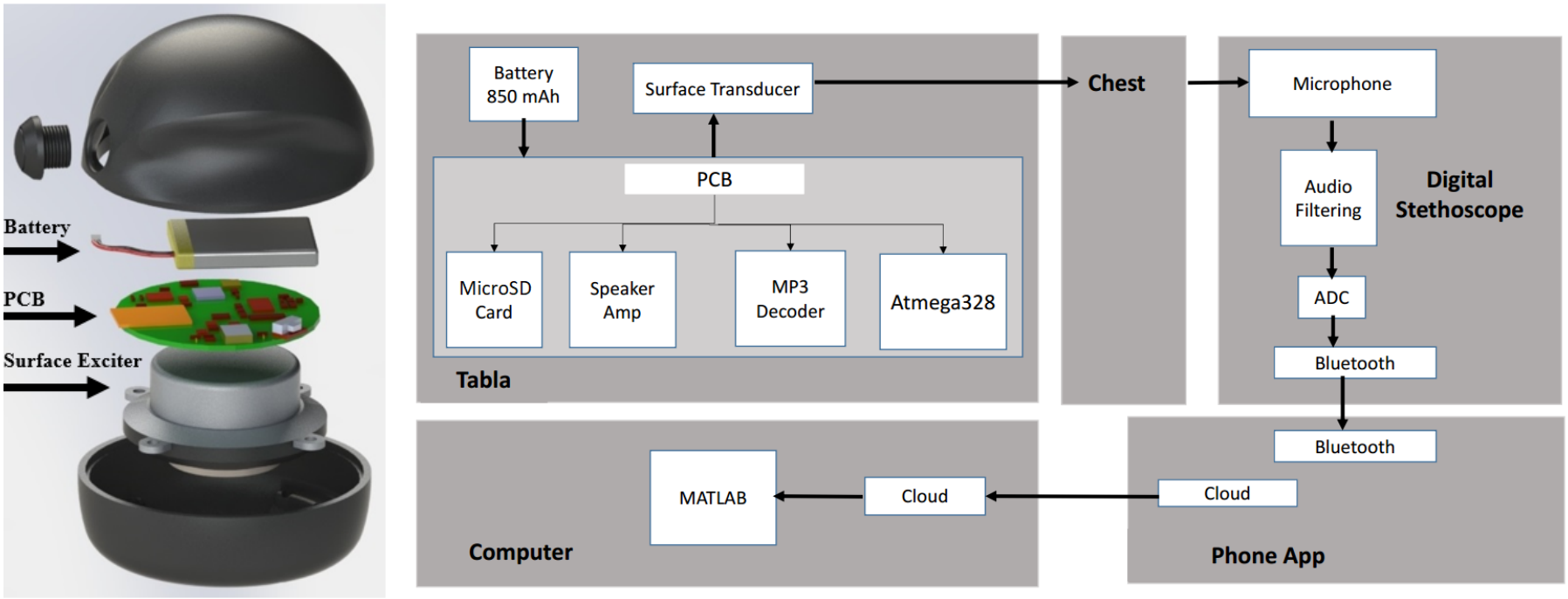

(a) Device assembly

(b) Block diagram of device

Figure 3.6: (**a**) The components of the device from top to bottom: 3D-printed plastic enclosure, button to start signal generation, Lithium polymer battery, printed circuit board (PCB), surface exciter; (**b**) the device prototype has four major components. Tabla transmits automated input into the chest and the Eko Core stethoscope (Eko Devices, Berkeley, CA) records output from the subject's back. The sound files are transmitted from the stethoscope via Bluetooth and recorded using a smartphone app; the data are then stored on the cloud, as described in Section 3.3. Figure from [133]

in Table 3.5.

Table 3.5: Actuator Pugh chart: Scored from 1 (low) to 5 (high).

		Actuator Choice			
Criteria	*Weight*	**Piezo**	**Solenoid**	**Speaker**	**Surf. Exciter**
Intensity	*5*	1	5	2	4
Portability	*3*	5	1	4	4
Cost	*3*	4	3	3	3
Battery	*2*	4	2	4	4
Weighted Score		40	41	39	**49**

Weights of criteria are determined from the design standards listed in Table 3.4. Intensity has the highest weight due to its effect on accuracy. Scores quantify relative performance with respect to each criteria, where 1 is the lowest possible score and 5 is the highest.

Piezoelectric transducers are compact and inexpensive, both desirable features; however, they did not produce a signal of measurable strength. Solenoids, in contrast, provided strong low-frequency signals, but are bulky and have high power needs, contributing to shorter device battery life. Bluetooth speakers have been developed to meet consumer market demand for low weight, small size, and long battery life. Despite being rated for use in the 20 Hz–20 kHz range, many handheld speakers cannot consistently generate frequencies < 100 Hz, which makes them inappropriate for use in this device. Surface exciters are a type of sound generator that are essentially speakers with no frame or cone; upon receiving an input signal, they vibrate an adjacent surface [134]. They are capable of consistently producing measurable sounds at frequencies as low as 50 Hz and are small enough to be incorporated in handheld devices. Based on these desirable characteristics, we chose to use a surface exciter (DAEX30 HESF-4, Dayton Audio, Springboro, OH, USA) in the design of the Tabla device.

As shown in the block labeled "Tabla" in Figure 3.6b, the actuator is driven by an am-

plifier circuit that uses MP3 data stored on a microSD card and processed by a VS1053B MP3 decoder chip (VLSI Solution, Tampere, Finland) controlled by an ATmega328p microprocessor (Atmel, San Jose, CA). The device has a handheld enclosure that contains the battery, surface exciter, and printed circuit board (PCB). This enclosure has a shell consisting of manufacturing-grade resins with the properties of injection-molded thermoplastics (Carbon 3D, Redwood City, CA, USA), designed using SolidWorks 3D CAD software (Dassault Systems, Waltham, MA, USA) and 3D printed via stereolithography with Carbon 3D (Carbon 3D, Redwood City, CA, USA).

MP3 Decoder

The VS1053b is a single chip Ogg Vorbis/MP3/AAC/WMA/MIDI audio decoder. It contains a high performance low-power DSP processor core, and working data memory, serial control and input data interfaces as well as a high-quality vairable sample-rate stereo ADC and stero DAC. It recieves its input bitstream through a serial input bus, which in our application is provided by the microcontroller via the SD card. The input stream is decoded and passed through a digital volume control to an 18 bit over sampling DAC. This allows the mp3 files from the SD card to be converted to an audio output that is fed directly into the amplifier circuit. The circuit for the MP3 decoder is shown in Figure 3.7.

Speaker Amplifier

Briefly, the amplification circuit consists of a Class-D audio power amplifier with volume control, dynamic range compression (DRC), and automatic gain control (AGC). This amplifier is a commercially available integrated circuit (TPA2016D2, Texas Instruments,

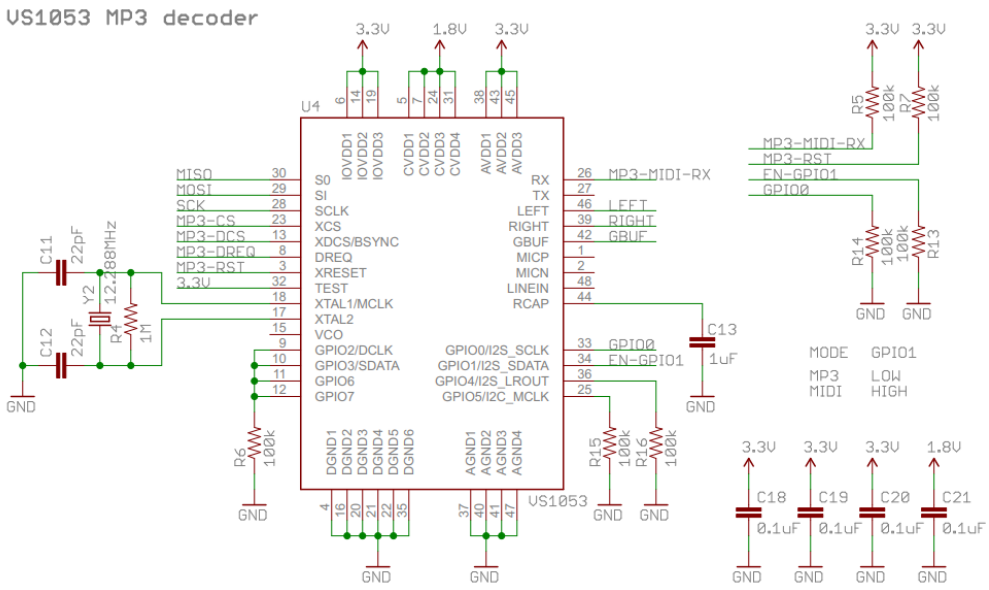

Figure 3.7: A commercially available MP3 decoder chip is used to decode the MP3 files from the SD card. The microcontroller coordinates this conversion. An external 12.28 Hz crystal is used to provide a clock signal to the decoder chip. This chip is driven by a battery power supply regulated to 3.3V.

Dallas, TX). The DRC and AGC function of the TPA2016D2 is programmable through a digital I2C interface. These functions can be configured automatically to prevent distortion of the audio signal. The gain can be selected from -28dB and +30dB in 1-dB steps, this is particularly important as finding the optimum level for chest transmission requires iterative testing.

The chip is capable of driving 1.5W/Ch at 3.6V into a 4Ω load which matches the specifications of the surface exciter and LiPo battery. The device also features independent software shutdown controls as well as thermal and short-circuit protection. These features make this chip ideal for cellular devices, PDA's and portable applications such as the Tabla device.

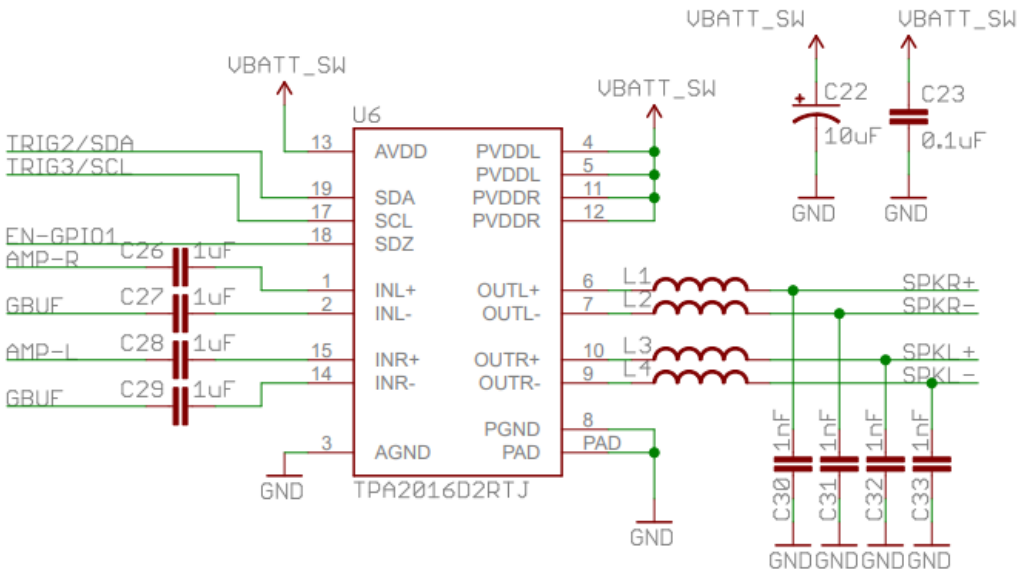

Figure 3.8: A commercially available audio amplifier front end amplifies the signal from the SD card, which is driven by a battery power supply regulated to 3.3V. The SPKR leads go to the surface exciter and the VBATT switches the power supply on and off for the amplifier.

Sensors

Like the choice of actuator, the choice of sensor was influenced by the UNICEF guidelines for devices of this type. There are a number of small digital stethoscopes on the market which provide high-quality data at a reasonable cost [135–137]. We compared different options and found that the Eko Core [136] stethoscope offers several features appropriate for our application. Notably, the Eko Core has a similar form to the traditional stethoscope and can function as a regular stethoscope if the microphone is turned off. In our initial product feasibility studies, we found familiarity of both form factor and procedure are important in increasing comfort with, and thus the adoption of, new devices among medical practitioners. Although the Eko Core was chosen for this study, other digital stethoscopes, such as the 3M Littmann (3M, Maplewood, MN) and Thinklabs One (Thin-

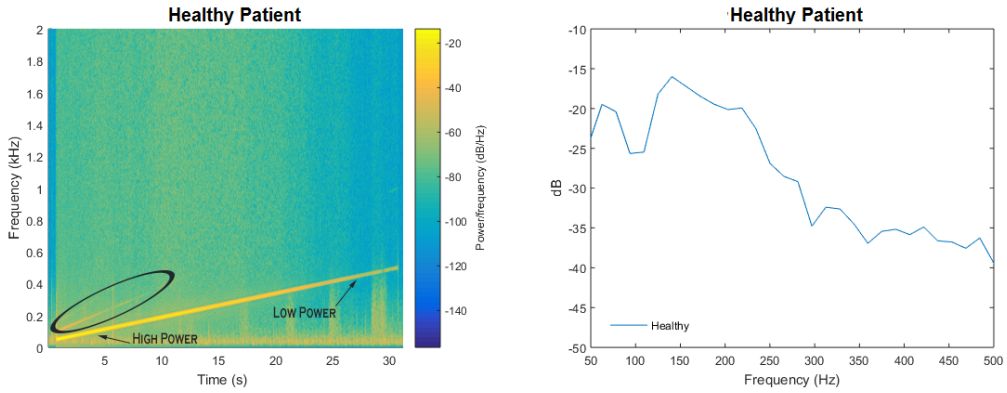

(a) Spectrogram (b) Transfer Function

Figure 3.9: (**a**) spectrogram of a chirp signal applied to the chest of a healthy subject. Resonance is represented by a bright spot, as indicated by the arrow on the left side of the figure. Along the line of the chirp, a comparison to a less-bright spot is indicated on the right; harmonics are indicated by the non-parallel lines (circled) above the chirp; (**b**) plotting power values along the line of the chirp yields a plot of the transfer function. Figure from [133]

klabs, Centennial, CO) should offer similar performance.

Wireless Bluetooth pairing of the stethoscope with a smartphone enables cloud storage of recorded data, facilitating its further use and analysis in telemedicine applications. In this proof-of-concept study, an iPhone 7 (Apple Inc., Cupertino, CA) was used for data collection; data were recorded locally and stored in the cloud (Figure 3.6b).

Signal

Considerations that influenced the choice of input signal were the ability to streamline information processing, which affects the ease of interpretation and training for users; and the ability to quickly assess the patient, which affects the time required for diagnosis.

There are a number of well-established approaches to system identification. The impulse response is a very brief, sharp input that most closely mimics the tapping of phys-

ical exams. Its main benefits are speed and uniform power distribution across frequency bands. However, because of its short duration, it requires a large signal to compensate for noise [138] and is very demanding of the actuator. The slow sine sweep uses slowly changing frequencies, which allow the system to settle to a steady state. The main benefit is a very high signal to noise ratio, but it takes several minutes to run the test. We chose to use a 'chirp', a sinusoidal signal characterized by rapid frequency change. This provides a balance between the slow sine sweep and impulse response, and has the added benefit that it is easy to automatically extract the transfer function.

We analyzed the data with a spectrogram, which is the result of performing successive discrete Fourier transforms within an overlapping time window to estimate signal power as a function of frequency and time. An illustration of the spectrogram is shown in Figure 3.9a. The transfer function is extracted by using power measurements along the line, which corresponds to the input chirp signal, shown in Figure 3.9b. The full test takes only 15 s.

3.4 Tabla System Load Testing

Before performing the clinical testing we performed load testing to determine the effect of different levels of pressure on both the Tabla device and the Eko Digital Stethoscope. We placed the device on a soft tissue phantom that is approximately 10 cm thick and measured the response on the other side using a noncontacting laser Doppler Vibrometer (LDV). In one case, the Tabla device was placed on the phantom, in the other two cases a force was applied on top of the Tabla device of 1.8 and 3.0 Newtons. The plots shown in Figure 3.10a show the frequency response of the Tabla device with the different amounts

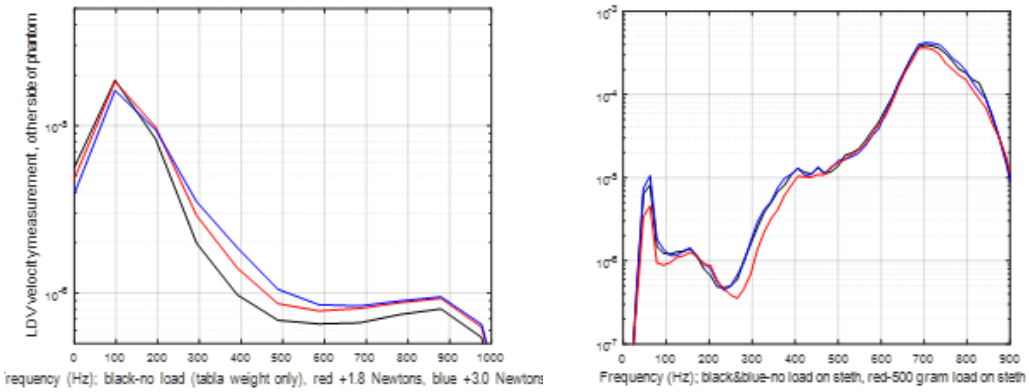

(a) Tabla Load Testing (b) Eko Load Testing

Figure 3.10: (**a**) frequency response of the Tabla device with different amounts of pressure applied; (**b**) frequency response of the Eko stethoscope with different amounts of pressure applied

of pressure applied. The stethoscope was also placed on a soft tissue phantom that has an embedded acoustic source that was driven with band-limited random noise. In one case, the stethoscope was placed on the surface, in the other case a mass of 500 grams was placed on top of the stethoscope. The plots shown in Figure 3.10b show the frequency response of the Eko Stethoscope with the different amounts of pressure applied. Although there is a small difference, the differences that we anticipate from structural lung changes should result in larger changes. To reduce this small difference as much as possible, the clinical protocol includes a specification on applied pressure to help standardize recordings.

3.5 Results and Discussion

In this section, we present and discuss several experiments performed with Tabla. In Section 3.5, we compare the measured acoustic properties of wet and dry sponges, which

share a similar density with the lungs [139]. In Section 3.5, we present results on the acoustic properties of the knee, which is composed of solid tissue, versus the stomach, which is hollow. Finally, in Section 3.5, we present preliminary clinical data collected at University of California, San Francisco (UCSF) Medical Center from five pneumonia patients and eight healthy subjects.

Water Filled Sponge vs. Air Filled Sponge

We use sponges as a bench-top model for pneumonia since they mimic the texture and density of the lungs [139]. Lung density normally ranges between 0.2–0.5 gm/mL [28]. A hydrophilated grouting sponge QEP 70005Q-6D (QEP, Boca Raton, FL, USA) was chosen for density comparable to human lung. When the sponge is dry, it is slightly lower in density than that of the lungs at 0.05 gm/mL. Our device was placed on one side of the sponge with the stethoscope placed on the other side. Next, the sponge was filled with water until an effective density of 0.6 gm/mL similar to the density of consolidation was obtained. A set of 10 measurements was taken for both the dry and wet sponge, and a mean was calculated.

The results are shown in Figure 3.11. For the dry sponge, we observe a resonant peak at 180 Hz and its first harmonic at 360 Hz, with higher frequencies being attenuated. The wet sponge behaves like a high-pass filter with decreased absorption of sound waves above 200 Hz; note that higher frequencies are less attenuated than in the dry sponge frequency response. These model findings are consistent with physical predictions that accumulation of water (which reduces acoustic mismatch) leads to improved transmission of higher frequencies. Specifically, the introduction of water led to an increase of

transmitted sound intensity at 500 Hz of approximately 40 dB.

Solid Tissue vs. Air-Filled Cavity Response

Solid areas of the body, such as bone, typically result in “dull” findings upon percussion [140]. Based on percussion data, the knee was chosen as a model for consolidation. The device was placed on the anterior portion of the knee, and the stethoscope placed on the posterior portion. Tympanic sound is found over air filled cavities, and represents the opposite extreme from ”dull” findings. Typical tympanic sound is found over the stomach, where percussion is commonly utilized to determine liver span [140]. The device was placed on the stomach and the stethoscope placed on the back; the findings can be seen in Figure 3.11. Note that, due to the increased thickness of the stomach, as well as the improved sound conduction of bone, the volume of the input signal was adjusted to compensate. Since we are concerned with frequency patterns rather than amplitude, this change should not interfere with our results.

The results are similar to the model system, with resonant peaks notable in the frequency response of the air filled stomach, and high-pass filter characteristics in the frequency response of the knee. For the stomach, resonant peaks can be seen between 200–400 Hz. However, frequencies above 400 Hz are filtered out. The response for the knee is similar to the wet sponge and appears to behave as a high-pass filter; however, the effect is less pronounced and begins to attenuate above 450 Hz. The measured increase in transmitted sound intensity of approximately 10 dB at 500 Hz is also less dramatic than in the sponge experiment, indicating that the difference between the stomach and the knee is less pronounced than the wet and dry sponges.

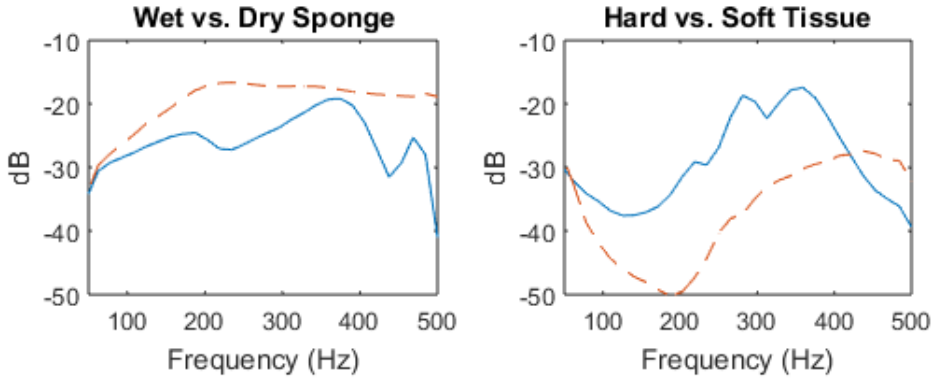

Figure 3.11: The frequency spectrum from 0–500 Hz for sound signals recorded for the wet (dotted line) vs. dry (solid line) sponge, and for the stomach (soft tissue, solid line) vs. knee (hard tissue, dotted line). Lines represent mean values from 10 consecutive measurements. The sponge experiment findings are consistent with physical predictions that accumulation of water, which reduces acoustic mismatch, leads to improved transmission of higher frequencies. The response for the knee is similar to the wet sponge and appears to behave as a high-pass filter; however, the effect is less pronounced and begins to attenuate above 450 Hz. Figure from [133]

Clinical Proof of Concept

Under an IRB-approved study at the University of California, San Francisco Medical Center, we have collected acoustic recordings from volunteer pneumonia patients using our prototype. At the beginning of the clinical examination, the patient was asked to sit up and the gown untied to ensure direct skin contact. Before recording began, each patient was asked to cough to clear their throat and then asked to breathe normally. For each subject, the device was placed over the manubrium, the stethoscope on the appropriate spot on the subject's back, and the input chirp signal applied. The stethoscope was applied at six locations on the back, corresponding to the different quadrants of the lungs. A 15-s sound recording was taken at each location to allow analysis for differences in sound transmission.

We obtained acoustic recordings from eight healthy subjects and five pneumonia pa-

tients, with several factors influencing inclusion in the initial study. The most important inclusion factor is that the patient had recently been diagnosed with pneumonia by chest X-ray. Healthy subjects consisted of individuals who did not have active respiratory symptoms or medical history of a confounding pulmonary pathology. The group of patients and healthy subjects were both restricted to English speakers between 18–85 years of age. The healthy group was 50% male with an average age of 27 ± 5. The patient group was 40% male with an average age of 72 ± 28.

Results from the left lower lobe of five pneumonia patients and eight healthy subjects are shown in Figure 3.12. The average frequency response was calculated from the left lower lobe recordings of the healthy subjects and pneumonia patients known to have left lower lobe consolidation. The range of frequency for the clinical data was expanded from 500 Hz to 1000 Hz; there is an overall decrease in power for the spectrum of the pneumonia patients, compared with the healthy subjects, that is most pronounced in the range of 100 to 300 Hz. Additionally, the resonance peak occurs at 148 Hz on the spectrum for healthy subjects, compared with 160 Hz for pneumonia patients. Due to differences between thorax size and pneumonia severity, specific spectral features vary between subjects.

3.6 Conclusions

Rapid prototyping was employed to develop a low cost, non-invasive acoustic device that uses frequency analysis to characterize structural changes in the lungs during pneumonia. Preliminary clinical results suggest that the frequency spectrum of pneumonia patients contains less power in the region of consolidation when compared with healthy

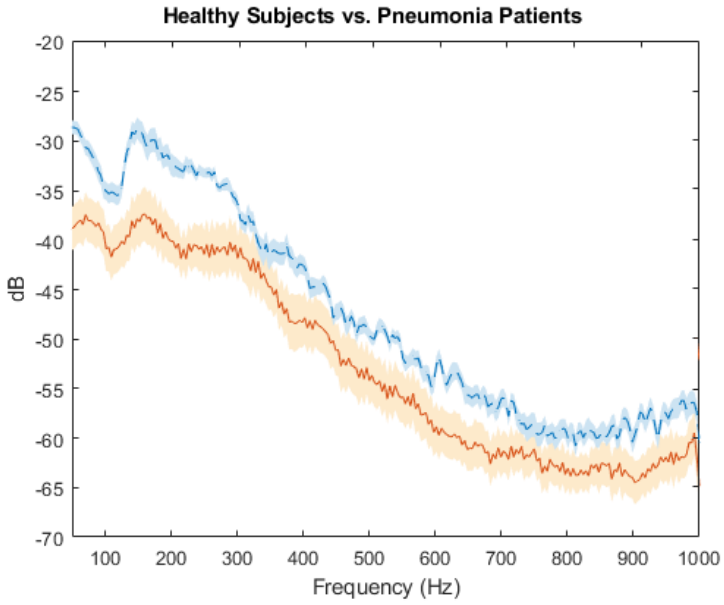

Figure 3.12: The frequency spectrum from 0–1000 Hz from the sound signal recorded from the left lower lobe of eight healthy subjects and five pneumonia patients, mean values are plotted for the pneumonia patients (solid line) and healthy subjects (dotted line) with standard error bars.

subjects. These data suggest that it is feasible to develop a low-cost diagnostic tool that uses acoustic analysis to aid in the pulmonary physical exam. Although these results are encouraging, there are limitations to this analysis. The recordings were collected from only 13 subjects, which prevented splitting the data into separate sets for training and testing and increased the risk of over-fitting. From a device perspective, shortening the length of the chirp input will be explored in order to gather recordings without the noise from patient breathing (apnea) and the trade-off for lower frequency resolution for shorter recordings will be investigated. Future work will explore the effect of clinical features such as age and gender, which influence thorax size and could therefore be confounding variables that affect the transfer function. By including these data as inputs, we anticipate

improved device performance. While our current focus is on the reliable diagnosis of pneumonia, the capabilities of our device could also be expanded to include detection of other pulmonary pathologies, such as pulmonary edema, chronic obstructive pulmonary disease, and atelectasis.

Chapter 4

Signal Processing and Analysis

Analysis of sound transmission in the chest cavity suggests that the chest, overall, acts as a low-pass filter absorbing higher frequencies as sound travels through it [17, 27, 28, 43, 50, 55, 57]. Spectral characteristics are affected by structural changes in the lungs caused by fluid or air accumulation, and can be studied and/or recognized using different techniques and classifiers in both the time and/or frequency domain.

4.1 Frequency range for analysis

Frequency analysis of lung sounds have shown to be a useful classifier for patients for diseases such as pneumonia, emphysema, pneumothorax, and asthma [4, 23, 42, 44]. The frequency range considered physiologically important for nearly all heart and lung sounds is up to 2000 Hz [23, 85]. In various studies, frequency ranges of interest included 0–2000 Hz for breath sounds [20, 23, 36, 39, 41, 42, 89] or sound evaluated at the chest [32, 41]. For sound through the mouth, several studies have used a range of 50–1600 Hz [32, 55, 56, 58]. In general, frequencies above 100 Hz are used to eliminate significant noise from

the heart and muscle, as well as 60 Hz electrical interference [141].

Frequency ranges for specific diseases

Pneumonia is often associated with crackles, which in one study was found to have an average frequency of 300 Hz [24, 38]. In a separate study, pneumonia was found to have a decrease in frequency response [77]. Another paper in line with these findings suggests that 300–600 Hz is important for pneumonia due to changes in bronchial breathing [141]. One review paper suggests a median frequency of 230 Hz for lung sounds [38].

For airway obstruction pathologies, such as asthma and COPD, the dominant relevant frequencies lie below 400 Hz [23]. The median frequency of lung sounds has been reported to be higher in asthmatic patients (239 Hz) than in healthy individuals (206 Hz) [41]; Schreur et al. found a lower median frequency of 165 Hz in allergen-induced asthma patients [142]. Another study found that asthmatic patients had wheezes and crackles with an average frequency of 300 Hz, while COPD patients had only crackles at the same average frequency, supporting the relevant frequency range below 400 Hz [24]. Patients with asthma also had a higher proportion of time spent wheezing at inspiration (10%) compared to COPD patients (1–2%) with average frequencies around 130–140 Hz [38]. Analysis strictly based on wheezes and crackles may not be a reliable method for diagnosing COPD, as a review paper found that the number of COPD crackles can vary per patient, but have an average lower inspiration frequency (233–311 Hz) than crackles in asthmatic patients (329 Hz) [38]. Pneumothorax has also been found to be associated with a significant drop in sound amplitude from 400–600 Hz [12].

4.2 Analysis methods

Several analysis methods are used for feature extraction from recordings of lung sounds. These analysis techniques are critical for classification by extracting distinctive features of sound such as wheezes, rhonchi, stridor, etc., which can be found in the time domain, frequency domain, or the time–frequency domain. We discuss frequently used methods, such as statistical analyses for time domain; the transfer function, Fourier transforms, and mel-frequency cepstrum analysis for the frequency domain; and wavelet analyses and the autoregressive (AR) model for the time-frequency domain.

Statistical analyses

Statistical methods, such as distribution features, higher-order statistics, and cross-correlation, have also been used to characterize lung sounds. While these methods are useful in both the time and frequency domain, they are especially important in the time domain, as the frequency domain often lends itself to other powerful analytical methods described below. Analysis in the time domain can also elicit unique information from non-periodic signals, such as crackles. Traditional frequency domain analyses assume stationarity that cannot be applied to such adventitious sounds and does not account for changes throughout the respiratory cycle [69].

Distribution features such as mean, median, mode, and variance can be useful in characterizing breath sounds and creating a mathematical model, such as wheezes which have biomodal distributions [69]. Breath sounds, however, are often more closely modeled as non-Gaussian, random processes, making distribution features less useful [38, 69]. Therefore, higher-order statistics, which measure deviations from the normal distribution, can

be more useful. Higher order statistics including skewness and kurtosis, have also been utilized for breath sound analysis [38, 69]. Notably, kurtosis is a sensitive but not very specific measure; a few outliers can heavily influence its value. This characteristic has been used in detecting the presence of crackles [69].

Cross-correlation is another useful method for analysis in the time domain, and works by detecting similarities between two signals. This has been used in previous studies to analyze the time delay of sound traveling through the parenchyma with multi-sensor arrays [51, 91], which can facilitate understanding of sound wave speed/propagation through the lungs, including changes that relate to different diseases.

Calculating sound intensity has also been used to produce images; notably, application of multi-sensor arrays to calculate intensity has been shown to be useful in both localizing the signal and understanding its timing in the breathing cycle [20, 31, 46]. An envelope can be used to represent the acoustic energy for each sensor to provide an acoustic heat map of the lungs [97, 143]. A Hilbert transform can be utilized to calculate this envelope of the acoustic signals to provide a measure of sound intensity [46].

Discrete Fourier transform

The Fourier transform (FT) is the most commonly used spectral analysis technique to calculate the frequency content of a signal [37, 40, 47, 49, 143]. The discrete Fourier transform (DFT) is a type of Fourier transform that is used to analyze discretely sampled data, such as digitized lung sounds. The DFT takes a signal from the time domain to the frequency domain, but operates on an assumption of stationary data over a time period. The short-time Fourier transform (STFT) sacrifices frequency resolution in order to keep the time

window short and more accurately track nonstationary signals [144]. The Fast Fourier transform (FFT) is an efficient algorithm used to calculate these Fourier transforms [145]. Different lung pathologies yield different sounds observed at the chest, such as wheezes and crackles, that contain different frequency ranges. Analysis of frequency range content and duration can be useful in distinguishing between diseases. Several studies have used different Fourier-related transforms to produce spectrograms or power spectral density (PSD) functions [47, 48, 146].

Frequency response function (FRF)

The FRF, which can be calculated a few different ways, is essentially the ratio of the DFT of an output signal to the DFT of an input signal. It assumes the input signal is well-defined or measurable. Analysis using FRFs involves examining the amplitude or power of a signal that is transmitted from the input to the output within a range of frequencies. Several studies have utilized the FRF to understand the physics of the lungs, notably the ways in which sound is transmitted through the varying geometries in the parenchyma at different frequencies, and which frequencies become attenuated [12, 19, 29, 32, 57, 77]. Specifically, the FRF can change with different conditions, such as pneumonia, due to changes to the geometry of the lung, which cause it to transmit or attenuate sound differently [47]. Several studies have used the FRF to detect excess fluid in or around the lung [77, 147–150] and pneumothorax [12].

Mel-frequency cepstrum

Similar to the DFT, mel-frequency cepstrum analysis is useful for feature extraction from audio signals. They closely follows the mel scale, which approximates the human hearing range [36]. This technique is commonly used in music information retrieval (MIR) to sort through different music types [151]. MFC is implemented using DFT coefficients that are filtered through the mel scale. The features extracted from MFC, outputting mel-frequency cepstrum coefficients (MFCC) that can then be fed into different classification schemes for automated lung sound analysis [36]. MFCC has been widely used in speech recognition and lung sound analysis in recent studies [36, 54, 62, 149, 152–156].

Wavelet and Hilbert–Huang transforms

Due to the non-stationary and non-periodic nature of breath sounds, the Fourier transform alone is insufficient to capture important time-domain characteristics of the signal [22, 157]. Using the wavelet transform (WT), partial time and frequency information can be utilized to help more accurately characterize the signal by means of windows of variable size [22, 144, 158]. Wavelet transforms focus on particular frequencies by applying successive high- and low-pass filters without the need to know a frequency range in advance [22]. Another method for modeling lung sounds this way is the Hilbert-Huang transform (HHT), used to extract oscillating components in the time-domain, which can be useful in determining characteristics of different lung sounds such as crackles [38], or denoising.

Several different wavelet transforms exist each with a different set of wavelet filters and characteristics [144, 159]. The Meyer wavelet filter, in particular, has been shown to

be successful in characterizing COPD and asthma by enhancing the signal of interest and allowing the use of cross-correlation and thresholding for detection [22]. Furthermore, the use of wavelet-based features has been proved effective by the work of Kandaswamy et al., who reported a classification accuracy of 100% of the type of adventitious sounds for the training set using wavelet decomposition and ANNs [144]. Other studies have also shown the applicability of WT in analyzing lung sounds [158].

Autoregressive (AR) modeling

Autoregressive (AR) modeling, also known as linear predictive coding (LPC), is particularly useful for time-varying signals. By assuming that each sample can be represented by a linear combination of previous samples [62], the model yields an output dependent on the bases given by the previous samples, scaled by stochastic predictor coefficients. Intersubject and even intrasubject variability with respect to microphone and utterance can lead to poor predictor coefficients with high error, but a previous study suggests that the use of AR with a moving-average (ARMA) model minimizes this variability [50]. Studies have utilized the AR model to estimate the power spectral density function [44, 50], basic feature extraction [160, 161], and extraction with reduced computational complexity [162].

4.3 Classification algorithms

When used in tandem with pre-processing techniques, classification algorithms have proven useful for automatic detection of adventitious lung sounds and/or diagnosis of

lung pathologies. In this section, we discuss the major classification algorithms that have been implemented with promising results.

Support vector machines (SVM)

The support vector machine (SVM) classifier is a kernel-based supervised learning algorithm particularly useful for binary and/or non-linear classification. Training SVM classifiers involves building a model, mapping a decision boundary for each class, and defining a hyperplane that separates the classes [36, 163]. Increasing the hyperplane margin, thus increasing the distance between the classes, helps improve classification accuracy. Only a few studies have implemented SVM for breath sound classification [163, 164]. Palaniappan et al. utilized SVM in order to classify healthy, pathological, and airway obstruction sounds, achieving a mean accuracy of 90.77% [36], but also showed that the k-nearest neighbors (KNN) algorithm was superior to SVM for generalization and classification [23]. Serbes et al. noted that improved pre-processing techniques boosted classification, with a maximum classification accuracy of crackles at 97.20% [159].

K-nearest neighbors (KNN)

K-nearest neighbors is an instance-based classification algorithm that has been used in several studies to classify recorded signals into different abnormal lung sound types [45, 49, 54, 149, 152, 160, 161]. The algorithm is trained on a data set, compressing the data into representative cluster centers for each abnormal sound; newly recorded data is mapped onto the same space, and the algorithm finds the K nearest neighbors, or data points, as measured by Euclidean distance [152]. The majority cluster center represented by these

neighbors corresponds to the class of the abnormal sound the data resembles. Rao et al. showed superior classification accuracy for pathology using KNN compared to Gaussian mixture models (GMM) and ANN [54]. Furthermore, for COPD specifically, using FOT measurements and utilizing KNN, SVM, and ANN showed consistently superior classification for KNN with an accuracy of 93–95% [165]. A study also comparing various pre-processing techniques in both KNN and SVM showed consistent superiority for KNN [149].

Artificial neural networks (ANN)

Neural networks have been used in several studies to automatically classify lung sounds, often yielding promising results [15, 40, 47, 109, 144, 146, 155, 158, 162, 163]. The most common method for training ANNs is the backpropagation algorithm [109]. ANNs work by modeling complex relationships between inputs and outputs. The model is formed by an interconnected group of artificial neurons that learns by adjusting its connective weights using training data in order to more accurately represent these relationships with minimal error [162, 163]. Although ANNs are widely represented in the literature due to their ability to classify both linear and non-linear data with high accuracy, they require a large data set to avoid over-fitting [54, 164].

Gaussian mixture model (GMM)

Gaussian mixture models (GMM) are widely used for speaker identification or verification [153]. Similarly to KNN, training data is used to obtain sound classes, which are represented by a GMM. Newly recorded data is mapped onto the same space and com-

pared to each GMM, with the final classification based on the highest maximum likelihood (ML) criterion [153, 166]. Several studies have used GMMs to classify lung sounds [62, 153, 154, 166]. Bahoura et al. showed superior sensitivity and specificity using MFCC combined to GMM to classify normal versus wheeze sounds compared to autoregressive methods with KNN and wavelet transform with ANN [62]. Comparatively, Mayorga et al. showed promising accuracy for crackles due to its characteristic frequency peaks [166], which contributed to a more robust GMM due to higher variance and distinctive mean. However, wheezes, crackles, and asthma-related signals performed poorly due to less defined or complex signals that could be improved with a larger dataset including different measurement locations and age groups and/or focus on a specific frequency band.

Other methods

The use of several other classification algorithms for lung sound analysis, such as fuzzy logic and hybrid algorithms, has been documented in the literature. Fuzzy logic has been used to score the severity of certain pathologies such as asthma and COPD based on variables acquired by the physician and the patient, such as coughing frequency, forced expiratory volume, or frequency of missing school/work [167]. This system allows the combination of acoustic variables such as IOS measurments of acoustic impedance with clinical variables to reach a classification decision. Badnjevic et al. combined fuzzy logic with ANNs, an approach they call a “neuro-fuzzy" system to obtain 99.41% classification accuracy for asthma patients and 99.19% classification accuracy for COPD patients, showing that a combination of methods can yield better accuracy [15]. They furthered the ANN-FL logic into an expert diagnostic system (EDS), yielding a sensitivity of 96%

and specificity of 98% in a prospective system [168]. Barua et al. were also able to achieve a high classification accuracy using ANN, but recommended further development to extract expert rules to obtain a human understanding of the network's knowledge. The authors suggested that obtaining these fuzzy logic decision rules could help create a more powerful hybrid neuro-fuzzy classifier, supporting the idea that hybrid algorithms yield superior classification [109]. In addition to superior classification, fuzzy-logic eliminates the black box nature inherent with ANNs, demystifying the logic behind its classifications, which is more user-friendly to doctors and upholds physician authority. Hybrid algorithms are a recent advance in classification methods and thus merit further study.

4.4 Methods

Approach and Statement of Contributions

The objective of this paper is to present an alternative to automated breath sound analysis that provides improved performance for lung pathology assessment. The key idea is to provide a fixed input signal to the chest, which sweeps across the frequencies of interest for analysis. By using a fixed input signal, we ensure that differences observed are purely a result of differences in the structure of the system being probed. This allows calculation of the acoustic frequency response of the chest and extraction of relevant features for classification.

The contributions of the paper are threefold. First, we present a noise-robust method of chirp signal tracking for acoustic system identification. Second, we provide a proposed set of classification features for healthy compared to pathological lungs, using both acous-

tic and clinical features for analysis. Finally, we present our classification results for the device and compare them to existing methods of breath sound analysis, comparing 216 recordings from six healthy subjects to 216 recordings from six patients. By using acoustic features to distinguish between these two groups, we achieved a classification accuracy of 92%.

Study Design and Subjects

The study was conducted at University of California, San Francisco Medical Center under approved institutional review board study number 15-16814. The study cohort consisted of patients with respiratory disease and healthy controls. The group of patients with respiratory disease consisted of English-speaking patients between 18–85 years of age who presented to the emergency department with a chief complaint of acute shortness of breath (dyspnea). Our study includes patients presenting with decompensated heart failure, chronic obstructive pulmonary disease (COPD), and asthma, the most common diagnoses among patients presenting to Emergency Department with a complaint of acute dypsnea and signs of respiratory distress [169]. The diagnosis of respiratory disease was provided by the treating physician, and was obtained from the medical chart for comparison. The healthy controls group consisted of individuals who did not have active respiratory symptoms or a medical history of confounding pulmonary pathology at the time of enrollment. All participants provided written informed consent prior to inclusion in the study.

Instrumentation

We used a hand-held acoustic device to emit a controlled audio signal into the chest [170]. The device consists of a lithium polymer battery, a printed circuit board (PCB), and surface exciter, all contained in a 3D-printed plastic enclosure. The signal is a chirp of uniform intensity that increases linearly from 50 Hz to 1000 Hz over a 14 second period. A 'chirp' signal was chosen to provide adequate power in each frequency band for analysis, and was based on preliminary studies with the device [138, 170]. For recording, we used the *Eko Core* digital stethoscope, which demonstrated a sufficiently flat frequency response in the frequency range of our analysis (50Hz–2000Hz)[136]. Since a fixed signal was used for both healthy subjects and patients, the transfer functions of the transducer and microphone were constant and did not contribute to differences between the two groups.

Table 4.1: Clinical features of healthy subjects and patients

Features	**Healthy Subjects**	**Patients**
Age	$27 \pm 5\%$	$54 \pm 12\%$
Gender	50% Male	50% Male
Height (cm)	166 ± 23	166 ± 8
Weight (kg)	72 ± 21	84 ± 20
Thorax Circ (cm)	95 ± 12	106 ± 10

Clinical features used to further refine analysis. Age, Gender, Height, Weight, Thorax Circumference were obtained from each subject.

Frequency Range Selection

COPD and asthma are highly prevalent diseases; both are associated with airway inflammation and obstruction, leading to air trapped in the lungs [171]. For asthma, the median

frequency of lung sound changes has been reported in the range of 240 Hz, while lung sound changes for COPD have been reported under 400 Hz [23, 41]. Heart failure and pleural effusion result in an analogous build-up of fluid in the lung tissue (parenchyma) and surrounding cavity due to leakage from the circulatory system. Diseases that result in trapped air and fluid lead to alterations in sound transmission due to the differences in acoustic characteristics of different media [28, 79]. The dominant frequency of parenchymal pathology ranges from 200 to 2000 Hz. Previous work investigating sound transmission in the chest cavity demonstrated significant attenuation at frequencies above 1000 Hz, suggesting an area of interest for analysis below this cutoff [28, 43, 50]. These frequency considerations led to the choice of stimulation frequencies between 50 to 1000 Hz.

Recording Procedure

The clinical study visit consisted of two types of audio recordings through the *Eko Core* digital stethoscope: percussion sounds and breath sounds. Recordings were obtained at six different locations: the right and left upper, middle, and lower lung fields. The recordings were taken from symmetric locations from the apices to the lung bases according to Bates' guide for physical examination [2]. Percussion sounds and breath sounds were each recorded in triplicate, leading to 36 recordings for each patient, each 15 seconds long. Percussion sounds were produced by the acoustic device, which emitted a controlled chirp held against the body of the sternum. Breath sounds consisted of recordings of the patient's respiration without the device. In additional to audio recordings, thoracic circumference and demographic data including age, gender, height, weight were

collected for each patient.

Audio Pre-Processing

Several pre-processing steps were performed to isolate the signal of interest. Each stethoscope recording was 15 seconds long; since the chirp lasted for 14 seconds, it was surrounded by periods of silence and low-energy background noise. Areas of silence are discarded when computing the features of the audio because certain features which rely on spectral energy would be adversely affected by their inclusion. To identify and crop the recordings to isolate the chirp, we used a sinusoidal model with sine tracking.

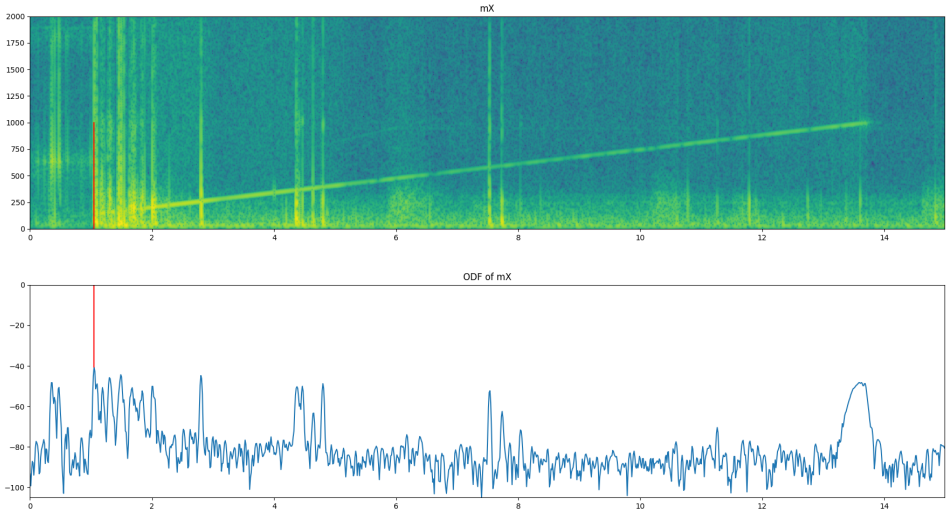

Figure 4.1: This ODF is tuned to detect acoustic events at 1000 Hz, unfortunately due to the presence of broadband noise, the largest peak at 1000 Hz does not occur at the end of the signal. This technique therefore is not appropriate for locating the end of the chirp.

An Onset Detection Function (ODF) is used to detect acoustic events, such as the onset of a certain frequency, in an audio stream [172]. In music information retrieval (MIR) ODFs are used to detect the beginning of a musical note or a percussion stroke. Typically,

ODFs will return a high value at the onset of an acoustic event of interest and are therefore typically well suited for chirp detection. We created an ODF to search for the end of the chirp and locate a peak of energy at 1000 Hz, as seen in Figure 4.1. Unfortunately, our signal contained broadband noise as seen in Figure 1 and it was essential that our algorithm be robust enough to detect chirp length with this noise. Due to the presence of broadband noise in the signal we explored an alternative processing technique, sinusoidal analysis.

Sinusoidal analysis approximates a signal with a sum of a finite number of sinusoidal with time-varying amplitude and frequency [173]. An input sound s(t) is modeled by

$$s(t) = \sum_{r=1}^{R} A_r(t) cos[\theta_r(t)]$$

where $A_r(t)$ and $\theta_r(t)$ are the instantaneous amplitude and phase function of the sinusoid, respectively. This model assumes that the sinusoids are stable partials of the sound and that each has a slowly changing amplitude and frequency. The sinusoidal model has several parameters that can be adjusted according to the sound being analyzed. Similar to the short-time Fourier transform (STFT), the sinusoidal model performs successive discrete Fourier transforms (DFT) by utilizing a moving windowing function.

Parameters were chosen specific to our stimulation signal. The size of our DFT was 2048 points, chosen to provide adequate frequency resolution for our sampling rate of 4 kHz. We chose the Blackman-Harris window because its main lobe includes most of the energy, which reduces the artifacts of windowing. For a chirp signal, the frequency continuously changes, which necessitates a shorter window. Thus, we chose a window size of 401 samples with additional points set to zero with zero padding. This window

was moved by a hop size of 50 samples to avoid artifacts that arise when the hop size is too large. For each frame of the STFT, the sinusoidal analysis identified the largest sinusoidal component. This sinusoid was tracked for the duration of the signal, and the time and frequency tuples were used to isolate the chirp, as seen in Figure 4.2. These parameter choices allowed the chirp to be isolated despite background noise and resulted in superior performance compared to standard methods of acoustic event detection which rely on energy changes between frames [172].

As a final pre-processing step, we applied a cross-fade (a 500 ms fade in and fade out), a technique used when the periodic timing of a signal is difficult to predict, in order to increase the fidelity of the DFT [174].

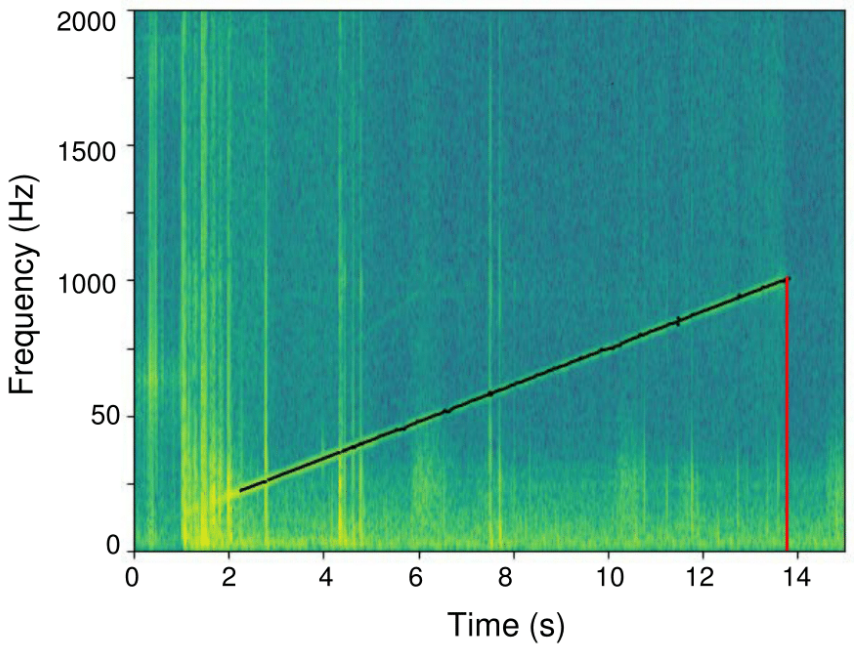

Figure 4.2: Sinusoidal modeling of the received signal results in improved chip isolation when compared with the standard onset detection. The model tracks the chirp and returns the value at 1000 Hz when the chirp terminates, shown here occurring at 13.8 seconds.

Frequency Principle Component Analysis

A three-component principal component analysis (PCA) was conducted on the spectra of chirp audio to determine which frequencies contributed most significantly to the variability between subject recordings. We used the FFT to find the power in the chirp within the range of 50 to 1000 Hz. We recorded the variability captured by each of the three principal components and examined which frequencies contributed most to these components. This analysis was completed at a resolution of 8 Hz. Our results were then compared to prior literature to determine if these frequencies corresponded to differences between healthy and diseased subjects.

Audio Features for Classification

From the processed data, we extracted specific features: the Mel-frequency cepstral coefficients (MFCCs) and the spectral centroid of the recordings. MFCCs are a set of coefficients that are commonly used in audio analysis to represent the frequency spectrum of a signal in a compact form [175]. The Mel scale approximates the human auditory system, giving higher weight to differences at lower frequencies. Since we are focusing on frequencies below 1000 Hz, this weighting is suitable for our analysis.

The spectral centroid is another commonly used audio feature that characterizes a spectrum by finding its center of mass [176]. It measures which frequencies are the most prominent across a signal by considering the spectrum as a distribution in which the values are the frequencies and the probabilities are the normalized amplitude. The spectral centroid provides a value for each frame of the signal; these values were then averaged to obtain the average spectral centroid value for the entire signal. The formula for calcu-

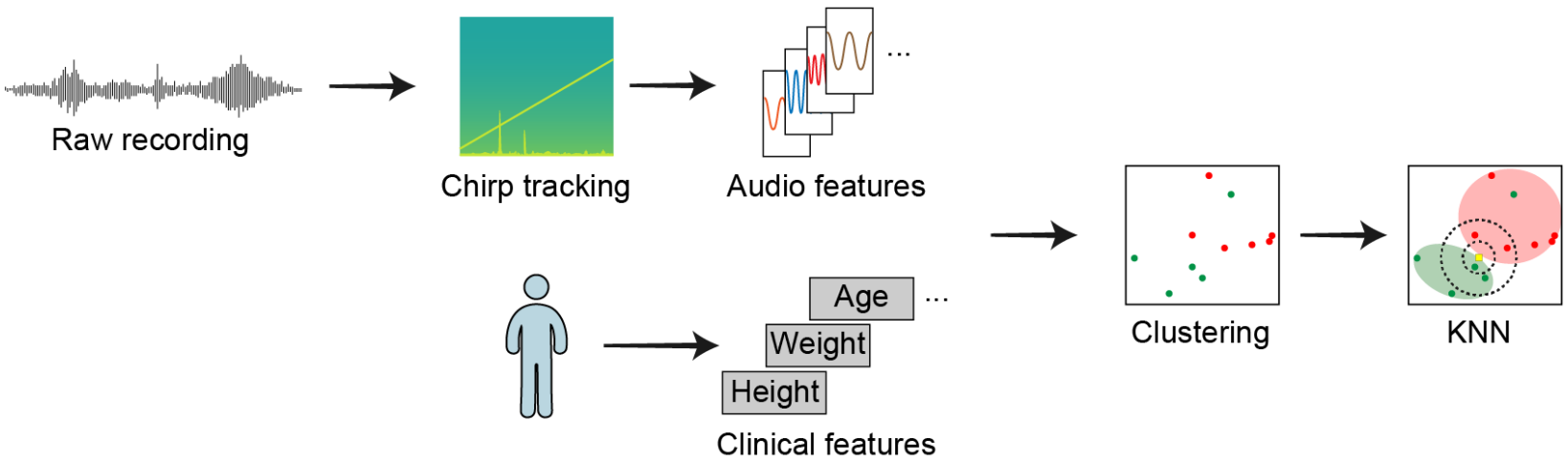

Figure 4.3: Block diagram of the data analysis process. Sounds were pre-processed using sinusoidal analysis to isolate the chirp. The audio was processed into acoustic features; other clinical features such as height and weight were recorded as clinical features. These features are plotted in the feature space to identify clusters. The feature vectors of sounds from the normal subjects are shown in green, while patient sounds are shown in red. Clustering of two example features (MFCC3 and MFCC8) from the total of 11 features are shown. The 11 features were analyzed using KNN to classify the sounds.

lation is shown below, where k is the frequency of the signal, l is the frame of the audio signal, $X_l(k)$ is the value of the DFT at point k for frame l, and N is the size of the DFT [176].

$$\text{Spectral Centroid} = \frac{\sum_{k=0}^{N/2} k \cdot X_l(k)}{\sum_{k=0}^{N/2} X_l(k)}$$

For each patient, we averaged the MFCC and spectral centroid values across three trials and six lung regions. An average was obtained because the lung pathologies tend to be diffuse processes affecting multiple lobes of the lung. The MFCC coefficents and spectral centroid value resulted in a set of 11 features to compare for each patient. The open source library Essentia was used to implement both the MFCC calculation and centroid calculation in Python [151].

Algorithmic Classification of Healthy or Diseased Lungs

We combined the audio features and patient features into a single feature set in order to classify the subject into the healthy or unhealthy classes; this process is illustrated in Figure 2. We used vector quantization to map our 11-dimensional vector to our 2-dimensional classification vector space [62].

We considered several vector quantization techniques including KNN, support vector machines (SVM), and gaussian mixture models (GMM) [177]. Although neural networks have been shown to produce a very high accuracy classification model for lung sounds [155], due to the size of our data set, the use of a neural network would most likely lead to over-fitting. The KNN algorithm has been demonstrated to be superior to SVM for breath sound (BS) analysis [23]. We performed a comparison of the three classification

techniques using the percussion sounds (PS) generated by the device. Our comparison of KNN, SVM and GMM also demonstrated superior accuracy for the KNN. These results together with KNN's improved interpretability versus GMM, led us to use KNN for our analysis.

The KNN algorithm was used to classify the feature set for each patient as either healthy or unhealthy. KNN classifies participant lung health by choosing the majority class of the K most similar patients. In this case, similarity is determined by the euclidean distance of audio and clinical features between patients. The K value refers to the number of 'neighbors' to query when assigning a point to a class. For the analysis, K values were compared across 1, 3, 5, and 7. Since the algorithm takes a majority vote of the closest neighbors to assign a class, even values of K are not used to prevent a tie during the vote. A value of 1 indicates that any point is assigned the class of its closest neighbor, although this value often leads to 100% clustering, it is susceptible to over-fitting. Higher accuracy at lower K values can be interpreted as more densely correlated classes; higher values of K can help account for more noise in the data as more data points are considered to assign a class.

4.5 Results & Discussion

We obtained acoustic recordings from six healthy subjects and six patients with lung disease. We first performed a three-component PCA analysis on the 50-1000Hz range of the spectra of chirp recordings. The three principle components accounted for 60, 12, and 5 percent of the variation among spectra. The 830-860Hz range contributed most significantly to the first component, while the 230-260Hz range were the most significant

Table 4.2: KNN with and without Clinical Features

Features	K = 1	K = 3	K = 5	K = 7
PS	100%	91.7%	66.7%	66.7%
PS + Clinical	100%	91.7%	91.7%	66.7%

The percussion recordings using the device, percussion sounds (PS) are evaluated with and without clinical features. The clinical features improve performance for the higher K values of 3.

frequencies in the second component. We used MFCC audio features, spectroid audio features, and patient clinical features processed with the KNN clustering algorithm to classify healthy and diseased lung states.

Our preliminary frequency analysis indicated that the frequency of greatest variability occurred in the 830-860 Hz range as well as in the 230-260 Hz range. The 230-260 Hz range variability lines up with previously reported frequency changes in asthma of 240 Hz [41]. The high level of variability at the 830-860 Hz range could be explained by changes in parenchymal fluid in heart failure and pleural effusion reported to be in the range of 200 to 2000 Hz [23]. However, due to this wide range, further investigation is needed to discriminate the frequency differences for specific disease states. This PCA result suggests that the presence of structural lung disease leads to detectable alterations in the sound transmission across the chest. Additional spectral characteristics such as MFCC and spectral centroid provide more generalizable information about the changes in acoustic transmission.

The accuracy of lung health classification from the controlled audio signal was tested across 12 patients and a variety of values of K for the KNN algorithm. Our highest classification accuracy was 91.7%, obtained by using the features from our acoustic device and the clinical features of each patient. Using our classifier on the recordings resulted in just

a single misclassification out of 12 subjects.

From Table 4.2, comparing the KNN classification accuracy obtained from just PS features and PS features combined with clinical features, we can see that the inclusion of clinical features improved accuracy when $K = 5$ from 66.7% to 91.7%. This aligns with the notion that these clinical features provide valuable information when classifying signal transmission. Sound transmission through the thorax is affected by the size of the chest which contributes to variability between subjects; by including thorax circumference and other clinical features we improve our classification accuracy.

Table 4.3: KNN between percussion sounds and breath sounds feature set with Clinical Features

Features	**K = 1**	**K = 3**	**K = 5**	**K = 7**
PS	100%	91.7%	91.7%	66.7%
BS	100%	75.0%	66.7%	66.7%
PS+BS	100%	75.0%	75.0%	58.3%

The percussion recordings using the device, percussion sounds (PS) are compared to the recordings of breath sounds (BS) from the patient. PS sounds can be seen to provide higher classification accuracy than BS.

From Table 4.3, we can see that classification using PS features outperformed classification based on BS features when $K = 3$ and $K = 5$. Not only did the PS features perform better, the introduction of BS features with PS features hindered classification accuracy when $K = 5$ and 7 compared to the PS features alone. Providing a controlled audio input across patients provides a cleaner signal than breath sounds which vary between patients and between trials. Furthermore, inclusion of BS appears to add noise to the system, reducing the accuracy of the KNN algorithm. The improved performance therefore motivates the use of a standardized audio signal rather than breath sounds for acoustic

analysis of lung fluid.

There are limitations to this analysis; the recordings were collected from 12 subjects, which prevented splitting the data into training and testing sets and increased the risk of over-fitting. Despite this limitation, because the clustering was performed identically for both the PS and BS features, the risk of overfitting would apply equally to both data sets. An additional limitation is the difference in age between the control group and the patient group. Future studies to control for age related lung changes will require a larger patient cohort with age matched controls.

This work also prompts further study of lung disease-specific classification to distinguish between respiratory conditions and to aid in differential diagnosis. Extending our analysis to allow for localized classification could be particularly helpful in conditions such as pneumonia, tuberculosis, or lung cancer, which can affect individual lobes of the lung. Larger disease-specific studies provide an opportunity to improve classification accuracy as different diseases lead to different structural changes. Another area of interest would be to measure changes in audio features over time, as a patient's clinical course and corresponding fluid buildup or trapped air in the lungs worsens or resolves. This has particularly relevant applications in respiratory conditions such as congestive heart failure, and could allow physicians the ability to monitor lung fluid status, reducing heart failure exacerbation and costly hospital admissions.

4.6 Conclusion

In this analysis we demonstrated that the presence of structural lung disease leads to detectable frequency differences using an PCA analysis of the frequencies from an FFT

of the recorded signal. KNN clustering of standard MFCC and spectroid audio features extracted from the recordings resulted in successful segmentation of healthy and pathological cases. Furthermore we demonstrated that classification of the standardized stimulation features outperforms classification based on breath sound features. This may be due to the amount of variability in breath sound recordings and is evidence toward one of our initial assumptions: a controlled, patient-independent input signal provides the most robust classification features. Future work will focus on collecting more patient data from specific disease states and applying more flexible classification techniques such as neural networks to extract new and more complex patterns from its features.

Chapter 5

Designing Human Subject Studies

Collaboration between physicians and biomedical researchers is essential to successful implementation of clinical feasibility studies. This process begins with acquisition of IRB approval from the ethics committee of the University, or an independent company. One of the largest challenges is coordination between biomedical researchers, clinical researchers and providers in order to ensure patient safety and satisfy research project requirements. The results from the human subjects studies for this dissertation are presented in detail in 3 and 4. In this chapter, we briefly review the steps taken to expand this study from benchtop studies to clinical studies, and present the findings from this dissertation in the context of other human subject studies in the field.

5.1 Designing a Clinical Protocol for Medical Device Studies

Although the methods of obtaining IRB approval differ from institution to institution, crafting a clinical research protocol is pivotal to translating research goals into goals of a clinical study in order to prepare for a successful IRB application. One important consideration when creating a protocol is to frame a broad IRB, focused on patient safety while still allowing for several areas of investigation. Our IRB covers the investigation of pulmonary pathology, so therefore, in addition to investigating pneumonia we have explored applications of the device to other pulmonary diseases such as Asthma and cardiogenic pulmonary edema secondary to congestive heart failure (CHF). The details of writing a clinical protocol are outlined in [178], however, we present several sections of the protocol for our pneumonia study to provide a framework to understand this process. The methods section, which contains the epidemiological design of the study as well as inclusion and exclusion criteria for patients. The measurements section is particularly interesting. The language of clinical research prefers the use of singular categorical or numeric variables for predictor and outcome variables. This is considerably different from engineering which has a much larger variety of data structures and methods of data visualization. It is however quite similar to format of feature vectors for classification problems. Although it may be challenging to represent the data from the device with a single variable, this method does allow for statistical estimation of the scale of clinical study needed for verification. The statistical calculations section helps to estimate the size of the clinical study needed to help provide a scope for the study. The quality control section describes how the quality of the clinical study will be maintained. This is particularly important as the

person collecting the clinical data is often different from the biomedical researchers and clinical researchers.

Methods

Study Design – Early in development of a diagnostic test, case control studies help to evaluate a test for its ability to distinguish between subjects with clear cut disease and healthy controls [12]. For our initial study we have therefore chosen to do a case-control analytic study, which will allow for further evaluation of the effect size of interest for future studies. The participants will have recordings taken during a 20 to 40-minute session. Measurements include electronic stethoscope recordings taken at six locations on the participant's back. The acoustic recordings will be processed to generate a mean "chest frequency response" value to compare measurements for pneumonia patients and healthy controls; therefore, it is an analytic and not a descriptive study. This is a preliminary observational study; no intervention or treatment is being given.

Study Participants – This study is part of a larger pilot study intended to utilize chest acoustics to help diagnose lung pathology. One of the primary aims of the parent study is determining the characteristic chest frequency response of pneumonia, CHF, and asthma. For the purposes of this smaller study, only pneumonia patients and healthy controls will be evaluated. Inclusion criteria for pneumonia patients include: age 18-85, evidence of lobar consolidation on chest x-ray, and ICD-10 diagnosis code for pneumonia. Inclusion criteria for healthy volunteers include: age 18-85, non-smoker, and no confounding medical history (e.g. lung pathology, heart pathology, cancer). Exclusion criteria for both groups include: participants that cannot understand English, are critically ill such that

participation would be dangerous or uncomfortable, and those with decreased decision making capacity.

Measurements

Another major decision point for a clinical study is the choice of which variables to focus on. For a diagnostic device, the predictor variable is the gold standard for diagnosing the disease and the outcome variable is the output from the device. Since clinical studies are challenging to conduct, other variables are collected to allow for additional investigations within the same clinical study.

Predictor variable: presence of lobar consolidation on chest x ray and ICD 10 diagnosis. Regionally isolated to: Right Upper Lobe (RUL), Right Middle Lobe (RML), Right Lower Lobe (RLL), Left Upper Lobe (LUL), and the Left Lower Lobe (LLL). In addition to the diagnosis, several predictor variables of interest will be collected from the patient including: age, gender, height, weight, and thorax circumference. The values for these measurements will be obtained by direct reporting from the patient, direct measurement and chart review. We will also restrict measurements to under 24 hours after the latest chest x-ray showing lobar consolidation since antibiotics will gradually improve the infection altering the acoustic signature.

Outcome variable: Change in chest frequency response, as determined through frequency analysis of the electronic stethoscope recordings.

Candidate covariates:

- Thorax circumference (in mm)
- Age (in years)

- Gender (female or male)
- Comorbidities (atelectasis, pleural effusion, lung fibrosis, pneumothorax, COPD, CHF)

Statistical Calculations

Because this is a pilot study designed to test feasibility and lead to preliminary results upon which a larger, more formal study will be based, the sample size can be set to the parameters of the study five pneumonia patients and eight healthy volunteers. From this starting point, better estimates of effect size can be calculated. A theoretical calculation of the sample size can be made based on studies of pneumothorax, a disease which effects chest frequency response in similar magnitude.

Our hypothesis is that the mean chest frequency drop is different in pneumonia patients than in healthy volunteers. The null hypothesis is that the mean chest frequency drop recorded is the same in pneumonia patients as healthy volunteers. Since the predictor variable is dichotomous (pneumonia vs. healthy) and the outcome is continuous (frequency level in decibels), we would want to use a test similar to the t-test to analyze our results. Although chest frequency response has not been obtained in pneumonia, studies in patients with pneumothorax are likely to have the opposite effect on chest frequency response as pneumonia and can be used as an estimate of effect size.

Standardized effect size was calculated from data in a recent paper by Mansy et al. [13] looking at the effect of pneumothorax on chest frequency response. Results were given in mean frequency drop in decibels. Pneumothorax was induced in patients as a normal part of a surgical procedure and measurements after pneumothorax induction

found a frequency drop of 8dB. We anticipate that the fluid accumulation in the lungs during pneumonia would lead to an opposite effect size of at least half this magnitude (i.e. 4dB). Using the calculator on "sample-size.net" for effect size given sample size utilizing the T-statistic and values (α=0.05, β=0.2, SD=2, N1=30, N2=30) we find that E=1.47, suggesting that the study has 80% power to detect an effect size of 3.5dB given a sample of five patients and eight controls. Given the effect size found in this experiment, we hope to motivate future larger studies investigating the link between pneumonia and chest frequency response.

Quality Control

Several measures will be taken to ensure quality control throughout this clinical study. Detailed coverage of this material will be assembled in an operations manual for the study. Clinical staff members will be trained in the use of the device and in the use of a case report form for data collection. In addition to device measurements, information on how each variable is measured will be included in the operations manual. Furthermore, certifications will take place on a monthly basis to ensure procedural integrity. For de-identified data management, a Google Drive spreadsheet will be used to provide flags for incomplete or out of range data entry. A quality control coordinator will check the spreadsheet weekly for compliance. During the study, individual meetings will be held weekly with each of the clinical staff. Furthermore, weekly staff meetings will be held with all members of the study. During recruitment of healthy volunteers, measurements will be compared across technicians to estimate inter-observer variability in device measurements.

5.2 From Bench to Bedside

Translational research refers to research which helps to turn studies that have been run in the lab into studies that can be run in the clinic. From a device perspective, this process can be assisted through the use of the software design life cycle which emphasizes iteration. A device can be made in a laboratory ensuring that all variables are controlled for and demonstrating the promise of a certain technique. The next step is to go to the end-users and ensure that a clinically-viable device, which satisfies clinical needs such as battery life, ease-of-use by staff, sanitation, and other important design metrics, can be constructed. Furthermore, a preliminary competitive analysis, market analysis and storyboarding of the main device use can help guide design. The storyboard for the device is included in this dissertation in Appendix A. At this point, design for manufacturing principles can be utilized to ensure that the cost of the device at scale will fall within an acceptable range. The cost of the individual devices can be reduced by utilizing 3D-printing instead of injection molding while in the early prototype phase. After assessing the performance of the device in IRB-approved studies, the Regulatory Path and Reimbursement Path must also be assessed. From an academic engineering perspective, much of the novelty is in benchtop and proof of concept data from patients. From a clinical perspective, large, randomized-controlled studies are the ideal for changing patient care. Designing cross-sectional, cohort or case control studies for medical devices serve as a middle ground in which greater attention must be paid to design of the devices for clinical use as well as quality assurance of the clinical protocol. Furthermore, providing open lines of communication between biomedical researchers, clinical research coordinators, and healthcare providers is essential to conduct an efficient study.

5.3 Human Subjects Studies

Respiratory diseases lead to structural lung changes that can be detected acoustically. The existence of such changes has spurred numerous studies utilizing both internal and external sounds to diagnose a variety of lung diseases. For the purposes of this review, we focus on pneumonia, asthma, COPD, pleural effusion and pneumothorax. We also include several miscellaneous studies with results that further elucidate different analysis methods. Table 5.1 summarizes human subject studies investigating acoustic changes in the diseases discussed in this review.

Acoustic detection of pneumonia and pleural effusion represents an important clinical need due to the high cost and radiation exposure of the gold standard chest X-ray (CXR). For example, the cost of deploying an x-ray machine in Northern India is estimated at $51,500 plus $5,900 per year to operate [7]. Several studies utilizing both internal and external sounds have been conducted to aid in pneumonia diagnosis. Three studies utilized multiple microphones to provide a sound map of the chest similar to a chest x-ray [20, 21, 95]. The highest reported sensitivity and specificity for pneumonia using this method was 70% and 80%, respectively [21]. Furthermore, inter-observer agreement for this method was high, with 80% agreement on the presence of an abnormality and inter-rater agreement of 90% [95]. Pleural effusion was detected with higher accuracy, with sensitivity of 95%, specificity of 88%, and 80% agreement on diagnosis compared to CXR [21, 94].

Another important clinical need is the ability to distinguish between pneumonia and atelectasis (lung collapse), a distinction chest x-ray cannot provide. Ultrasound has been used to rule out atelectasis with a specificity of 94% and sensitivity of 61% [116]. Breath sounds have also been analyzed for pneumonia patients with standard electret micro-

phones. In that study, 29% of pneumonia patients had wheezes, 29% had rhonchi and 87% had crackles [24]. The average frequency of the crackles which correlated most closely with diagnosis of pneumonia was found to be 300 Hz at inspiration and 285 Hz at expiration for pneumonia [24]. A more recent proof-of-concept study examining the use of external sound for pneumonia diagnosis utilized an external surface exciter with a linear chirp from 50–1000 Hz to detect pneumonia [77]. That study reported frequency changes between healthy and consolidated lung.

Discrimination between asthma and COPD also represents an important clinical problem, as current diagnosis is largely based on clinical observation. Quantifying the findings for these diseases provides a route for faster and more consistent diagnosis. The diagnosis of both asthma and COPD is based on signs of airway obstruction, causing COPD to be often misdiagnosed as asthma due to the overlapping symptoms [143]. One study, however, was able to differentiate between the two with 85% accuracy; its approach was based on dynamic images of lung activity acquired during a 12 second recording using an array of stethoscopes on the back [143].

Several studies on asthma have highlighted characteristics that could differentiate between the two disorders; one large study found that a majority of asthmatic patients had wheezes and crackles with an average frequency of 300 Hz, while a majority of COPD patients only had crackles with a similar average frequency [24]. An algorithm for wheeze peak detection was developed and tested on asthmatic patients with a sensitivity of 100%, 87.8%, and 71% for high, middle, and low flow rates, respectively, potentially allowing clinicians to diagnose asthma versus COPD based on the presence of wheezing episodes [179]. A study of asthmatic patients who had taken bronchodilator drugs showed a decreased in centroid frequency during forced expiration from 500 Hz to 200 Hz, suggesting

that the frequency characteristics of breath sounds can be used to detect response to treatment [44].

Similarly, studies have focused on the various acoustic characteristics present in COPD patients. In a study of COPD patients with a history of smoking, these individuals were shown to have larger peak signal amplitudes from 0–5 kHz when compared with healthy subjects [59]. This suggests a frequency range of interest for COPD detection. Furthermore, another study evaluated eleven different parameters to diagnose COPD, such as lead and lag time of inspiration at different locations and ratio of inspiratory to expiratory time; the authors concluded that all 11 parameters possessed differences between COPD and healthy patients that were statistically significant, suggesting that further study into these differences should be carried out [180].

The use of IOS, which measures lung function parameterized by airway acoustic input impedance, has also shown potential to differentiate asthma and COPD. In studies of COPD patients, IOS analyses showed changes in reactance are correlated with changes in airflow obstruction [107, 181], while another study using asthmatic children showed measurement of changes in resistance rather than reactance better indicated asthmatic patients [104, 108]. In spite of these promising results, a large 3-year clinical trial found that although IOS could differentiate COPD patients amongst healthy patients and determine the degree of severity of airflow limitation, measurement data from COPD patients was similar to that of healthy non-smokers. The authors concluded that IOS cannot yet replace spirometry but may instead prove valuable in distinguishing between different subgroups of COPD [60]. While IOS is a valuable tool, more portable acoustic methods of monitoring COPD patients for acute exacerbation, allowing patients to monitor their own health over time, have been demonstrated [182].

Similar to pneumonia, the current standard for diagnosing pneumothorax (PTX) includes radiography, which is both expensive and not readily available [13]. Several studies have examined changes in sound and frequency transmission due to the presence of air accumulation between the chest wall and lungs, which would affect how sound is transferred due to the existence of another interface. One study utilizing external stimuli found that a significant decrease in sound transmission and the power spectral density (PSD) function was evident using 400–600 Hz sound inserted at the mouth and measured over the chest [12]. In another study using an array of stethoscopes on the back, abnormalities of the pleural space were identified with a sensitivity of 100% and specificity of 87% [183]. Another study using ultrasound used the disappearance of lung sliding to represent the air pocket from PTX that causes the lung–wall interface to appear motionless [52]. This method had a sensitivity of 95.3% and specificity of 91.1%.

Several studies have investigated the broader question of how accurately lung pathology can be distinguished from healthy lung. Although this approach does not provide direct clinical benefit, it provides a foundation upon which future studies can build and demonstrates a variety of analysis methods and sensor technologies. Ultrasound has shown promise in prediction of consolidated lung, as well as for detecting fluid accumulation [53, 111]. One analytical method of interest is the use of MFCC coefficients combined with KNN to develop an automated method of extracting data from the frequency domain and classify the sounds into diseased and healthy categories.

Two recent studies utilizing this method demonstrated the use of this approach for breath sounds as well as external sounds. A 2015 study used a digital stethoscope to record lung sounds for classification of abnormal lung sounds achieving a classification accuracy of 91.3% [152]. A 2018 study extended this work to external sounds, using a

surface exciter placed on the chest and a digital stethoscope placed on the back, achieving a classification accuracy of 91.7% for distinguishing between healthy subjects and patients with lung pathology [54]. Finally, regular use of an array of stethoscopic measurements on the back has shown potential in preventative medicine, where it has been used to track the progression of lung disease in smokers. Changes in the intensity of breath sounds were correlated with pack-year history among smokers [184].

Table 5.1: Comparison of acoustic methods for lung disorder diagnosis

[Ref]	Sensor Type	(n)	Comparison	Results
		Pneumonia		
[21]	Contact microphone array	20	CXR	Study found that the system provided 70% sensitivity & 80% specificity in diagnosing patients with pneumonia without workup.
[20]	Condenser microphone array	5	CXR	Built a spatial representation similar to CXR, with high active area in lower lung corresponding to lung consolidation.
[116]	Ultrasound imaging	58	Fibroscopy or bacteriology	Evaluated the ability of ultrasound to differentiate between pneumonia and atelectasis. Dynamic air bronchograms were used to rule out atelectasis, with a specificity of 94% and sensitivity of 61%.
[24]	Condenser microphone array	122	Physician diagnosis	29% of symptomatic patients were found to have wheezes, 29% were found to have rhonchi, and 87% were found to have crackles.
[77]	Condenser microphone	13	CXR	Encouraging results from proof-of-concept study with eight healthy subjects and five lobar pneumonia patients.
		Pleural Effusion		
[21]	Condenser microphone array	20	CXR	Pleural effusion was detected with a 95% sensitivity and 88% specificity.

Cont. on next page

(Ref)	Sensor Type	(n)	Comparison	Results
[94]	Condenser microphone array	56	CXR, Ultrasound	Agreement of diagnosis via clinical assessment compared to CXR was 80%, and with ultrasound was 75%.
		Asthma		
[143]	Condenser microphone array	31	Spirometry	Found 81% and 74% accurate in differentiating between COPD and asthma; 85% overall accuracy when using quantitative data in addition to generated images.
[24]	Condenser microphone array	51	Physician diagnosis	59% of symptomatic patients were found to have wheezes, 27% were found to have rhonchi, and 65% were found to have crackles.
[179]	Contact microphone	16	Spirometry	An algorithm for wheeze peak detection and grouping to find episodes was used. The algorithm has a sensitivity of 100%, 87.8%, and 71% for high, middle, and low flow respectively.
[44]	Contact microphone	17	Spirometry	Patients with bronchial asthma who had taken bronchodilator drugs showed a decrease in centroid frequency after taking the drugs during forced expiration.

Cont. on next page

(Ref)	Sensor Type	(n)	Comparison	Results
[108]	IOS	132	Spirometry	While spirometry did not show significantly different results between asthmatic and healthy children, IOS indicated significant differences in resistance at 10 Hz and bronchodilator responses at 5 and 35 Hz.
[109]	IOS	41	Spirometry	An ANN achieved a generalized classification accuracy of 94.44% in detecting airway obstruction from asthmatic children using their IOS patterns and age, weight, and height demographics.
		COPD		
[143]	Contact microphone array	35	Spirometry	81% and 74% accurate in differentiating between COPD and asthma; 85% overall accuracy when using quantitative data in addition to generated images.
[24]	Condenser microphone array	94	Physician diagnosis	39% of symptomatic patients had wheezes, 26% had rhonchi, and 71% had crackles.
[59]	Condenser microphone	11	–	Discriminated between “normal" smokers’ lungs and the presence of COPD in smokers by noting peak signal amplitudes in COPD patients were slightly larger at frequencies from 0–5 kHz.

Cont. on next page

(Ref)	Sensor Type	(n)	Comparison	Results
[180]	Condenser microphone array	90	Physician diagnosis	11 parameters, including inspiratory/expiratory crackle rate and ratio of inspiration to expiration time, were found to be statistically significant in diagnosing COPD.
[107]	IOS	180	Spirometry	Measured reactance, particularly at 5 Hz, was shown to be correlated with forced expiratory values and changes caused by airflow obstruction.
[60]	IOS	2609	Spirometry, CT	IOS showed reduced impedance in COPD patients and could identify different subgroups of COPD patients based on severity. Data did not suggest IOS is an appropriate replacement for spirometry.
[182]	Condenser microphone	16	Hospital visit	Promising results in predicting acute exacerbation COPD (AECOPD) were reported.
[12]	Condenser microphone	19	Surgically induced	The occurence of PTX was associated with a drop in sound amplitude most noticeable in mid-frequency ranges (400–600Hz). Increasing the frequency further decreased amplitude due to increased tissue damping.

Cont. on next page

(Ref)	Sensor Type	(n)	Comparison	Results
[183]	Contact microphone array	14	CXR	Using dynamic breath sound distribution images generated from the VRI, diagnosing PTX had a sensitivity of 100% and specificity of 87%.
[52]	Ultrasound	43	CT, CXR	On the basis of lung sliding in ultrasound, diagnosis of pneumothorax had 95.3% sensitivity and 91.1% sensitivity.
		Miscellaneous		
[53]	Ultrasound	121	CXR	Ultrasound was used to find echographic comets to determine extent of extravascular lung water; significant correlation was found between ultrasound and CXR methods (r = 0.78).
[111]	Ultrasound	39	CXR	Sonographic air bronchograms (92.30%), fluid bronchograms (92.30%), and superficial fluid alveolograms (100%) were observed.
[152]	Condenser microphone	20	–	Using a stethoscope for recording and a condenser mic to upload lung sound data for processing, this study achieved 95% identification for normal lung sounds and 91.3% for abnormal sounds.
[54]	Condenser microphone	12	Physician diagnosis	A classification accuracy of 91.7% was achieved by analyzing a chirp signal inserted into the patient chest using MFCC and KNN.

Cont. on next page

(Ref)	Sensor Type	(n)	Comparison	Results
[184]	Contact microphone array	151	CXR, Spirometry, Auscultation	Smokers showed a significant reduction of vibrational energy compared to nonsmokers, particularly with increase in pack-year of cigarette smoking.

This table provides a comparison of different methods of acoustic detection for lung disorders. The lung disorder being detected is listed alongside the number of subjects in the study (n), the gold standard used for comparison and the major outcomes of the study. *CXR = Chest x-ray, IOS = Impulse oscillometry system, VRI = Vibration response imaging, COPD = Chronic obstructive pulmonary disorder.*

Chapter 6

Conclusions

Recent advances in acoustic monitoring for pulmonary diseases indicate the strong potential of these measurements to address a wide variety of clinical needs, in particular, providing quantitative metrics of lung health without the dangers and expense of radiography, and without the requirement for patient compliance associated with spirometry. In addition to these key advantages, acoustic monitoring also provides a route to telemedicine applications that can allow patients to be monitored outside of the clinic. Acoustic measurements can be taken with highly precise instrumentation, or with inexpensive sensors, making acoustic devices well suited for hospital-grade diagnostics as well as home monitoring of chronic diseases. Despite the rich potential of acoustic monitoring, the physiological origins of the signals should be studied further with greater standardization and larger scale human studies to ensure maximum interpretability of these signals. Finally, an extensive open database – not just for breath sound recordings but also featuring responses to external stimuli, processing tools, and even microcontroller code – needs to be made available. Such as database would truly expand the capabil-

ity of researchers to investigate these phenomena, apply them to their own studies, and establish techniques that can facilitate their translation into the clinic.

6.1 Automating the pulmonary physical exam

The pulmonary physical exam consists of several techniques designed to assess the health of the patient's lungs. These techniques include the analysis of both internal and external sound sources using a variety of methods. Each of these methods helps to detect different diseases and provides an encouraging alternative to more expensive methods of imaging, however, the qualitative nature of these techniques and differences in application of these techniques limits their clinical utility. The goal of this dissertation is to provide an automated method of assessing lung pathology and to review the current state-of-the-art methods for acoustic assessment of the respiratory system.

Transmission of sound into the respiratory system is a more recent method of acoustic analysis of the lungs. This dissertation explored the use of an external sound source to send sound of low frequencies (under 1kHz) into the chest in order to determine the effects of pulmonary pathologies on sound transmission through the thorax. Because fluid in the lungs changes the characteristics of sound transmission, the frequency response can be used to assess changes in the lungs. In this technique, a chirp with a frequency range of 50 to 1000 Hz was used to probe the thorax and assess sound transmission. After signal conditioning and computation of the frequency response, this method was presented as proof of concept for detection of lobar pneumonia. There are several advantages to an external acoustic signal, including non-invasiveness, lack of radiation, low cost, standardized input and simplicity.

In order to create a device which would fit seamlessly into the physical exam, UNICEF design requirements were consulted for the ideal characteristics of a low cost pneumonia detection tool. The device characteristics were optimized for signal-to-noise ratio, portability, cost, and battery life. Additionally, the device pairs with a digital stethoscope in order to leverage physician familiarity and improve interoperability. Furthermore, testing was conducted to ensure that the user differences in application pressure of the device did not have a large impact on the signal. After performing bench-top experiments on materials with density similar to the lungs as well as hard and soft tissue, this method was applied to patients with lobar pneumonia and to healthy volunteers. In an IRB-approved study at the University of California, San Francisco Medical center, data was collected from eight healthy subjects and five pneumonia patients. The frequency response was analyzed and plotted for the two groups. The results indicated considerable differences between the frequency response for pneumonia patients and healthy subjects.

Although the use of the frequency response presents encouraging physical intuition, the large amount of data presented in graphical format presents challenges for rapid clinical interpretation and raises the barrier for training. In order to reduce this burden, a data pipeline was developed to process the data and classify the recording as pathological or healthy. This could provide a screening tool for detection of common pulmonary pathologies such as COPD, asthma, pneumothorax and pneumonia. In addition to compressing the audio data to a more interpretable number of discrete values, the addition of other clinical variables such as the patients height and weight can help to improve the accuracy of the system.

Another important distinction that we highlighted was assessing the difference between internal and external sounds for pulmonary pathology assessment, specifically, the

differences between using breath sounds compared with a fixed input percussion signal. We found that not only did percussion sound features result in improved classification, but the inclusion of breath sound features hindered classification accuracy. This suggests that the use of a fixed signal provides a more standardized method for pulmonary exam automation.

Although these results are encouraging, larger scale clinical trials need to be conducted in order to validate these findings. The results obtained in this dissertation are examined alongside other human subject studies in the field of acoustic pulmonary diagnosis. This review highlights the importance of standardization of these methods and the need for larger scale clinical assessment. In order to get these studies out of the lab and into the clinic, a focus on the end user is equally important.

6.2 Challenges and prospects: The path to standardization

Acoustic methods of pulmonary diagnosis are valuable indicators of respiratory health. Several factors have prevented clinical application of recent experimental advances in the field. In spite of decades of research in the area of breath sound analysis, standardized information for sensor usage, signal processing, nomenclature, and frequency or time information in the context of pathologies remains a challenge, arguably deterring the wider adoption of lung sound analysis in the clinic. Standardization of information with regards to the acoustic characteristics and physics of the lungs, especially with different pathologies, was undertaken by CORSA [63], but its recommendations still have not been widely adopted, and an updated standard is overdue [38]. Differing methods as to what to sense (internal vs. external sounds) and how to analyze these signals, has made it

difficult to begin translation of these methods into the clinic. Specifically, future work should focus on expanding the human subject studies in each disease to provide adequate samples for clinical application.

Translational challenges act as the main barrier between the different groups working on advancing acoustic analysis of the lungs. The creators of a device may not understand the different nomenclature or needs of physicians, and physicians may not have the engineering experience required to communicate sensor, processing, and/or classification specifications. As a result, research into both internal and external methods of acoustic analysis to diagnose the lungs has used a wide array of sensors, usually microphones or accelerometers, which have different specifications, yielding different measurements. With advances in transducer fabrication methods, such as using MEMS technology, and other sensor research, we finally land on a description of the ideal sensor, one that is lightweight, reliable, and sensitive, which will help standardize our understanding of the characteristics of the lungs with respect to internal and external sounds.

In addition to translational challenges between clinicians and device engineers, those working on signal processing and classification techniques also need to be included in future collaborations. Despite the value of machine-learning algorithms, it is important that they provide outputs that can be interpreted by a clinician rather than automatically outputting a diagnosis. Acoustic information can provide a digital biomarker for diagnosis or likelihood scores but should not be used to classify the patient without the context provided by a clinician and a thorough medical history.

Further research is needed to understand the clinical utility of analyzing external sound through the parenchyma instead of internal breath sounds. The analysis of sounds acquired through the parenchyma has the benefit of providing a controllable, well-characterized

input signal that lends itself to application of new advances, including signal processing and classification schemes. The frequency ranges for the diseases discussed in this review are presented to provide a foundation for researchers in the field to develop such a system, consistent with CORSA, as well as other relevant research. Similarly, the use of an array of sensors is a notable method to improve SNR and provide localization information that invites further research. There are different external methods of sensor actuation with regard to location and system. The ideal actuator should be selected based on size (which influences portability, cost, and comfort), intensity at frequencies of interest, and current draw, which affects battery life. The ideal system would also help with monitoring, as aforementioned; integration with the electronic health record (EHR) could contribute to online databases for pathologies, facilitating further research into changes in lungs parameters in response to disease.

6.3 Looking ahead: Telemedicine and mobile health

Outside the hospital, the capability of wirelessly transmitting and storing data is increasingly becoming a standard feature in medical devices [77, 182, 185]. This capability offers the potential to develop and advance the field of telemedicine, which will allow physicians to access live data on the acoustic biomarkers for their patients' lung health and change the course of their care accordingly [182, 185]. This can be done through mobile solutions, such as apps, which are widely available. Certain digital stethoscopes have already provided this platform [135–137], but it has yet to be established for multisensor recording systems. Notably in the field of lung diagnosis, a telehealth system was prospectively studied by Gurbeta et al. for use in diagnosing patients with COPD

and asthma based on neural network and fuzzy logic systems with promising results [186]. This system showed the potential of telemedicine and mobile health for improving quality of care in low-resource settings and less mobile patients. Integration of new technologies with these modern systems (EHR, mobile) is essential because it not only provides better means of monitoring, but also gives context to the treatment of patients with respect to differing demographics and conditions. Creation of such a database will facilitate development of more accurate sensors and analytical techniques in the future.

6.4 Recommendations

The results of this dissertation show that external sound excitation is a promising technique in the diagnosis of pneumonia and other pulmonary pathologies. However, the following recommendations are made for future research in this area.

- In these studies, a digital stethoscope with an electret microphone was used as the sensing component. This was chosen to leverage physician familiarity and reduce interoperability. However, the use of a piezoelectric microphone would be beneficial in reducing surrounding noise. There are trade-offs to this choice, and peizoelectric microphones require considerable signal conditioning; however, for low-resource regions and loud hospital environments this feature is desirable and likely would yield more accurate results.

- In addition to the use of piezoelectric sensors, using a sensor array as several studies have indicated would provide a richer source of spatial information. This approach,

however, should be weighed against the increased cost to determine which device provides the largest amount of clinical utility.

- In these studies, thorax circumference was used as a method of normalization between patients. However, this is a proxy for lung volume which would be a preferred metric by which to normalize patient data. Spirometry can help to provide lung volume and could be used adjunctively to improve performance.

- In these studies, inhalation and exhalation were not controlled and the patients were asked to breath normally while the Tabla system recorded measurements for fifteen seconds. Although asking these patients to hold their breath may not be feasible, the direct effect of breath holding should be investigated. Additionally, reduction of the recording time to less than fifteen seconds at the cost of frequency resolution could be weighed against the benefits of a fixed lung volume.

- In these studies, chest excitation was explored. However, sound input through the mouth provides another avenue of research. It was found through user studies that patients do not prefer mouth based sound input, and there are infection concerns with that design. On the other hand, chest excitation provides a route of sound transmission directly through the rib-cage that is not desirable which may be mitigated through this alternative method. Both methods should be compared in larger scale clinical trials to compare and validate their performance.

Appendix A

Device Storyboard

Creating a storyboard provides a platform to show design ideas and give a rationale for usage. It clearly indicates the functionality of a device and what the user interface looks like. Each scene shows a major task that the device performs. This helps to ensure that the device design is user-centric and carefully thought out. Shown below is the storyboard for the Tabla device.

Panel 1:
Attending - “Alright Mr. Jones, I’m going to move the stethoscope down your back; each time I move it I’m going to ask you to take a deep breath for me.”
Resident (toward Medical Student) - “Were listening for crackles, that would suggest pneumonia.”
(Chart on patient’s bed says pneumonia.)

Attending - "Next I'm going to be tapping on your back."
(Attending leans in slightly to hear the dullness or resonance.
Resident (towards medical student) - "We're listening for dullness."

Panel 3:
Attending - "Alright you two, come take a listen."
Resident (listening to patient with stethoscope.)

Panel 4:
Medical Student (Tapping on patient's back trepidatiously.)
Resident - "You may need to tap harder."

Panel 5:
Attending - "Crackles were heard in the lower right lobe consistent with the dullness to percussion."
Resident - "Lungs sounded clear to me, what do you think?"
(Medical student looks nervous.)

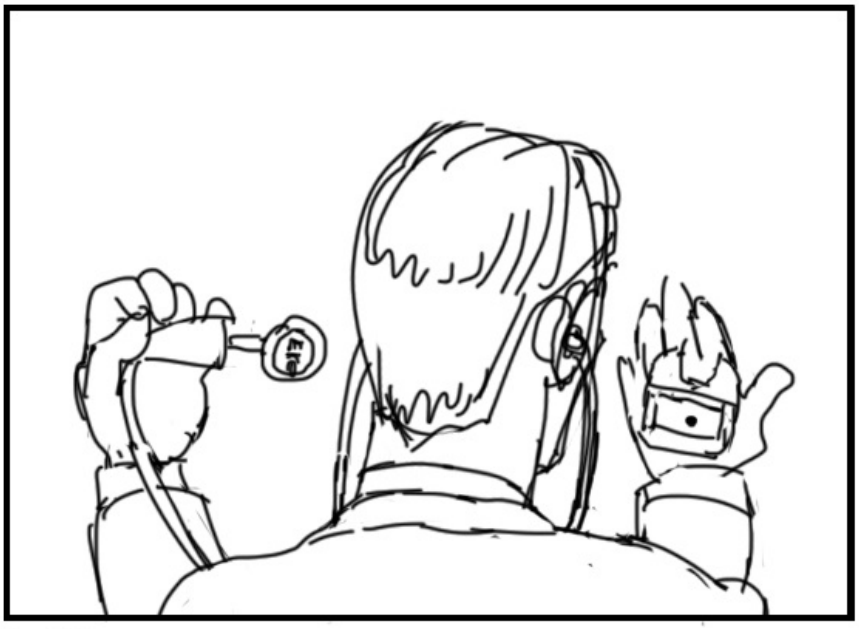

Panel 6:
(Medical student pulls out Eko digital stethoscope, and tabla attachment.)
Medical student - "Glad I brought these today!"

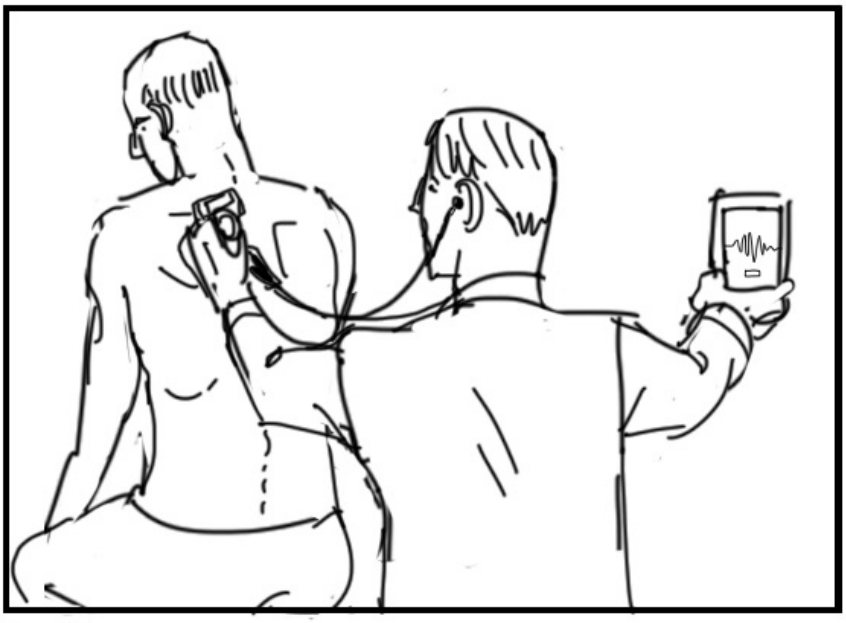

Panel 7:
(Closeup of patient's back, back of medical student with phone in view with audio waveform and record button.)
Medical student - "First I'll record the breath sounds."

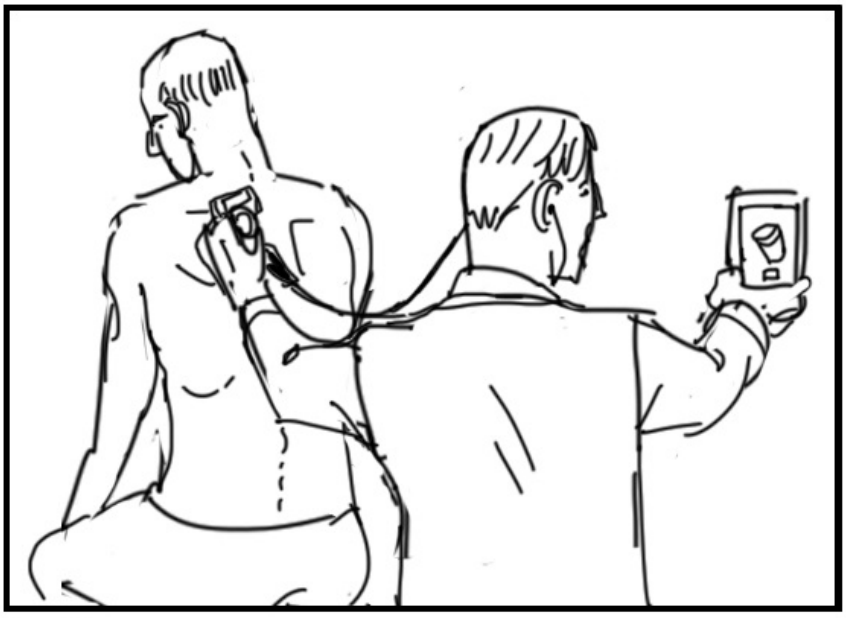

Panel 8:
(Closeup of patient's back, back of medical student with phone in view with phone in veiw with a tabla drum on the scren and tap button.)
Medical student - "Next I'll send in the taps."

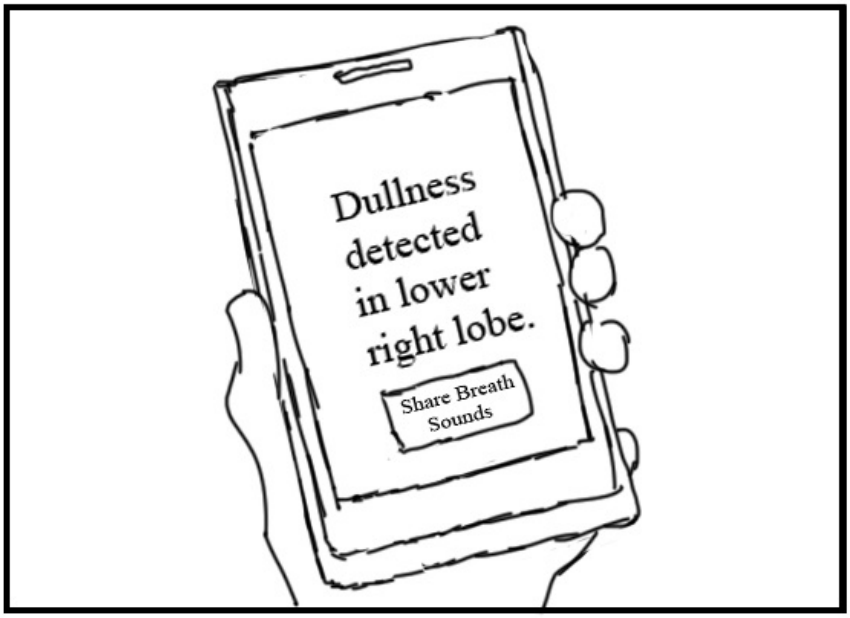

Panel 9:
(Closeup of Phone.)
"Dullness detected in lower right lobe."
(Share breath sounds button) - > clicked with finger.

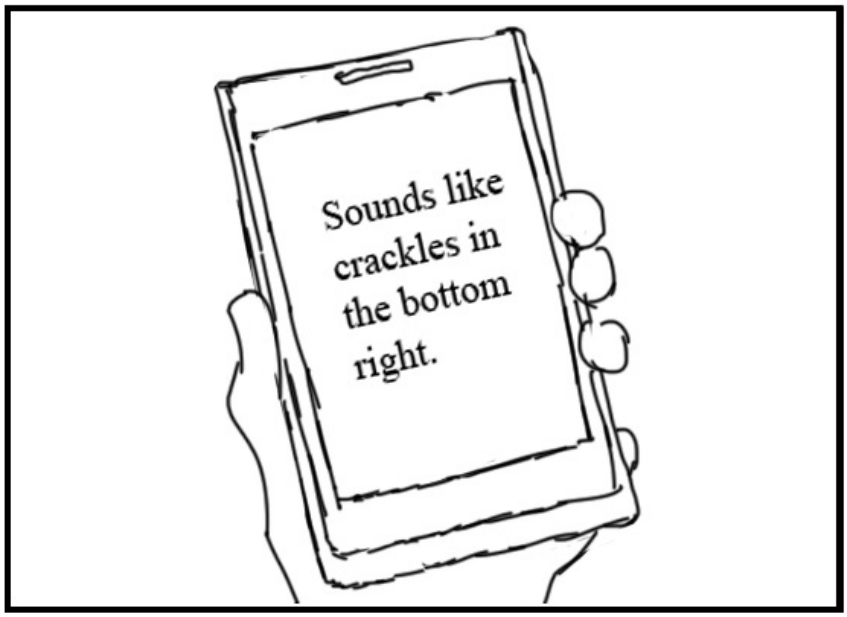

Panel 10:
(Closeup of phone.)
Pulmonologist friend text message - "Sounds like crackles in the bottom right."

Panel 11:
Medical student - "Patient presents with clinical symptoms of pneumonia, physical exam confirms dullness to percussion in the bottom right as well as crackles on auscultaion."
(Attending and Resident look impressed.)

Bibliography

[1] A. Ahmed and M.A. Graber. *Evaluation of the adult with dyspnea in the emergency department In: UpToDate*. Ed. by T.W. Post. UpTodate, 2018.

[2] Lynn Bickley and Peter G Szilagyi. *Bates' guide to physical examination and history-taking*. Lippincott Williams & Wilkins, 2012.

[3] Jean Claude Yernault and AB Bohadana. "Chest percussion". In: *European Respiratory Journal* 8.10 (1995), pp. 1756–1760.

[4] Ying Peng et al. "Sound transmission in the chest under surface excitation: an experimental and computational study with diagnostic applications". In: *Medical & biological engineering & computing* 52.8 (2014), pp. 695–706.

[5] Joyce E Wipf et al. "Diagnosing pneumonia by physical examination: relevant or relic?" In: *Archives of Internal Medicine* 159.10 (1999), pp. 1082–1087.

[6] Arnon Cohen and Dorota Landsberg. "Analysis and automatic classification of breath sounds". In: *IEEE Transactions on Biomedical Engineering* 9 (1984), pp. 585–590.

[7] Duncan Smith-Rohrberg Maru et al. “Turning a blind eye: the mobilization of radiology services in resource-poor regions”. In: *Globalization and health* 6.1 (2010), p. 18.

[8] Christoph F Dietrich et al. “Ultrasound of the pleurae and lungs”. In: *Ultrasound in Medicine and Biology* 41.2 (2015), pp. 351–365.

[9] Adam Rao et al. “Acoustic methods of pulmonary disease diagnosis”. In: *IEEE reviews in biomedical engineering* (2018).

[10] JohnR Guarino. “Auscultatory percussion of the chest”. In: *The Lancet* 315.8182 (1980), pp. 1332–1334.

[11] Joshua P Metlay, Wishwa N Kapoor, and Michael J Fine. “Does this patient have community-acquired pneumonia?: Diagnosing pneumonia by history and physical examination”. In: *Journal of the American Medical Association* 278.17 (1997), pp. 1440–1445.

[12] Hansen A Mansy et al. “Pneumothorax effects on pulmonary acoustic transmission”. In: *Journal of applied Physiology* 119.3 (2015), pp. 250–257.

[13] HA Mansy et al. “Pneumothorax detection using pulmonary acoustic transmission measurements”. In: *Medical and Biological Engineering and Computing* 40.5 (2002), pp. 520–525.

[14] Abraham Bohadana, Gabriel Izbicki, and Steve S Kraman. “Fundamentals of lung auscultation”. In: *New England Journal of Medicine* 370.8 (2014), pp. 744–751.

[15] Almir Badnjevic et al. “Neuro-fuzzy classification of asthma and chronic obstructive pulmonary disease”. In: *BMC medical informatics and decision making* 15.3 (2015), S1.

[16] M Contoli et al. “The small airways and distal lung compartment in asthma and COPD: a time for reappraisal”. In: *Allergy* 65.2 (2010), pp. 141–151.

[17] Malay Sarkar et al. “Auscultation of the respiratory system”. In: *Annals of thoracic medicine* 10.3 (2015), p. 158.

[18] René Théophile Hyacinthe Laennec and John Forbes. *A Treatise on the Diseases of the Chest, and on Mediate Auscultation*. Samuel S. and William Wood, 1838.

[19] Arnon Cohen. “Signal processing methods for upper airway and pulmonary dysfunction diagnosis”. In: *IEEE Engineering in Medicine and Biology Magazine* 9.1 (1990), pp. 72–75.

[20] Martin Kompis, Hans Pasterkamp, and George R Wodicka. “Acoustic imaging of the human chest”. In: *Chest* 120.4 (2001), pp. 1309–1321.

[21] Ram Mor et al. “Breath sound distribution images of patients with pneumonia and pleural effusion”. In: *Respiratory care* 52.12 (2007), pp. 1753–1760.

[22] A Marshall and S Boussakta. “Signal analysis of medical acoustic sounds with applications to chest medicine”. In: *Journal of the Franklin Institute* 344.3-4 (2007), pp. 230–242.

[23] Rajkumar Palaniappan, Kenneth Sundaraj, and Sebastian Sundaraj. “A comparative study of the svm and k-nn machine learning algorithms for the diagnosis of

respiratory pathologies using pulmonary acoustic signals". In: *BMC bioinformatics* 15.1 (2014), p. 223.

[24] Raymond LH Murphy. "In defense of the stethoscope". In: *Respiratory Care* 53.3 (2008), pp. 355–369.

[25] Robert Loudon and Raymond LH Murphy Jr. "Lung sounds". In: *American Review of Respiratory Disease* 130.4 (1984), pp. 663–673.

[26] Salvatore Mangione and Linda Z Nieman. "Pulmonary auscultatory skills during training in internal medicine and family practice". In: *American journal of respiratory and critical care medicine* 159.4 (1999), pp. 1119–1124.

[27] Paul Forgacs. "The functional basis of pulmonary sounds". In: *Chest* 73.3 (1978), pp. 399–405.

[28] David A Rice. "Transmission of lung sounds". In: *Seminars in respiratory medicine*. Vol. 6. 03. Copyright© 1985 by Thieme Medical Publishers, Inc. 1985, pp. 166–170.

[29] George R Wodicka et al. "A model of acoustic transmission in the respiratory system". In: *IEEE Transactions on Biomedical Engineering* 36.9 (1989), pp. 925–934.

[30] Zoujun Dai et al. "Comparison of poroviscoelastic models for sound and vibration in the lungs". In: *Journal of vibration and acoustics* 136.5 (2014), p. 050905.

[31] R Phillip Dellinger et al. "Dynamic visualization of lung sounds with a vibration response device: a case series". In: *Respiration* 75.1 (2008), pp. 60–72.

[32] VI Korenbaum et al. "Comparison of the characteristics of different types of acoustic sensors when recording respiratory noises on the surface of the human chest". In: *Acoustical Physics* 59.4 (2013), pp. 474–481.

[33] John E Aldrich. “Basic physics of ultrasound imaging”. In: *Critical care medicine* 35.5 (2007), S131–S137.

[34] Daniel A Lichtenstein. “Ultrasound in the management of thoracic disease”. In: *Critical care medicine* 35.5 (2007), S250–S261.

[35] Shuang Leng et al. “The electronic stethoscope”. In: *Biomedical engineering online* 14.1 (2015), p. 66.

[36] Rajkumar Palaniappan and Kenneth Sundaraj. “Respiratory sound classification using cepstral features and support vector machine”. In: *Intelligent Computational Systems (RAICS), 2013 IEEE Recent Advances in*. IEEE. 2013, pp. 132–136.

[37] Arati Gurung et al. “Computerized lung sound analysis as diagnostic aid for the detection of abnormal lung sounds: A systematic review and meta-analysis”. In: *Respiratory medicine* 105.9 (2011), pp. 1396–1403.

[38] Kostas N Priftis, Leontios J Hadjileontiadis, and Mark L Everard. *Breath Sounds: From Basic Science to Clinical Practice*. Springer, 2018.

[39] H Pasterkamp, S Patel, and GR Wodicka. “Asymmetry of respiratory sounds and thoracic transmission”. In: *Medical and Biological Engineering and Computing* 35.2 (1997), pp. 103–106.

[40] Kevin E Forkheim, David Scuse, and Hans Pasterkamp. “A comparison of neural network models for wheeze detection”. In: *WESCANEX 95. Communications, Power, and Computing. Conference Proceedings., IEEE*. Vol. 1. IEEE. 1995, pp. 214–219.

[41] Yating Hu et al. “Physiological acoustic sensing based on accelerometers: A survey for mobile healthcare”. In: *Annals of biomedical engineering* 42.11 (2014), pp. 2264–2277.

[42] Heinrich D Becker. “Vibration response imaging–finally a real stethoscope”. In: *Respiration* 77.2 (2009), pp. 236–239.

[43] Noam Gavriely, YORAM Palti, and Gideon Alroy. “Spectral characteristics of normal breath sounds”. In: *Journal of Applied Physiology* 50.2 (1981), pp. 307–314.

[44] José Antonio Fiz et al. “Analysis of tracheal sounds during forced exhalation in asthma patients and normal subjects: bronchodilator response effect”. In: *Chest* 116.3 (1999), pp. 633–638.

[45] Yasemin P Kahya, Ugur Cini, and O Cerid. “Real-time regional respiratory sound diagnosis instrument”. In: *Engineering in Medicine and Biology Society, 2003. Proceedings of the 25th Annual International Conference of the IEEE*. Vol. 4. IEEE. 2003, pp. 3098–3101.

[46] A Torres-Jimenez et al. “Asymmetry in lung sound intensities detected by respiratory acoustic thoracic imaging (RATHI) and clinical pulmonary auscultation”. In: *Engineering in Medicine and Biology Society, 2008. EMBS 2008. 30th Annual International Conference of the IEEE*. IEEE. 2008, pp. 4797–4800.

[47] Lemuel R Waitman et al. “Representation and classification of breath sounds recorded in an intensive care setting using neural networks”. In: *Journal of clinical monitoring and computing* 16.2 (2000), pp. 95–105.

[48] RJ Riella, P Nohama, and JM Maia. “Method for automatic detection of wheezing in lung sounds”. In: *Brazilian Journal of Medical and Biological Research* 42.7 (2009), pp. 674–684.

[49] Mireille Oud, Edo Hans Dooijes, and Jaring S van der Zee. “Asthmatic airways obstruction assessment based on detailed analysis of respiratory sound spectra”. In: *IEEE transactions on biomedical engineering* 47.11 (2000), pp. 1450–1455.

[50] Amon Cohen and AD Berstein. “Acoustic transmission of the respiratory system using speech stimulation”. In: *IEEE transactions on biomedical engineering* 38.2 (1991), pp. 126–132.

[51] Vladimir Korenbaum and Anton Shiriaev. “Sound propagation through human lungs, under transmission sounding with acoustic signal of 80-1000 Hz frequency band”. In: *Proceedings of Meetings on Acoustics 169ASA*. Vol. 23. 1. ASA. 2015, p. 020002.

[52] Daniel A Lichtenstein and Yves Menu. “A bedside ultrasound sign ruling out pneumothorax in the critically III: lung sliding”. In: *Chest* 108.5 (1995), pp. 1345–1348.

[53] Zoltan Jambrik et al. “Usefulness of ultrasound lung comets as a nonradiologic sign of extravascular lung water”. In: *American Journal of Cardiology* 93.10 (2004), pp. 1265–1270.

[54] Adam Rao et al. “Improved Detection of Lung Fluid with Standardized Acoustic Stimulation of the Chest”. In: *IEEE journal of translational engineering in health and medicine* (2018).

[55] MP Jones and DW Thomas. "Acoustic detection of physiological change within the thorax". In: *Acoustic Sensing and Imaging, 1993., International Conference on*. IET. 1993, pp. 201–205.

[56] GR Wodicka et al. "Spectral characteristics of sound transmission in the human respiratory system". In: *IEEE transactions on biomedical engineering* 37.12 (1990), pp. 1130–1135.

[57] MUHAMMAD Mahagnah and NOAM Gavriely. "Gas density does not affect pulmonary acoustic transmission in normal men". In: *Journal of Applied Physiology* 78.3 (1995), pp. 928–937.

[58] VI Korenbaum et al. "Acoustic equipment for studying human respiratory sounds". In: *Instruments and Experimental Techniques* 51.2 (2008), pp. 296–303.

[59] V Goncharoff, JE Jacobs, and DW Cugell. "Wideband acoustic transmission of human lungs". In: *Medical and Biological Engineering and Computing* 27.5 (1989), pp. 513–519.

[60] Courtney Crim et al. "Respiratory system impedance with impulse oscillometry in healthy and COPD subjects: ECLIPSE baseline results". In: *Respiratory medicine* 105.7 (2011), pp. 1069–1078.

[61] TJ Royston et al. "Modeling sound transmission through the pulmonary system and chest with application to diagnosis of a collapsed lung". In: *The Journal of the Acoustical Society of America* 111.4 (2002), pp. 1931–1946.

[62] Mohammed Bahoura. "Pattern recognition methods applied to respiratory sounds classification into normal and wheeze classes". In: *Computers in biology and medicine* 39.9 (2009), pp. 824–843.

[63] ARA Sovijärvi, J Vanderschoot, and JE Earis. *Computerized Respiratory Sound Analysis (CORSA): Recommended Standards for Terms and Techniques: ERS Task Force Report*. Munksgaard, 2000.

[64] AK Siddiqui and S Ahmed. "Pulmonary manifestations of sickle cell disease". In: *Postgraduate medical journal* 79.933 (2003), pp. 384–390.

[65] Zhen Wang, Smith Jean, and Thaddeus Bartter. "Lung sound analysis in the diagnosis of obstructive airway disease". In: *Respiration* 77.2 (2009), pp. 134–138.

[66] Hans Pasterkamp, Steve S Kraman, and George R Wodicka. "Respiratory sounds: advances beyond the stethoscope". In: *American journal of respiratory and critical care medicine* 156.3 (1997), pp. 974–987.

[67] Styliani A Taplidou and Leontios J Hadjileontiadis. "Wheeze detection based on time-frequency analysis of breath sounds". In: *Computers in biology and medicine* 37.8 (2007), pp. 1073–1083.

[68] Sandra Reichert et al. "Analysis of respiratory sounds: state of the art". In: *Clinical medicine. Circulatory, respiratory and pulmonary medicine* 2 (2008), CCRPM–S530.

[69] Noam Gavriely and David W Cugell. *Breath sounds methodology*. cRc PrEss, 1995.

[70] MA Spiteri, DG Cook, and SW Clarke. "Reliability of eliciting physical signs in examination of the chest". In: *The Lancet* 331.8590 (1988), pp. 873–875.

[71] Joshua P Metlay and MD Kapoor. "Community-Acquired Pneumonia?" In: *Jama* 278 (1997), pp. 1440–1445.

[72] B Maitre, T Similowski, and JP Derenne. "Physical examination of the adult patient with respiratory diseases: inspection and palpation". In: *European Respiratory Journal* 8.9 (1995), pp. 1584–1593.

[73] Shriprakash Kalantri et al. "Accuracy and reliability of physical signs in the diagnosis of pleural effusion". In: *Respiratory medicine* 101.3 (2007), pp. 431–438.

[74] GR Wodicka, PD DeFrain, and SS Kraman. "Bilateral asymmetry of respiratory acoustic transmission". In: *Medical and Biological Engineering and Computing* 32.5 (1994), pp. 489–494.

[75] Abraham B Bohadana, Fernando TV Coimbra, and José RF Santiago. "Detection of lung abnormalities by auscultatory percussion: a comparative study with conventional percussion". In: *Respiration* 50.3 (1986), pp. 218–225.

[76] Abraham B Bohadana, R Patel, and Steve S Kraman. "Contour maps of auscultatory percussion in healthy subjects and patients with large intrapulmonary lesions". In: *Lung* 167.1 (1989), pp. 359–372.

[77] Adam Rao et al. "Tabla: A Proof-of-Concept Auscultatory Percussion Device for Low-Cost Pneumonia Detection". In: *Sensors* 18.8 (2018), p. 2689.

[78] GR Wodicka et al. "Phase delay of pulmonary acoustic transmission from trachea to chest wall". In: *IEEE transactions on biomedical engineering* 39.10 (1992), pp. 1053–1059.

[79] DAVID A Rice. "Sound speed in pulmonary parenchyma". In: *Journal of Applied Physiology* 54.1 (1983), pp. 304–308.

[80] J.L. Prince and J. Links. *Medical Imaging Signals and Systems*. Pearson Education, 2014. ISBN: 9780133583151. URL: https://books.google.com.au/books?id=KpNyBAAAQBAJ.

[81] A Murray and JMM Neilson. "Diagnostic percussion sounds: 1. A qualitative analysis". In: *Medical and biological engineering* 13.1 (1975), pp. 19–28.

[82] Ying Peng et al. "Sound transmission in porcine thorax through airway insonification". In: *Medical & biological engineering & computing* 54.4 (2016), pp. 675–689.

[83] HA Mansy, TJ Royston, and RH Sandler. "Use of abdominal percussion for pneumoperitoneum detection". In: *Medical and Biological Engineering and Computing* 40.4 (2002), pp. 439–446.

[84] HA Mansy, TJ Royston, and RH Sandler. "Acoustic characteristics of air cavities at low audible frequencies with application to pneumoperitoneum detection". In: *Medical and Biological Engineering and Computing* 39.2 (2001), pp. 159–167.

[85] Manuel Abella, John Formolo, and David G Penney. "Comparison of the acoustic properties of six popular stethoscopes". In: *The Journal of the Acoustical Society of America* 91.4 (1992), pp. 2224–2228.

[86] Jeffrey J Goldberger and Jason Ng. *Practical signal and image processing in clinical cardiology*. Springer, 2010.

[87] L Vannuccini et al. "Capturing and preprocessing of respiratory sounds". In: *European Respiratory Review* 10.77 (2000), pp. 616–620.

[88] Dmitry Sergeevich Zhdanov et al. “Short review of devices for detection of human breath sounds and heart tones”. In: *Biology and Medicine* 6.3 (2014), p. 1.

[89] Uzair Mayat et al. “Towards a low-cost point-of-care screening platform for electronic auscultation of vital body sounds”. In: *Humanitarian Technology Conference (IHTC), 2017 IEEE Canada International*. IEEE. 2017, pp. 1–5.

[90] G Nelson, R Rajamani, and A Erdman. “Vibro-acoustic model of a piezoelectric-based stethoscope for chest sound measurements”. In: *Measurement Science and Technology* 26.9 (2015), p. 095701.

[91] Tim Bergstresser et al. “Sound transmission in the lung as a function of lung volume”. In: *Journal of Applied Physiology* 93.2 (2002), pp. 667–674.

[92] S Charleston-Villalobos et al. “Respiratory acoustic thoracic imaging (RATHI): assessing deterministic interpolation techniques”. In: *Medical and Biological Engineering and Computing* 42.5 (2004), pp. 618–626.

[93] Brian Henry and Thomas J Royston. “Localization of adventitious respiratory sounds”. In: *The Journal of the Acoustical Society of America* 143.3 (2018), pp. 1297–1307.

[94] Devanand Anantham et al. “Vibration response imaging in the detection of pleural effusions: a feasibility study”. In: *Respiration* 77.2 (2009), pp. 166–172.

[95] Konstantinos Bartziokas et al. “Vibration response imaging: evaluation of rater agreement in healthy subjects and subjects with pneumonia”. In: *BMC medical imaging* 10.1 (2010), p. 6.

[96] Zhen Wang et al. “Asynchrony between left and right lungs in acute asthma”. In: *Journal of Asthma* 45.7 (2008), pp. 575–578.

[97] Shaul Lev et al. “Computerized lung acoustic monitoring can help to differentiate between various chest radiographic densities in critically ill patients”. In: *Respiration* 80.6 (2010), pp. 509–516.

[98] Suranan Noimanee et al. “Design considerations for aural vital signs using PZT piezoelectric ceramics sensor based on the computerization method”. In: *Sensors* 7.12 (2007), pp. 3192–3208.

[99] Jens Kirchner, Sara Souilem, and Georg Fischer. “Wearable system for measurement of thoracic sounds with a microphone array”. In: *SENSORS, 2017 IEEE*. IEEE. 2017, pp. 1–3.

[100] Hans Pasterkamp et al. “Measurement of respiratory acoustical signals: comparison of sensors”. In: *Chest* 104.5 (1993), pp. 1518–1525.

[101] Michael Talbot-Smith. *Audio engineer's reference book*. Focal Press, 2012.

[102] Ion Boldea and Syed A Nasar. “Linear electric actuators and generators”. In: *Electric Machines and Drives Conference Record, 1997. IEEE International*. IEEE. 1997, MA1–1.

[103] M Redwood. “Transient performance of a piezoelectric transducer”. In: *The journal of the acoustical society of America* 33.4 (1961), pp. 527–536.

[104] Bill Brashier and Sundeep Salvi. “Measuring lung function using sound waves: role of the forced oscillation technique and impulse oscillometry system”. In: *Breathe* 11.1 (2015), p. 57.

[105] HJ Smith, P Reinhold, and MD Goldman. “Forced oscillation technique and impulse oscillometry”. In: *European Respiratory Monograph* 31 (2005), p. 72.

[106] Koundinya Desiraju and Anurag Agrawal. “Impulse oscillometry: the state-of-art for lung function testing”. In: *Lung India: official organ of Indian Chest Society* 33.4 (2016), p. 410.

[107] Su-Gang Gong et al. “Evaluation of respiratory impedance in patients with chronic obstructive pulmonary disease by an impulse oscillation system”. In: *Molecular medicine reports* 10.5 (2014), pp. 2694–2700.

[108] Tae Won Song et al. “Utility of impulse oscillometry in young children with asthma”. In: *Pediatric Allergy and Immunology* 19.8 (2008), pp. 763–768.

[109] Miroslava Barúa et al. “Classification of impulse oscillometric patterns of lung function in asthmatic children using artificial neural networks”. In: *Engineering in Medicine and Biology Society, 2005. IEEE-EMBS 2005. 27th Annual International Conference of the*. IEEE. 2006, pp. 327–331.

[110] Zareth Irwin and Justin O Cook. “Advances in point-of-care thoracic ultrasound”. In: *Emerg Med Clin North Am* 34.1 (2016), pp. 151–7.

[111] Rémi Targhetta et al. “Sonographic approach to diagnosing pulmonary consolidation”. In: *Journal of ultrasound in medicine* 11.12 (1992), pp. 667–672.

[112] Luna Gargani and Giovanni Volpicelli. “How I do it: lung ultrasound”. In: *Cardiovascular ultrasound* 12.1 (2014), p. 25.

[113] Mohammad Al Deeb et al. “Point-of-care ultrasonography for the diagnosis of acute cardiogenic pulmonary edema in patients presenting with acute dyspnea: a systematic review and meta-analysis”. In: *Academic Emergency Medicine* 21.8 (2014), pp. 843–852.

[114] Daniel A Lichtenstein et al. “Ultrasound diagnosis of alveolar consolidation in the critically ill”. In: *Intensive care medicine* 30.2 (2004), pp. 276–281.

[115] Miguel A Chavez et al. “Lung ultrasound for the diagnosis of pneumonia in adults: a systematic review and meta-analysis”. In: *Respiratory research* 15.1 (2014), p. 50.

[116] Daniel Lichtenstein, Gilbert Mezière, and Julien Seitz. “The dynamic air bronchogram: a lung ultrasound sign of alveolar consolidation ruling out atelectasis”. In: *Chest* 135.6 (2009), pp. 1421–1425.

[117] Alexandre Grimberg et al. “Diagnostic accuracy of sonography for pleural effusion: systematic review”. In: *Sao Paulo Medical Journal* 128.2 (2010), pp. 90–95.

[118] Pan-Chyr Yang et al. “Value of sonography in determining the nature of pleural effusion: analysis of 320 cases.” In: *AJR. American journal of roentgenology* 159.1 (1992), pp. 29–33.

[119] Khaled Alrajhi, Michael Y Woo, and Christian Vaillancourt. “Test characteristics of ultrasonography for the detection of pneumothorax: a systematic review and meta-analysis”. In: *Chest* 141.3 (2012), pp. 703–708.

[120] Xiaoming Zhang et al. “Noninvasive ultrasound image guided surface wave method for measuring the wave speed and estimating the elasticity of lungs: A feasibility study”. In: *Ultrasonics* 51.3 (2011), pp. 289–295.

[121] Armen P Sarvazyan et al. “Shear wave elasticity imaging: a new ultrasonic technology of medical diagnostics”. In: *Ultrasound in Medicine and Biology* 24.9 (1998), pp. 1419–1435.

[122] Armen P Sarvazyan, Matthew W Urban, and James F Greenleaf. "Acoustic waves in medical imaging and diagnostics". In: *Ultrasound in Medicine and Biology* 39.7 (2013), pp. 1133–1146.

[123] Shigao Chen, Mostafa Fatemi, and James F Greenleaf. "Quantifying elasticity and viscosity from measurement of shear wave speed dispersion". In: *The Journal of the Acoustical Society of America* 115.6 (2004), pp. 2781–2785.

[124] Man Zhang et al. "Quantitative characterization of viscoelastic properties of human prostate correlated with histology". In: *Ultrasound in Medicine and Biology* 34.7 (2008), pp. 1033–1042.

[125] Xiaoming Zhang, RR Kinnick, and James F Greenleaf. "Viscoelasticity of lung tissue with surface wave method". In: *Ultrasonics Symposium, 2008. IUS 2008. IEEE*. IEEE. 2008, pp. 21–23.

[126] Yogesh K Mariappan et al. "MR elastography of human lung parenchyma: technical development, theoretical modeling and in vivo validation". In: *Journal of Magnetic Resonance Imaging* 33.6 (2011), pp. 1351–1361.

[127] Yogesh K Mariappan et al. "Estimation of the absolute shear stiffness of human lung parenchyma using 1H spin echo, echo planar MR elastography". In: *Journal of Magnetic Resonance Imaging* 40.5 (2014), pp. 1230–1237.

[128] BC Goss et al. "Magnetic resonance elastography of the lung: technical feasibility". In: *Magnetic resonance in medicine* 56.5 (2006), pp. 1060–1066.

[129] John P Marinelli et al. “Quantitative assessment of lung stiffness in patients with interstitial lung disease using MR elastography”. In: *Journal of Magnetic Resonance Imaging* 46.2 (2017), pp. 365–374.

[130] Xiaoming Zhang, Thomas Osborn, and Sanjay Kalra. “A noninvasive ultrasound elastography technique for measuring surface waves on the lung”. In: *Ultrasonics* 71 (2016), pp. 183–188.

[131] Pneumonia Acute Respiratory Infection Diagnostic Aid Target Product Profile E. Kadilli. Available online: https://www.unicef.org/supply/files/Pneumonia_Diagnostics_Aid_Device_TPP_Introduction.pdf. accessed on 12 November 2016.

[132] Robert P Baughman and Robert G Loudon. “Sound Spectral Analysis of Voice-Transmitted Sound 1, 2”. In: *American Review of Respiratory Disease* 134.1 (1986), pp. 167–169.

[133] Adam Rao et al. “Tabla: An acoustic device designed for low cost pneumonia detection”. In: (2017), pp. 172–175. DOI: 10.1109/HIC.2017.8227612.

[134] Dayton Audio (2017, Sep.) Understanding Exciters - Principles and Applications. URL: https://www.parts-express.com/pedocs/buyer-guides/understanding-and-using-dayton-audio-exciters.pdf.

[135] Littmann (2017, Mar.) 3M Littmann Electronic Stethoscope. URL: http://www.littmann.com/3M/en_US/littmann-stethoscopes/products/$\sim$/3M-Littmann-Stethoscopes/Electronic-Stethoscopes.

[136] Eko Devices (2017, Mar.) Eko Core Digital Stethoscope. URL: https://ekodevices.com/.

[137] ThinkLabs (2017, Mar.) ThinkLabs One Digital Stethoscope. URL: http://www.thinklabs.com/.

[138] James Derek Smith. *Vibration measurement and analysis*. Butterworth-Heinemann, 2013.

[139] Elena Nioutsikou et al. "Quantifying the effect of respiratory motion on lung tumour dosimetry with the aid of a breathing phantom with deforming lungs". In: *Physics in Medicine and Biology* 51.14 (2006), p. 3359.

[140] Bhuiyan Md Moinuddin. "Automated Classification of Medical Percussion Signals for the Diagnosis of Pulmonary Injuries". PhD thesis. University of Windsor, 2013.

[141] Volker Gross et al. "The relationship between normal lung sounds, age, and gender". In: *American journal of respiratory and critical care medicine* 162.3 (2000), pp. 905–909.

[142] HJ Schreur et al. "Lung sounds during allergen-induced asthmatic responses in patients with asthma." In: *American journal of respiratory and critical care medicine* 153.5 (1996), pp. 1474–1480.

[143] Kalpalatha K Guntupalli et al. "Evaluation of obstructive lung disease with vibration response imaging". In: *Journal of Asthma* 45.10 (2008), pp. 923–930.

[144] A Kandaswamy et al. "Neural classification of lung sounds using wavelet coefficients". In: *Computers in biology and medicine* 34.6 (2004), pp. 523–537.

[145] James W Cooley and John W Tukey. "An algorithm for the machine calculation of complex Fourier series". In: *Mathematics of computation* 19.90 (1965), pp. 297–301.

[146] S Rietveld, Mireille Oud, and Edo Hans Dooijes. "Classification of asthmatic breath sounds: preliminary results of the classifying capacity of human examiners versus artificial neural networks". In: *Computers and Biomedical Research* 32.5 (1999), pp. 440–448.

[147] Roy L Donnerberg et al. "Sound transfer function of the congested canine lung". In: *Respiratory Medicine* 74 (1980), pp. 23–31.

[148] Hamed Minaei Zaeim et al. "Evaluation of the use of frequency response in the diagnosis of pleural effusion on a phantom model of the human lungs". In: *Engineering in Medicine and Biology Society (EMBC), 2014 36th Annual International Conference of the IEEE*. IEEE. 2014, pp. 3418–3421.

[149] Feng Yang et al. "Lung water detection using acoustic techniques". In: *Engineering in Medicine and Biology Society (EMBC), 2012 Annual International Conference of the IEEE*. IEEE. 2012, pp. 4258–4261.

[150] K Mulligan, A Adler, and R Goubran. "Detecting regional lung properties using audio transfer functions of the respiratory system". In: *Engineering in Medicine and Biology Society, 2009. EMBC 2009. Annual International Conference of the IEEE*. IEEE. 2009, pp. 5697–5700.

[151] Dmitry Bogdanov et al. "ESSENTIA: an open-source library for sound and music analysis". In: *Proceedings of the 21st ACM international conference on Multimedia*. ACM. 2013, pp. 855–858.

[152] Chin-Hsing Chen et al. “Using k-nearest neighbor classification to diagnose abnormal lung sounds”. In: *Sensors* 15.6 (2015), pp. 13132–13158.

[153] M Bahoura and C Pelletier. “Respiratory sounds classification using cepstral analysis and Gaussian mixture models”. In: *Engineering in Medicine and Biology Society, 2004. IEMBS'04. 26th Annual International Conference of the IEEE*. Vol. 1. IEEE. 2004, pp. 9–12.

[154] Jen-Chien Chien et al. “Wheeze detection using cepstral analysis in gaussian mixture models”. In: *Engineering in Medicine and Biology Society, 2007. EMBS 2007. 29th Annual International Conference of the IEEE*. IEEE. 2007, pp. 3168–3171.

[155] Murat Aykanat et al. “Classification of lung sounds using convolutional neural networks”. In: *EURASIP Journal on Image and Video Processing* 2017.1 (2017), p. 65.

[156] Selim Aras, Ali Gangal, and Yilmaz Bulbul. “Classification of healthy and pathologic lung sounds recorded with electronic auscultation”. In: *Signal Processing and Communications Applications Conference (SIU), 2015 23th*. IEEE. 2015, pp. 252–255.

[157] Leon Cohen. *Time-frequency analysis*. Vol. 778. Prentice hall, 1995.

[158] Amjad Hashemi, Hossein Arabalibiek, and Khosrow Agin. “Classification of wheeze sounds using wavelets and neural networks”. In: *International Conference on Biomedical Engineering and Technology*. Vol. 11. IACSIT Press. 2011, pp. 127–131.

[159] Gorkem Serbes et al. “Feature extraction using time-frequency/scale analysis and ensemble of feature sets for crackle detection”. In: *Engineering in Medicine and Biology Society, EMBC, 2011 Annual International Conference of the IEEE*. IEEE. 2011, pp. 3314–3317.

[160] Sameer S Alsmadi and Yasemin P Kahya. "Online classification of lung sounds using DSP". In: *Engineering in Medicine and Biology, 2002. 24th Annual Conference and the Annual Fall Meeting of the Biomedical Engineering Society EMBS/BMES Conference, 2002. Proceedings of the Second Joint*. Vol. 2. IEEE. 2002, pp. 1771–1772.

[161] Bülent Sankur et al. "Comparison of AR-based algorithms for respiratory sounds classification". In: *Computers in Biology and Medicine* 24.1 (1994), pp. 67–76.

[162] Ross Folland et al. "Comparison of neural network predictors in the classification of tracheal–bronchial breath sounds by respiratory auscultation". In: *Artificial intelligence in medicine* 31.3 (2004), pp. 211–220.

[163] B Flietstra et al. "Automated analysis of crackles in patients with interstitial pulmonary fibrosis". In: *Pulmonary medicine* 2011 (2011).

[164] Rajkumar Palaniappan, Kenneth Sundaraj, and Nizam Uddin Ahamed. "Machine learning in lung sound analysis: a systematic review". In: *Biocybernetics and Biomedical Engineering* 33.3 (2013), pp. 129–135.

[165] Jorge LM Amaral et al. "Machine learning algorithms and forced oscillation measurements applied to the automatic identification of chronic obstructive pulmonary disease". In: *Computer methods and programs in biomedicine* 105.3 (2012), pp. 183–193.

[166] P Mayorga et al. "Acoustics based assessment of respiratory diseases using GMM classification". In: *Engineering in Medicine and Biology Society (EMBC), 2010 Annual International Conference of the IEEE*. IEEE. 2010, pp. 6312–6316.

[167] Maryam Zolnoori et al. "Fuzzy rule-based expert system for assessment severity of asthma". In: *Journal of medical systems* 36.3 (2012), pp. 1707–1717.

[168] Almir Badnjevic, Lejla Gurbeta, and Eddie Custovic. "An Expert Diagnostic System to Automatically Identify Asthma and Chronic Obstructive Pulmonary Disease in Clinical Settings". In: *Scientific reports* 8.1 (2018), p. 11645.

[169] Patrick Ray et al. "Acute respiratory failure in the elderly: etiology, emergency diagnosis and prognosis". In: *Critical care* 10.3 (2006), R82.

[170] Chen Bao-Shuvo Roy Adam Rao Jorge Ruiz. "Tabla: An Acoustic Device Designed for Low Cost Pneumonia Detection". In: *Proceedings of the IEEE-NIH Healthcare Innovations and Point of Care Technology (HI-POCT)*. Bethesda, MD, USA, 2017.

[171] Mohammad Obadah Nakawah, Clare Hawkins, and Farouk Barbandi. "Asthma, chronic obstructive pulmonary disease (COPD), and the overlap syndrome". In: *The Journal of the American Board of Family Medicine* 26.4 (2013), pp. 470–477.

[172] Juan Pablo Bello et al. "On the use of phase and energy for musical onset detection in the complex domain". In: *IEEE Signal Processing Letters* 11.6 (2004), pp. 553–556.

[173] Xavier Amatriain et al. "Spectral processing". In: *Zölzer U, editor. DAFX-Digital Audio Effects. Chichester: John Wiley & Sons; 2002.* (2002).

[174] Mark Kahrs and Karlheinz Brandenburg. *Applications of digital signal processing to audio and acoustics*. Vol. 437. Springer Science & Business Media, 1998.

[175] Todor Ganchev, Nikos Fakotakis, and George Kokkinakis. "Comparative evaluation of various MFCC implementations on the speaker verification task". In: *Proceedings of the SPECOM*. Vol. 1. 2005, pp. 191–194.

[176] Geoffroy Peeters. "A large set of audio features for sound description (similarity and classification) in the CUIDADO project". In: (2004).

[177] Lie Lu, Hong-Jiang Zhang, and Stan Z Li. "Content-based audio classification and segmentation by using support vector machines". In: *Multimedia systems* 8.6 (2003), pp. 482–492.

[178] Stephen B Hulley. *Designing clinical research*. Lippincott Williams & Wilkins, 2007.

[179] Antoni Homs-Corbera et al. "Time-frequency detection and analysis of wheezes during forced exhalation". In: *IEEE Transactions on Biomedical Engineering* 51.1 (2004), pp. 182–186.

[180] Andrey Vyshedskiy and Raymond Murphy. "Acoustic biomarkers of Chronic Obstructive Lung Disease". In: *Research Ideas and Outcomes* 2 (2016), e9173.

[181] Umme Kolsum et al. "Impulse oscillometry in COPD: identification of measurements related to airway obstruction, airway conductance and lung volumes". In: *Respiratory medicine* 103.1 (2009), pp. 136–143.

[182] Miguel Angel Fernandez-Granero, Daniel Sanchez-Morillo, and Antonio Leon-Jimenez. "Computerised analysis of telemonitored respiratory sounds for predicting acute exacerbations of COPD". In: *Sensors* 15.10 (2015), pp. 26978–26996.

[183] Montserrat Blanco et al. "Distribution of Breath Sound Images in Patients with Pneumothoraces Compared to Healthy Subjects". In: *Respiration* 77.2 (2009), pp. 173–178.

[184] Mordechai Yigla et al. "Vibration response imaging technology in healthy subjects". In: *American Journal of Roentgenology* 191.3 (2008), pp. 845–852.

[185] Aparna Lakhe et al. "Development of digital stethoscope for telemedicine". In: *Journal of medical engineering & technology* 40.1 (2016), pp. 20–24.

[186] Lejla Gurbeta et al. “A telehealth system for automated diagnosis of asthma and chronical obstructive pulmonary disease”. In: *Journal of the American Medical Informatics Association* (2018).

Publishing Agreement

It is the policy of the University to encourage the distribution of all theses, dissertations, and manuscripts. Copies of all UCSF theses, dissertations, and manuscripts will be routed to the library via the Graduate Division. The library will make all theses, dissertations, and manuscripts accessible to the public and will preserve these to the best of their abilities, in perpetuity.

Please sign the following statement:

I hereby grant permission to the Graduate Division of the University of California, San Francisco to release copies of my thesis, dissertation, or manuscript to the Campus Library to provide access and preservation, in whole or in part, in perpetuity.

Author Signature

5/10/19

Date